TOXICOKINETIC MODELS OF DERMAL EXPOSURE TO JET FUEL

David Kim

A dissertation submitted to the faculty of the University of North Carolina at Chapel Hill in partial fulfillment of the requirements for the degree of Doctor of Philosophy in the Department of Environmental Sciences and Engineering.

Chapel Hill
2006

Approved by,

Advisor: Leena A. Nylander-French
Reader: Melvin E. Andersen
Reader: Louise M. Ball
Reader: Dana Loomis
Reader: Stephen M. Rappaport

ABSTRACT

DAVID KIM: Toxicokinetic models of dermal exposure to jet fuel
(Under the direction of Leena A. Nylander-French)

Dermal exposure to Jet-Propulsion Fuel 8 (JP-8) is prevalent in the United States Air Force. Although a large amount of exposure data was generated from previous occupational studies, dermal exposure to JP-8 was poorly characterized and quantitative estimates of the contribution of dermal exposure to the internal dose of JP-8 were unavailable. To fill this data and knowledge gap, a controlled dermal exposure study was designed to quantify the toxicokinetic behavior of naphthalene, 1-methyl naphthalene, 2-methyl naphthalene, decane, undecane, and dodecane. Further, a toxicokinetic model was constructed; this model provided the basis for the development of a physiologically-based toxicokinetic (PBTK) model of dermal and inhalation exposure to JP-8. The PBTK model was used to quantify the contribution of dermal exposure to the internal dose of naphthalene. Results of this research suggest that the apparent human permeability coefficient is 10-fold lower than estimates made *in vitro*. Further, simulations of dermal exposure to JP-8 suggested that the tape-strip method can be used to differentiate exposure groups in epidemiology studies. The median relative contribution of dermal exposure to the internal dose of naphthalene was 1.7% (10^{th} percentile = 0.3% and 90^{th} percentile = 6.9%). The overall implication of these findings is that protection from dermal exposure to JP-8 can reduce the internal dose of naphthalene. However, for most of the US Air Force personnel, the major contribution to the internal dose was from inhalation exposure. The two most significant contributions to the scientific understanding of JP-8 exposures were (1) improved characterization of dermal exposures, and (2) quantitation of the toxicokinetic behavior of aromatic and aliphatic hydrocarbons. Overall, this research has presented a new direction for toxicokinetic modeling human exposures to complex chemical mixtures. This modeling strategy may be used to better assess the risks associated with JP-8 exposures in human populations.

To my wife, Christina

and to my parents, Ki-Hwan and Hyun-Soon.

ACKNOWLEDGEMENTS

Twenty years from now you will be more disappointed by the things that you didn't do than by the ones you did do. So throw off the bowlines. Sail away from the safe harbor. Catch the trade winds in your sails. Explore. Dream. Discover.

Mark Twain

I am glad that I did this. Four years ago I committed to something that I did not know much about. Now that I am here, and am able to look back from a higher perch, what I see is not disappointing but utterly satisfying. I am indebted to many for giving me this perspective: Leena Nylander-French for her vision and support, which have made all of this possible; Melvin Andersen for his teaching and rebuking; Stephen Rappaport for his humor and research technician; Dana Loomis for provocation of deeper thought; and Louise Ball, for opportunity and space. Time is irrefutably the most highly prized commodity in modern times; next is, arguably, space. Louise Ball provided much of both, giving me an opportunity to teach her class and providing me the use of her laboratory for the human volunteer study. I am also grateful to my colleagues and friends: Suramya, Joachim, Connie, Sheila, Evelyn, Pete, Sung, Yu-Sheng, Jon, Bill, Berin, Jan, Kenny, Linda, Rong, Jacob and Anjolie, Meredith, Pat and Brenda, Andy, Chot, Cruz, James, Paul Michael, Janet, Christine, Stephen, and my volleyball community. We've had many petty discussions and some that led to enlightening research ideas; I appreciate all the conversations that we have had together. I am especially grateful to my parents for their unconditional love, especially when I was a "stressed out doctoral student". Lastly, but mostly, I thank my wife, Christina, for taking care of me and allowing herself to be taken care of when we both needed each other so much. Thank you.

This study was supported by NIEHS (P42-ES05948, P30ES10126, and T32-ES07018), by US Air Force through a subcontract with Texas Tech University (1331/0489-01), and by NIOSH (T42/CCT410423-09)

TABLE OF CONTENTS

LIST OF TABLES

LIST OF FIGURES

ABBREVIATIONS

A_{exp}	Area of exposure
ATD	Automatic Thermal Desorption
ATSDR	Agency for Toxic Substances and Disease Registry
AUC	Area under the curve
BMI	Body Mass Index
CI	Confidence interval
cm	Centimeter
C_{PBZ}	Concentration in the personal breathing zone
C_{max}	Maximum Concentration
CTS	Central Testing Site
D	Diffusion coefficient
∂C	concentration gradient
DTK	Dermatotoxicokinetic
∂x	thickness
EPA	Environmental Protection Agency
$f_{fat,ve}$	Fraction of fat in the viable epidermis
$f_{fat,b}$	Fraction of fat in the blood
GC	Gas chromatography
MS	Mass spectrometry
h	Hour
HS-SPME	Headspace solid phase microextraction
$INHAL_{adj}$	Adjusted air concentration of naphthalene
$INHAL_{est}$	Estimated air concentration of naphthalene
$INHAL_{pred}$	Predicted air concentration of naphthalene
IRB	Institutional Review Board
J	Flux

JP-8	Jet-propulsion fuel 8
K_{eff}	Effective permeability coefficient
K_M	Michaelis-Menten Constant
K_{ow}	Octanol-water partition coefficient
K_p	Permeability coefficient
K_{ps}	Permeability coefficient for the stratum corneum
K_{pv}	Permeability coefficient for the viable epidermis
L	Liter
LOD	Limit of detection
LR	Likelihood ratio
MBDE	Mass balance differential equation
mg	Milligram
min	Minute
ml	Milliliter
MW	Molecular weight
NATO	North Atlantic Treaty Organization
ng	Nanogram
NHANES	National Health and Nutrition Examination Survey
OEL	Occupational Exposure Limit
OR	Odds Ratio
$P_{b:a}$	Blood:air partition coefficient
PBTK	Physiologically Based Toxicokinetic
PID	Photoionization detector
PBZ	Personal breathing zone
$P_{sc:ve}$	Stratum corneum:viable epidermis partition coefficient
$P_{ve:b}$	Viable epidermis:blood partition coefficient
PDMS	Polydimethylsiloxane
$P_{f:b}$	Fat:blood partition coefficient

$P_{o:b}$	Other tissue:blood partition coefficient
QC	Cardiac Output
QE	Blood flow rate to skin
QF	Blood flow rate to fat
QL	Blood flow rate to liver
QO	Blood flow rate to other tissues
QP	Pulmonary ventilation rate
QSAR	Quantitative Structure Activity Relationship
QSPR	Quantitative Structure Permeation Relationship
SC	Stratum corneum
SD	Standard deviation
t	Time
TEWL	Trans-epidermal water loss
t_{max}	Time at maximum concentration
US	United States
V_b	Volume of blood
V_f	Volume of fat
V_{max}	Maximum rate of metabolism
V_o	Volume of other tissue
V_{sc}	Volume of stratum corneum
V_{ve}	Volume of viable epidermis

CHAPTER 1

BACKGROUND AND SIGNIFICANCE

Military activities require the use of hazardous chemicals, which can be emitted into the air, soil, and water. These hazards present a risk to personnel, their families, and surrounding communities. The single largest chemical exposure found on military bases of North Atlantic Treaty Organization (NATO) nations is jet-propulsion fuel 8 (JP-8) (Zeiger and Smith 1998). JP-8, which replaced JP-4, is less volatile and does not contain the lower molecular weight hydrocarbons found in gasoline. As a result, exposure by inhalation may potentially be lower, but dermal exposure may play a more significant role in causing adverse health effects. In this section, the current state of knowledge of dermal exposure to JP-8 is examined. First, the local and systemic health effects of JP-8 are discussed briefly. Second, a large body of literature in the area of dermal exposure assessment to chemicals is examined. Specific studies of dermal exposure to JP-8 are then critiqued in the context of this broader picture of the literature.

1.1 Health effects of dermal exposure to JP-8

JP-8 is composed of many hydrocarbons. These include benzene, toluene, naphthalene, and aliphatic compounds such a nonane and decane (McDougal *et al.* 2000). For some chemicals (e.g., benzene) more is known about the adverse health effects than others (e.g., dodecane). It is impractical to summarize the health effects caused by each and every known component of JP-8. In this section, the health effects of bulk exposure to JP-8 will be reviewed with examples drawn from studies of specific components of JP-8.

1.1.1 Metabolism of JP-8 components

JP-8 has been divided into aromatic and aliphatic components, using naphthalene and dodecane as markers of exposure to each fraction respectively (Baynes *et al.* 2001). Metabolic products are often the compounds that cause toxicity. The metabolism of naphthalene has been studied extensively (ATSDR 1995; Buckpitt and Bahnson 1986; US EPA 1998). Primary metabolism of naphthalene by the cytochrome P450 monooxygenases results in naphthalene-1,2-oxide. This epoxide rearranges to 1- and 2-naphthols. The epoxide also undergoes phase II metabolism, such as conjugation with glucuronic acid, sulfate, or glutathione to form more water soluble compounds. The naphthols can be hydrated by epoxide hydrolase to form naphthalene-1,2-dihydrodiol, which itself can be converted to 1,2-naphthalenediol by catechol reductase. The 1,2-naphthalenediol can undergo further oxidation to 1,2-naphthoquinone, and also form 1,4-naphthoquinone. Further, 1-naphthol can also produce 1,4-naphthoquinone. Naphthalene metabolism has been studied in lung tissue (Buckpitt and Bahnson 1986) but not in the skin. The metabolism of dodecane is not well characterized but is believed to undergo oxidation reaction to a ketone through an intermediate hydroxylation step (Subcommittee on Jet-Propulsion Fuel 8 2003).

1.1.2 Local health effects

Dermal exposure to JP-8 has been associated with irritation and sensitization. Skin irritation is a non-immune related response that is caused by direct damage to the stratum corneum of the skin. This can result in redness of the skin, blisters, and scales. A common method of assessing damage to the skin is to measure the trans-epidermal water loss (TEWL). TEWL is the rate at which water vapor is lost from the skin; this has been used to determine the efficiency of the barrier function of the skin (Gioia and Celleno 2002). Damage done to the skin by chemical and/or physical agents causes the barrier function to be compromised, resulting in an increase of TEWL. Exposures to skin *in vitro* have shown elevated TEWL and erythema in pigs (Singh *et al.* 2003). Chemical exposures can also cause an immune-related response called allergic contact dermatitis. Aliphatic and aromatic components of JP-8 have been shown to increase expression of IL-8, IL-1 α, TNF-α, and MCP-1α in *in vitro* systems of human epidermal keratinocytes (Babu *et al.* 2004; Chou *et al.* 2003).

1.1.3 Systemic health effects

The systemic health effects of dermal exposure to JP-8 are not expected to be different from inhalation exposure. The immune system has been implicated as a potential target for JP-8 exposures (Rhodes *et al.* 2003). In this study, fuel system maintenance personnel had higher counts of white blood cells, neutrophils, and monocytes when compared to personnel in the low-exposure group (e.g., military police). The effects of JP-8 exposure on the central nervous systems has also been investigated in US Air Force employees (Smith *et al.* 1997). A significant association was found between JP-8 exposure and increased postural sway, suggesting subtle effects on vestibular/proprioception function.

The carcinogenic potential of exposure to jet fuel in humans has been suggested from population-based epidemiological studies (Parent *et al.* 2000; Siemiatycki *et al.* 1987). Siemiatycki *et al*. (1987) investigated, using a case-referent study design, the association between exposures to 12 petroleum derived liquids and cancers among 3726 subjects living in Montreal, Canada. The most relevant finding from this study was an association between jet-fuel exposure and kidney cancer, with an odds ratio (OR) of 3.4 [95% confidence interval (CI) = 1.5-7.6]. Other cancers associated with jet fuel were cancers of the colon and rectum. Cancer of the kidneys was confirmed in a study conducted by Parent *et al*. (2000). They used a case-control design consisting of 142 known cases of renal cell carcinoma, 1900 controls with cancer at other sites, and 533 population-based controls. Exposures were assigned using a questionnaire that asked questions about lifestyle and detailed descriptions of each subject's job history. Excess risk of renal cell cancer was associated with exposure to jet fuel (OR = 3.5, 95% CI = 1.4-8.7), aviation gasoline (OR = 3.5, 95% CI = 1.4-8.6), and jet fuel engine emissions (OR = 2.7, 95% CI = 0.9-8.1). Odds ratios were adjusted for respondent status (self or proxy), age, smoking, BMI, and occupational confounders (i.e., exposures to other substances like butadiene, styrene, chromium etc.). The main limitation of these epidemiological studies is that the exposures were assessed using self-reported information about each subject's occupation, and not from occupational hygiene measurements. Therefore, the route of exposure was not known and, thus, exposure assessment was subject to misclassification.

Numerous other studies exist showing the relationship between exposure to jet fuel and/or components thereof, and effects on the respiratory tract, nervous system, liver, kidney, cardiovascular system, reproduction and development, and genotoxicity. Many of these are summarized in the report by the subcommittee on JP-8 (Subcommittee on Jet-Propulsion Fuel 8 2003).

1.2 Dermal exposure assessment

The three main routes of human exposure to chemicals are inhalation, ingestion, and dermal absorption. In the past, exposure assessment has focused on inhalation exposures because it is considered the most important route of exposure. Consequently, many studies have been conducted to measure inhalation exposures and to examine consequent effects both locally and systemically. For the most part, the dermal route of exposure has been neglected, making it difficult to assess its importance relative to other routes of exposure like inhalation and ingestion (Semple 2004). Recent interest in dermal exposure assessment has been spawned by decreasing inhalation exposures to chemicals in the workplace. Hence, it is suggested that dermal exposures may be relatively more important in contributing to total body burden. This has motivated the occupational and environmental exposure assessment community to develop methods for understanding the process of dermal exposure so that dermal exposure to chemicals can be better evaluated and controlled. Such is the case for JP-8 on military bases. Very few studies of JP-8 exposures in the field exist. This section reviews the current state of knowledge regarding the measurement of dermal exposure to chemicals and to JP-8.

1.2.1 Conceptual model for dermal exposure assessment

Chemicals that deposit on the skin may undergo numerous processes that make assessment of exposure difficult. These processes include washing, evaporation, storage, and penetration. Simple measurement of the amount of chemical on the surface of the skin at one time-point will not capture the total amount of chemical deposited during a work shift, for example. Further, the exposure intensity, the surface area of skin exposed, the frequency of skin washing, the presence of clothing or protective equipment, and repeated exposures will modify the amount of chemical exposure.

Consequently, the variability in dermal exposures to chemicals necessitates a framework for assessing exposures.

A conceptual model has been proposed to aid in identifying the key processes of dermal exposure (Schneider *et al.* 1999). The model describes the transfer of contaminants among compartments, ultimately leading to dermal exposure. The main compartments are the source compartment, air, surface contaminant layer, outer clothing contaminant layer, inner clothing contaminant layer, and skin contaminant layer. The model describes the transport of the contaminant mass between compartments. Conversion into concentration takes into account the mass of the outermost skin layer plus all other substances. As a first approximation, this is the volume of bulk liquid for contaminants that have low volatility.

1.2.2 Sampling methods for measuring dermal exposure

As in any exposure assessment, sampling instruments are required to quantify the amount of chemical that one is exposed to. Preferably, the sampling instrument can accurately and precisely measure the intensity of exposure, and is simple enough for use in the field. Currently, there are numerous methods for measuring dermal exposures; most have focused on the sampling of the skin contaminant layer, as defined in the conceptual model described above.

There is no standard instrument to employ when measuring dermal exposure to chemicals. Rather, instruments are chosen based on properties of the chemical, such as molecular weight, solubility in water, and reactivity. The sampling instruments can be classified into three techniques based on surrogate skin, removal, and a fluorescent tracer (Fenske 1993). Surrogate skin techniques use patch sampling or whole-body sampling. In patch sampling, absorbent patches are placed under a worker's clothing prior to exposure. After exposure, the patches are removed and analyzed. In whole-body sampling, the objective is to measure the amount of chemical that is deposited on the clothing or skin. Workers are outfitted with overalls of certain material (e.g., cotton) before exposure; the overalls are analyzed using an appropriate method after exposure. The removal technique involves washing (Brouwer *et al.* 2000), wiping (Wheeler and Stancliffe 1998), or tape stripping (Loffler *et al.* 2004; Reddy *et al.* 2002) where part of the stratum corneum is stripped off and depth

profiling is possible. These techniques use solvents, gauze pads, or adhesive tapes to measure chemicals remaining on the skin after exposure. The third technique uses a fluorescent compound to determine the area of exposure and to quantify the mass deposited onto the skin (Cherrie *et al.* 2000); however, this technique is limited by cost and availability of equipment, and is not as widely used in the field as other techniques.

1.2.3 Measurement of dermal exposure to JP-8 in the workplace

Occupational exposure to JP-8 can occur quite frequently because JP-8 is the most common source of chemical exposure for military personnel. Exposures can occur during spills, transportation and storage of fuel, fueling, general maintenance and operation of aircrafts, cold engine starts, and performance testing (Subcommittee on Jet-Propulsion Fuel 8 2003). Personnel exposed during these scenarios are ground crew, fuelers, maintenance workers, general troops, and cleanup crew. Other scenarios where JP-8 exposure can occur are during the fueling of military tent heaters, and cleaning and degreasing with fuel. Inhalation exposure is highly possible during hot temperatures (e.g., during the Persian Gulf War). Inhalation exposures have been documented previously (Egeghy *et al.* 2003; Pleil *et al.* 2000). The work by Egeghy *et al*. (2003) used benzene and naphthalene as markers for exposure to JP-8. They found that dermal contact with JP-8 significantly contributed to the exposure of workers in the high-exposed group.

There is a paucity of field studies that have measured human dermal exposure to JP-8. Results of an acute dermal exposure study have been reported (Chao *et al.* 2005). The dermal exposure measurements were conducted using a tape-strip technique (Chao and Nylander-French 2004). This technique measured the amount of JP-8 in the stratum corneum of the skin from successive tape strips of the skin of the fuel-cell maintenance personnel (Chao *et al.* 2005). The mass of naphthalene did not change much between successive tape strips at the same site of exposure, suggesting that some components of JP-8 penetrated the skin. The average whole-body dermal exposure to naphthalene was 5.84 ± 1.34 $\ln(ng \cdot m^{-2})$ for the low-exposure group, 6.18 ± 1.35 $\ln(ng \cdot m^{-2})$ for the medium-exposure group, and 8.34 ± 2.23 $\ln(ng \cdot m^{-2})$ for the high-exposure group. Further study of the determinants of dermal exposure discovered that skin irritation, use of booties,

working inside the fuel tank, and the duration of JP-8 exposure were significant factors that explained whole body dermal exposure to JP-8. One of the limitations of this study was that only naphthalene was measured and not other components of JP-8. Thus, only a snapshot of JP-8 was taken, and dermal exposure to other components of JP-8 remains unknown.

1.3 Structure and Function of the Skin

While the assessment of dermal exposure involves measurement of the amount of chemical on the skin, it does not measure the amount of uptake into the body. However, chemicals deposited onto the skin can be absorbed into the skin to cause local effects, pass through the skin to cause systemic effects, or evoke allergic reactions both locally and systemically. As part of a dermal exposure assessment plan, it is important to understand the extent to which chemicals absorb into the skin and become systemically available. This will aid in the control of harmful exposures. The skin is composed of two layers: (1) the epidermis, which provides much of the barrier function, and (2) the dermis, which is a highly vascularized layer containing protein filaments, blood vessels, nerves, lymphatics, and epidermal appendages (Montagna and Parakkal 1974). The epidermis has further been divided into the outer layer called the stratum corneum and the inner layer called the viable epidermis. The sections below focus on the structure and function of the layers of the epidermis.

1.3.1 Structure and function of the stratum corneum

Traditionally, the stratum corneum was considered to be an inert and homogenous tissue (Montagna and Parakkal 1974). However, current research has shown that the stratum corneum is in fact structurally and biochemically complex (Harding 2004; Marks 2004). The stratum corneum is an approximately 15 μm thick membrane comprised of ordered corneocytes each less than 1 μm in thickness. The overall thickness of the stratum corneum depends on anatomical location, and can range from 5 μm in the scrotum to over 600 μm on the feet (Poet and McDougal 2002). Corneocytes originate from the keratinocytes of the basal layer of the viable epidermis through a process of programmed cell differentiation called keratinization. The corneocytes in the stratum corneum are connected by desmosomal proteins through lipids in the intercorneocyte space (Elias 1989; Kalinin *et*

al. 2001). The main lipids are ceramides (50% by mass), fatty acids (10-20% by mass), and cholesterol (25% by mass) (Madison 2003). The corneocytes embedded in the lipid lamellae make the stratum corneum hydrophobic.

The main function of the stratum corneum is to control the movement of materials in and out of the body. Of primary importance is the movement of water. Under normal circumstances, 0.5 L of water is lost through the stratum corneum each day; however, damage to the stratum corneum, as in psoriasis, can result in over 6 L lost per day (Marks 2004). Another important function is to prevent xenobiotics from entering into the body. The lipid lamellae, not the hair follicles and appendages of the stratum corneum, is believed to be the most important route of penetration for lipophilic chemicals (Marks 2004).

1.3.2 Structure and function of the viable epidermis

The viable epidermis consists of living cells with a proliferating basal layer. The four different cell types are keratinocytes, melanocytes, Langerhan's cells, and Merkel cells (Montagna and Parakkal 1974). The keratinocytes are metabolically active cells, which accumulate keratin as they differentiate into corneocytes of the stratum corneum. Melanocytes are cells that contain melanosomes, which produce melanin. Langerhan's cells are dendritic cells, which capture antigens and present them to lymphocytes for the initiation of an immune response (Elias 1989). Merkel cells occur in the basal layer and are the terminal points to sensory nerve endings. The overall thickness of the viable epidermis is from 50-100 μm depending on the location on the body. The viable epidermis is a relatively hydrophilic skin layer.

The viable epidermis has many more functions than the stratum corneum. One of these is protection from solar radiation. Melanin granules are formed within the melanocytes and transferred to the keratinocytes for absorption of UV radiation. The viable epidermis has an immunologic function via Langerhan's cells. The viable epidermis is also involved in transmission of sensory signals via Merkel cells. Of notable mention is the presence of both phase I and phase II metabolism enzymes in the viable epidermis, such as families of cytochrome P450, esterases, and β-glucoronidase

(Mukhtar 1992). The presence of these enzymes suggests that chemicals may be metabolized in the viable epidermis.

1.3.3 Studies of percutaneous absorption

Chemical exposures on the skin set up a concentration gradient between the surface and the richly perfused dermis. This gradient results in a transfer of mass that is dependent on the properties of the chemical and the layer(s) through which the chemical must traverse. The mass transfer, or flux, of chemical across a thin homogeneous membrane has been described by Fick in his first law, which states that:

$$J = -D \frac{\partial C}{\partial x} \quad (1)$$

where:

J is the flux of material across the membrane ($mg/cm^2 \cdot h$)

D is the diffusion coefficient (cm^2/h)

∂C is the concentration gradient across the membrane (mg/cm^3)

∂x is the thickness of the membrane (cm)

Assuming that there is no chemical in the dermis prior to exposure, the following expression for the permeability coefficient is defined (Moss *et al.* 2002):

$$K_p = \frac{J}{C} \quad (2)$$

where:

K_p is the permeability coefficient (cm/h)

J is the steady-state flux ($mg/cm^2 \cdot h$)

C is the concentration of chemical on the surface of the skin (mg/cm^3)

Both *in vitro* and *in vivo* studies have been conducted to estimate K_p values for various compounds (Borras-Blasco *et al.* 2004; Pillai *et al.* 2004; Venier *et al.* 2004).

The study of percutaneous absorption of chemicals *in vivo* in humans is difficult and few methods exist. One such method makes use of tracers (e.g., ^{14}C) and tracks the amount of the tracer retained in the body (plasma) or excreted in feces and urine (West *et al.* 1987). Another approach is to monitor the loss of material as it penetrates the skin (Wester and Maibach 1989). It is assumed that the difference between the applied dose and the residual dose is the amount of chemical absorbed. One method that is gaining popularity involves tape stripping of the stratum corneum. In this method, the chemical is applied to the stratum corneum for a short period of time, removed by successive tape applications, and urine/blood/feces are monitored to determine penetration across the skin (Rougier *et al.* 1987; Wester *et al.* 1998). The tape-strip method has also been used with Fick's law of diffusion to estimate permeability coefficients (Pirot *et al.* 1997; Reddy *et al.* 2002). This technique does not require sampling of biological media, such as urine and blood, but uses a quick and non-invasive tape-strip method to measure amounts of a chemical in successive layers of the stratum corneum. Hence both depth-profiling and time-course information is available to estimate dermal absorption parameters.

The ideal way to measure penetration of chemicals is by applying a chemical to human volunteers. Often, this is not feasible because many chemicals are too harmful to test in humans. More often, skin penetration tests have been conducted *in vivo* in animals or *in vitro* using diffusion cell systems. Popular animal models are the mouse, rat, rabbit, pig, and monkey (Poet and McDougal 2002). Animal studies have shown that the pig is the best model as it most closely predicts penetration of chemicals across human skin (Poet and McDougal 2002). More common is the use of diffusion cells with excised skin to study percutaneous absorption. The basic design is a donor cell wherein which the chemical is applied, a receptor cell into which the chemical is received, and a flap of skin that separates the two cells. The receptor solution (e.g., polyethylene glycol-20 oleyl ether and physiological saline) is sampled at various points in time and analyzed using analytical chemistry techniques, such as gas chromatography mass spectrometry (GC-MS) combined with head space solid phase microextraction (HS-SPME). Fick's law of diffusion is then used to mathematically

estimate the permeability coefficient. The advantage of these *in vitro* experiments is that they can be used to estimate the amount of a chemical penetrating across animal skin. However, their relevance to humans is inherently questionable because of the use of animal skin, skin viability, and perfusion of the skin *in vitro*. Nevertheless, this design has been widely used for penetration studies of metals (Larese Filon *et al.* 2004), chemical warfare agents (Chilcott *et al.* 2001), and drugs (Wagner *et al.* 2000).

The percutaneous absorption of JP-8 components has been characterized using diffusion cells (McDougal *et al.* 2000; Muhammad *et al.* 2004). McDougal *et al.* (2000) used male rat skin with surface area of 4.9 cm^2 to measure the permeability of JP-8 components. They used a mixture of polyethylene glycol-20 oleyl ether (6% Volpo 20) and saline as their receptor solution. The aromatic components of JP-8 had permeability coefficients that are significantly larger than the aliphatic components. For example, naphthalene had a permeability coefficient of $5.1x10^{-4}$ cm/h whereas dodecane had a permeability coefficient of $1.4x10^{-5}$ cm/h. Muhammed *et al.* (2004) also studied the permeation of JP-8 components using diffusion cells, but they improved on the work of McDougal *et al*. (2000) by using porcine skin. They measured permeability coefficients of $2.1x10^{-4}$ cm/h for naphthalene and $2.5x10^{-6}$ cm/h for dodecane, both smaller than reported by McDougal *et al*. (2000) for rat skin. *In vivo* studies of the percutaneous absorption of JP-8 components in humans have not been reported.

1.4 Mathematical descriptions of percutaneous absorption

In order to make predictions of the quantity of chemical that penetrates the skin, and is available for systemic circulation, a mathematical description is needed. This can be as simple as measuring the percent absorbed (Bronaugh and Franz 1986; Ross *et al.* 2004). However, the main limitation of measuring percent absorbed is that it is appropriate only under tightly controlled experimental conditions. In most situations, the process of absorption is non-linear with regard to length of exposure and concentration on the surface of the skin. In this section, several mathematical descriptions for percutaneous absorption of chemicals are examined.

1.4.1 Quantitative Structure-Activity/Permeation Relationship models

Quantitative Structure Activity Relationship (QSAR) models attempt to relate the biological activity of a chemical to its physicochemical and structural properties using statistical methods (Basak *et al.* 2003; Beliveau *et al.* 2003; Hawkins *et al.* 2004; Moss *et al.* 2002). The variables used for prediction of percutaneous absorption should be relevant to the particular diffusion process. Classical approaches have used three classes of descriptors: (1) hydrophobicity, (2) electronic properties, and (3) steric properties. Based on permeability studies, a predictive equation has been built for 93 compounds using the two descriptors: octanol-water partition coefficient (K_{ow}) and molecular weight (MW) (Guy and Potts 1992). The model has the following functional form:

$$\log(K_p) = 0.71 \times \log(K_{ow}) - 0.0061 \times MW - 6.3 \quad (3)$$

The R^2 was 0.67; however, Guy and Potts (1992) did not examine outliers and various Gauss-Markov assumptions, which state that (1) the expected value of the errors is zero, (2) all errors have the same variance, and (3) the errors are not correlated. Since then, further developments have included hydrogen bonding (Lien and Gao 1995) and melting point (Barratt 1995). The main weakness of QSAR models is that they treat the skin as one compartment, namely the stratum corneum, assuming that the viable epidermis presents relatively little barrier function to the percutaneous absorption of chemicals.

1.4.2 Two-compartment skin models

The composition of the stratum corneum and viable epidermis, both which a chemical must penetrate to become systemically available, is very different. The stratum corneum is comprised of dead cells and is very hydrophobic, whereas the viable epidermis is comprised of viable cells and is less hydrophobic. Thus, the application of Fick's law of diffusion may be inappropriate for chemicals that do not undergo diffusion via the lipid pathway but are transported through appendages (e.g., hair follicles) or undergo reactions with proteins. Also, a simple diffusion model may not be realistic for compounds that are held in the stratum corneum or viable epidermis such that there is a lag-time

before the compounds enter the blood. A more apt description of percutaneous absorption for such chemicals may be to treat the skin as two compartments with a different set of descriptors for each compartment.

Two-compartment models have been constructed in the past, and used to successfully predict exposures to chemicals (McCarley and Bunge 2001; Shatkin and Brown 1991). Two-compartment models treat the stratum corneum and viable epidermis differently. These models may also include a compartment representing the outer surface layer and a dermis layer that is highly vascularized and removes the chemical from the skin quite readily. The rate constants for the two-compartment model constructed by Shatkin and Brown (1991) are functions of the partition coefficients, the thicknesses of the skin compartments, the fat content, molecular weight of the chemical, and diffusivity coefficients. The limitation of the two-compartment models is that there are more parameters needed in the mathematical description of percutaneous absorption, and these parameters may not always be available for the compound of interest.

1.4.3 Physiologically based toxicokinetic models

The disposition of compounds that penetrate the skin and become available for systemic circulation can be described using physiologically based pharmacokinetic (PBTK) models. In PBTK models, the body is compartmentalized into various tissue groups, enabling the calculation of the tissue dose of parent chemical and metabolites. The parameters in a PBTK model are derived from relevant physicochemical, physiological, and biochemical properties of various tissues and the chemical of interest (Brown *et al.* 1997). Each compartment is described by a mass balance differential equation (MBDE), and the set of equations is solved using numerical methods. Further information about PBTK modeling, its history and application in chemical risk assessment can be found in recent reviews (Andersen 2003; Reddy *et al.* 2005).

1.4.4 Mathematical descriptions of the percutaneous absorption of JP-8

PBTK models have been developed for some JP-8 components (Perleberg *et al.* 2004; Quick and Shuler 1999; Willems *et al.* 2001). The decane model by Perleberg *et al*. (2004) was constructed for

inhalation exposure to decane in rats. They found that the toxicokinetic behavior of decane could not be adequately explained by a flow-limited system. Therefore, diffusion-limited equations were fit for brain, bone marrow, skin, fat, and spleen. Further, a PBTK model for inhalation, ingestion, intravenous dosing, and intraperitoneal injection of naphthalene has been constructed (Quick and Shuler 1999). This PBTK model consisted of 5 major tissue groups (lung, liver, fat, richly perfused tissue, poorly perfused tissue). Willems *et al*. (2001) built upon this work by constructing a PBPK model for exposures to naphthalene in rats and mice. All compartments except the blood compartment were treated as diffusion-limited. They examined the inhalation and intravenous routes of exposure. None of these models included the dermal route of exposure. Therefore, extrapolations to occupational exposure conditions are limited to inhalation exposures only.

1.5 Specific aims of this project

The primary objective of this project was to characterize the toxicokinetic behavior of aromatic and aliphatic hydrocarbons following dermal exposure to JP-8. This objective was met by collecting dermal exposure data and constructing mathematical models of the skin. A model was selected and expanded to include both the dermal and the inhalation routes of exposure. A secondary objective of this investigation was to integrate complex chemical exposure and biomarker data into a PBTK model that could be used to improve assessment of human health risks. The specific aims were:

Specific Aim 1: Examine the absorption and the penetration of JP-8 components across human skin *in vivo*, and contrast the results to rat or pig skin studies.

Specific Aim 2: Determine the structure of a mathematical model that optimally predicts the toxicokinetic behavior of aromatic and aliphatic hydrocarbons following dermal exposure to JP-8.

Specific Aim 3: Compare the contribution of dermal and inhalation exposures to the internal dose of naphthalene in the US Air Force personnel.

CHAPTER 2

DERMAL ABSORPTION AND PENETRATION OF JET FUEL COMPONENTS IN HUMANS

David Kim, Melvin E. Andersen, and Leena A. Nylander-French

Reprinted from Toxicology Letters, doi:10.1016/j.toxlet.2006.01.009, Kim D, Andersen ME, Nylander-French LA, Dermal absorption and penetration of jet fuel components in humans, Copyright (2006), with permission from Elsevier

2.1 Abstract

Jet Propulsion Fuel 8 (JP-8) is the largest source of chemical exposures on military bases. Dermal exposure to JP-8 has been investigated *in vitro* using rat or pig skin, but not *in vivo* in humans. The purpose of this study was to investigate the absorption and penetration of aromatic and aliphatic components of JP-8 in humans. A surface area of 20 cm^2 was delineated on the forearms of human volunteers and 1 ml of JP-8 was applied to the skin. Tape-strip samples were collected 30 min after application. Blood samples were taken before exposure (t = 0 h), after exposure (t = 0.5 h), and every 0.5 hour for up to 4 hours past exposure. The tape-strip samples showed evidence of uptake into the skin for all JP-8 components. The blood data was used to estimate an apparent permeability coefficient (K_p). The rank order of the apparent K_p was naphthalene > 1-methyl naphthalene = 2-methyl naphthalene > decane > dodecane > undecane. This rank order is similar to results from rat and pig skin studies. However, this study demonstrates that rat and pig models of the skin over predict the internal dose of JP-8 components in humans.

2.2 Introduction

Jet Propulsion Fuel 8 (JP-8) is the standard fuel for military aircrafts and vehicles, and is the single largest source of chemical exposure found on military bases of the NATO nations (Zeiger and Smith 1998). Possible adverse health effects associated with JP-8 include neurological effects and cancers (Babu *et al.* 2004; Parent *et al.* 2000; Rhodes *et al.* 2003; Siemiatycki *et al.* 1987; Smith *et al.* 1997). The main route of exposure inferred in these studies is inhalation; however, JP-8, which replaced JP-4, is less volatile and does not contain the lower molecular weight hydrocarbons found in gasoline. As a result, dermal exposure to JP-8 has been observed to affect the levels of urinary naphthalene metabolites, a biomarker of exposure to JP-8 (Chao *et al.* 2005; Chao *et al.* 2006). However, it is not well understood how chemical components of JP-8 are absorbed into the skin and how they become systemically available. Three types of study designs have been implemented to study dermal exposures to JP-8; these are field studies, *in vitro* experiments using excised skin, and *in vivo* studies using animal models.

Field studies of JP-8 use on military bases have identified sources of exposure as spills during transportation and storage of fuel, fueling, general maintenance and operation of aircrafts, cold engine starts, and performance testing (Subcommittee on Jet-Propulsion Fuel 8 2003). Inhalation exposures are evident during these work processes (Egeghy *et al.* 2003; Pleil *et al.* 2000), but skin as a route of exposure is less well-characterized as only one field study has measured human dermal exposure to JP-8 (Chao *et al.* 2005; Chao *et al.* 2006).

In order to estimate the amount of JP-8 that penetrates the skin, measurements of both the applied dose and the internal dose are needed. Diffusion cells and excised skin from animals have been used to estimate the extent of absorption and penetration of JP-8 components (Baynes *et al.* 2001; Kanikkannan *et al.* 2001a; Kanikkannan *et al.* 2001b; McDougal *et al.* 2000; Muhammad *et al.* 2004). McDougal *et al.* (2000) used male rat skin (surface area of 4.9 cm^2) and a mixture of polyethylene glycol-20 oleyl ether (6% Volpo 20) and saline as the receptor solution to measure the permeability of JP-8 components. They found that the aromatic components of JP-8 had permeability coefficients significantly larger than the aliphatic components. These results were confirmed in a pig-skin study (Muhammad *et al.* 2004).

Although *in vitro* studies are valuable for determining the permeation rates and the amount that is available for systemic circulation, they need validation under *in vivo* conditions to be usable in risk assessment. However, few studies of *in vivo* exposures to JP-8 exist. One of these exposed weanling pigs to 0.5 ml of JP-8 over an area of 3.14 cm^2 for 0.5 h (Singh *et al.* 2003). They found that more hexadecane (0.43 %) than xylene (0.17%) or heptane (0.14%) was absorbed into the skin after 0.5 h exposure. Blood measurements were not made, so permeability coefficients could not be calculated for comparison to *in vitro* experiments.

The primary objective of our study was to examine the absorption and penetration of JP-8 components across human skin after the fuel was applied to the forearms of human volunteers. Building upon the results of previous studies (Chao and Nylander-French 2004; McDougal *et al.* 2000; Muhammad *et al.* 2004; Singh *et al.* 2003), an appropriate blood sampling regimen was established for the current study to examine the amount of chemical that penetrates the skin and becomes systemically available. The study design incorporated a validated tape-strip technique to quantify concentrations in the stratum corneum (Chao *et al.* 2005; Chao and Nylander-French 2004). The main hypothesis of the current study is that single-dose application data from controlled human exposures to jet fuel can be used to quantify the absorption and penetration of aromatic and aliphatic components of JP-8 for humans *in vivo*.

2.3 Methods

2.3.1 Study volunteers

Ten healthy adult volunteers (5 males and 5 non-pregnant females) with no occupational exposure to jet fuel were recruited for participation. No restrictions on age, race, gender, or skin type were applied other than that the group was to be equally divided between males and females. If volunteers had a history of cardiovascular disease or atopic dermatitis, were current smokers, or were on prescription medication for a current or chronic illness, they were excluded from the study. Volunteers were not permitted to drink any alcoholic beverages 24 hours before or during the experiment. Individuals occupationally exposed to compounds chosen to represent JP-8 were also excluded (e.g., auto mechanics). Approval for this study was obtained from the Office of Human

Research Ethics (School of Public Health, The University of North Carolina at Chapel Hill, Chapel Hill, NC). Informed consent was received from all study volunteers.

2.3.2 General procedure

Upon arrival at the laboratory, the study volunteer was given a protective laboratory coat that was worn for the duration of the experiment. A passive monitor was attached to the lapel of the volunteer to monitor levels of JP-8 in the personal breathing zone. The volunteer's forearms were examined for obvious skin defects (abrasions, inflammation) that could enhance or impair the penetration of JP-8. The exposure chamber shown in Figure 1 (20.3 cm width $\times$ 20.3 cm length $\times$ 18.8 cm height and total volume of 7706 cm^3) was placed inside a fume hood to prevent possible inhalation of JP-8. After the volunteer was seated comfortably, one forearm was placed palm up inside the exposure chamber, and two aluminum application wells (dimensions 2.5 cm $\times$ 4.0 cm = 10 cm^2 per well) were pressed against the skin to prevent JP-8 from spreading during the experiment. The exposure chamber was sealed for the duration of the experiment (0.5 h).

At the end of the 0.5 h exposure period, the two exposed skin sites were wiped with a gauze pad and tape-stripped as many as 10 times. Tape strips were placed in 10 ml of acetone containing 1 μg/ml of internal standards (naphthalene-d_8). All tape-strip samples were stored in 20 ml vials (I-CHEM, Rockwood, TN) and refrigerated at 4°C. Blood samples were drawn from the unexposed arm at baseline, 0.5 h, 1 h, 1.5 h, 2 h, 2.5 h, 3 h, and 3.5 h and collected in 6 ml test tubes containing sodium heparin (Vacutainer, Franklin Lakes, NJ). The blood samples were transferred to 15 ml centrifuge tubes (Fisherbrand, Pittsburgh, PA) and stored at -80°C until analysis.

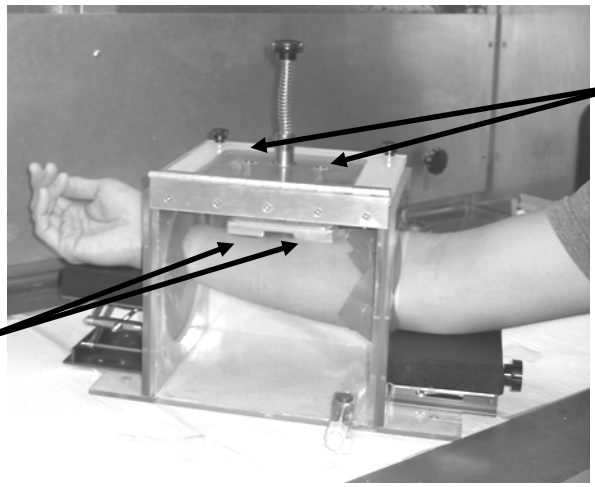

Figure 1. Schematic of the exposure chamber and aluminum application wells. The exposure was done inside a fume hood to prevent inhalation exposure to JP-8 components.

2.3.3 Dosing

The volume of JP-8 to be applied to the skin in order to have sufficient concentrations in blood was estimated using the limit of detection (LOD) of a published analytical method and estimates of permeability coefficients from an *in vitro* study (McDougal *et al.* 2000; Waidyanatha *et al.* 2003). Although the method by Waidyanatha *et al*. (2003) was developed for the analysis of naphthalene in urine, a similar LOD (5.0×10^{-4} ng/ml) was assumed to apply for blood samples. Three times the LOD was assumed to be adequate for detection in blood. A permeability coefficient of 5.1×10^{-4} cm/h was used to back extrapolate to surface levels of JP-8. It was determined that 1 ml of JP-8 should produce measurable blood concentrations. Neat JP-8 was applied to the volar forearm using a 0.5 ml gas-tight syringe through two openings on top of the exposure chamber; 0.5 ml was applied to each of two wells for a total of 1.0 ml JP-8 on an area of 20 cm^2. Upon application, the openings were sealed to prevent loss from the chamber.

2.3.4 Tape-strip samples

Adhesive tape strips (Cover-Roll™ tape; Beiersdorf, Germany) with dimensions 2.5 cm × 4.0 cm (10 cm^2) were used to remove skin containing JP-8 from the stratum corneum. The tape strips had

the same dimensions as the aluminum application wells. Clean forceps were used to remove each tape strip without cross-contamination; the time it took to apply and remove 10 tape strips was recorded. To minimize pressure-induced vasodilation, no direct pressure was applied to the exposed sites during the exposure, tape strip was applied to the skin by one finger stroke with sufficient minimal pressure to adhere the tape to the skin, and forceps were used to remove the tape. This tape-strip method has been previously validated for multifunctional acrylates and jet fuel (Chao and Nylander-French 2004; Nylander-French 2000). Tape-stripping has also been used in dermatopharmacokinetic studies of therapeutic agents (Loden *et al.* 2004; Shah 2001; Shah *et al.* 1998).

2.3.5 Chemicals

Six aromatic and aliphatic components of JP-8 were investigated in this study. The aromatic components were naphthalene, 1-methyl naphthalene, and 2-methyl naphthalene, and the aliphatic components were decane, undecane, and dodecane. These aromatic and aliphatic components were chosen because they represent the most abundant hydrocarbons in JP-8 by mass percentage (McDougal and Rogers 2004). The reagents naphthalene, 1-methyl naphthalene, 2-methyl naphthalene, decane, undecane, and dodecane were purchased from Sigma-Aldrich (St. Louis, MO). Napthalene-d_8 and dodecane-d_{26} (internal standards) were purchased from Cambridge Isotope Laboratories (Andover, MA). Acetone and methanol (HPLC grade) were purchased from Sigma-Aldrich (St. Louis, MO). JP-8 was collected for U.S. EPA directly from bulk storage at Warner Robins Air Force Base, Georgia. Chemical characterization of this fuel was determined by dissolving 1 µl of fuel in 10 ml of acetone with internal standard. The physico-chemical properties of the three aromatic and three aliphatic compounds analyzed in this study are shown in Table 1.

Table 1. Physico-chemical properties of naphthalene, 1-methyl naphthalene, 2-methyl naphthalene, decane, undecane, and dodecane. Permeability coefficients (K_p) are taken from McDougal *et al.* (2000).

Property	Naphthalene	1-methyl Naphthalene	2-methyl Naphthalene	Decane	Undecane	Dodecane
			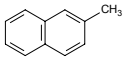			
Chemical formula	$C_{10}H_8$	$C_{11}H_{10}$	$C_{11}H_{10}$	$C_{10}H_{22}$	$C_{11}H_{24}$	$C_{12}H_{26}$
MW (g/mol)	128.3	142.2	142.2	142.3	156.3	170.3
Concentration in JP-8 (mg/ml)	3.0	2.5	2.1	28.3	111.2	102.9
K_p (cm/h)	$5.1x10^{-4}$	$1.6x10^{-4}$	$1.6x10^{-4}$	$5.5x10^{-5}$	$2.5x10^{-5}$	$1.4x10^{-5}$

2.3.6 Chemical analysis

Personal breathing-zone (PBZ) samples were thermally desorbed with a Perkin Elmer automatic thermal desorption (ATD) 400 system (Perkin Elmer, Norwalk, CT) for 2 min at 225°C onto a cold trap. The cold trap was subsequently heated to 225°C and transferred to a transfer line at 200°C. The samples were analyzed with a Hewlett Packard 6890 Series II gas chromatograph (GC) equipped with a DB-1 column (60 m × 0.53 mm × 1.5 µm; J&W Scientific, Folsom, CA) and a photoionization detector (PID; HNU Systems, Inc., Newton, MA). The GC oven conditions were as follows: 40°C for 5 min, 10°C/min to 75°C, 5.5°C/min to 175°C, and 50°C/min to 260°C for 6 min.

Tape-strip samples were analyzed by gas chromatography mass spectrometry (GC-MS). A Thermoquest Trace GC (Thermo Electron Corporation, Austin, TX) coupled with a Combi Pal autosampler (CTC Analytics, Zwingen, Switzerland) and a Finnigan Polaris Q quadrupole ion trap MS (Thermo Electron Corporation, Austin, TX) in electron ionization mode, was used for the chemical analysis. Separation of the sample was done with a fused-silica capillary column coated with a mixture of 5% diphenyl/95% dimethyl polysiloxane (30 m × 0.25 mm × 0.25 µm; RTX-5MS, Restek

Corporation, Bellefonte, PA). The oven temperature was 40°C (3 min) and then 10°C/min to 290°C (10 min). About 1 µl of sample was directly injected into the inlet. The injector and auxiliary temperatures were kept at 280°C and 300°C, respectively. Samples were injected in the splitless mode; the split valve was kept closed for 2 min. Helium was used as the carrier gas (1.0 ml/min) with vacuum compensation enabled. The MS conditions were as follows: source temperature 200°C; full-scan mode (60-160 amu) with electron impact ionization (70 eV). The ions used for quantitation were m/z 128 (naphthalene), 142 (1-methyl and 2-methyl naphthalene), 136 (naphthalene-d_8), 71 (n-decane, n-undecane, n-dodecane), and 98 (dodecane-d_{26}). The number of microscans was set at 2 and the max ion time at 200 ms. Samples were quantified using an 11-point calibration curve with concentrations ranging from 0 to 11 µg/ml. A typical chromatogram for a tape-strip sample is shown in Figure 2.

Blood samples were analyzed using head-space solid-phase microextraction (HS-SPME) and the GC-MS system described above. Modifications were made from published methods (Cardinali *et al.* 2000; Waidyanatha *et al.* 2003). Briefly, whole blood (1 ml) was added to a 10 ml headspace vial with crimp top (Microliter, Suwanee, GA) containing 3 ml of deionized water, 2 g of NaCl, and 2 µl of 5 ng/ml internal standard. The vial was put into an aluminum block (CTC Analytics, Zwingen, Switzerland) for heating and agitating at 45ºC and 250 rpm (1 min). A 100 µm polydimethyl-siloxame (PDMS) fiber (Supelco, Bellefonte, PA) was inserted into the head-space of the vial for 20 min. The needle containing the SPME fiber was withdrawn and introduced into the inlet of the GC for 20 min. The inlet temperature was set at 230°C; an IceBlue septum (Restek, Bellefonte, PA) and a liner with an internal diameter of 0.8 mm (SGE, Austin, TX) were used. All other GC-MS conditions were the same as for the analysis of tape-strip samples. Quantification was carried out using an 8-point calibration curve ranging from 0 to 3 ng/ml. A typical chromatogram for a blood sample is shown in Figure 3. Much cleaner chromatograms were obtained from blood samples relative to tape-strip samples because of the use of the SPME device.

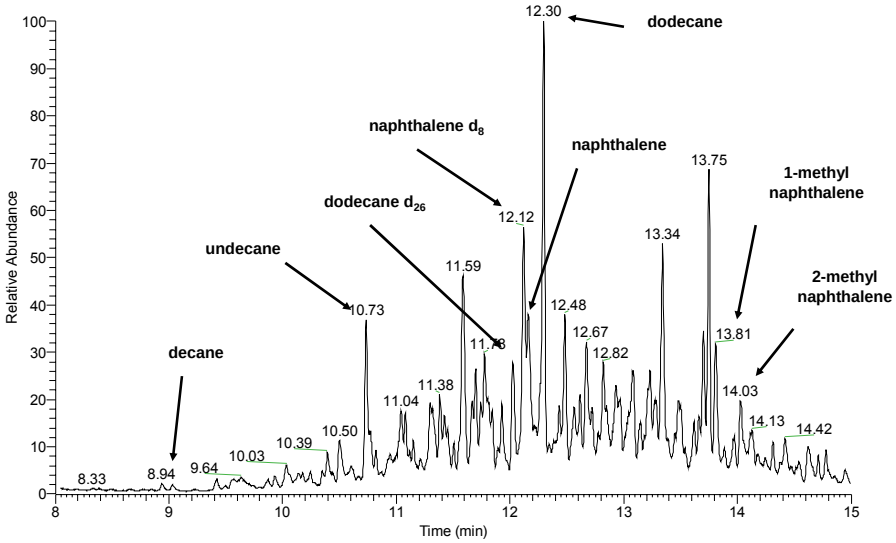

Figure 2. MS chromatogram (total ion count) from the first tape-strip sample collected from one study volunteer.

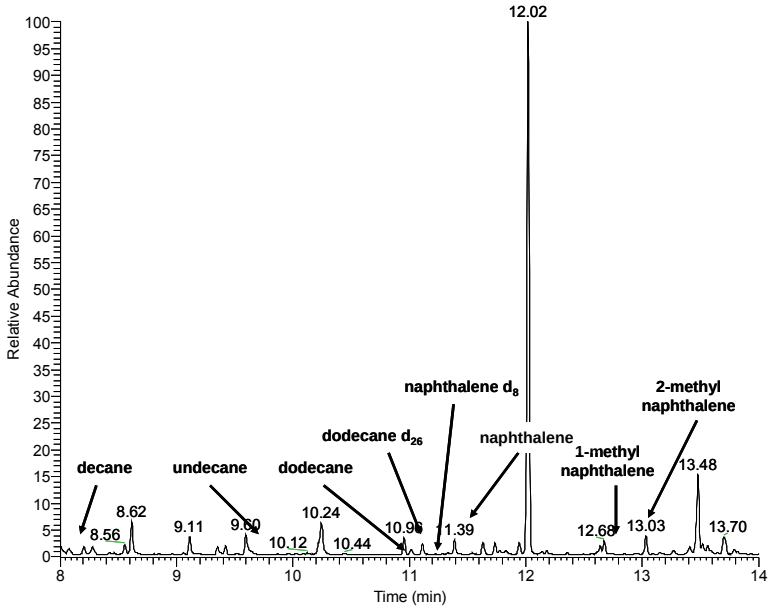

Figure 3. MS chromatogram (total ion count) from one blood sample. This blood sample was collected 1 hour after the end of exposure. The cleaner spectrum compared to the tape-strip sample in Figure 2 is due to the use of the HS-SPME device.

2.3.7 Data analysis

Exploratory analyses of skin and blood concentrations of JP-8 components were conducted using descriptive statistics. The skin and blood concentrations were plotted as functions of time. The first tape strip was not included in these plots because of potential residual contamination from the dose applied to the skin (Pershing *et al.* 2002; Pershing *et al.* 2003; Shah 2001; Shah *et al.* 1998). The volume of blood was estimated using allometric relationships (Davies and Morris 1993). The equation is Volume of blood (V_b) = 72.447 $\times$ (body weight in kg)$^{1.007}$. V_b was used to estimate the total mass of naphthalene, 1-methyl naphthalene, 2-methyl naphthalene, decane, undecane, and dodecane in the blood of each volunteer. The steady state flux (J, μg/cm^2 per h) was estimated from the slope of the linear portion of the cumulative mass per cm^2 *vs.* time curve. The slope of the curve during the uptake period (i.e., exposure duration) was estimated for each subject. The permeability coefficient (K_p, cm/h) was estimated by dividing the flux by the concentration of the chemical ($C_{JP\text{-}8}$, μg/cm^3) in the 1 ml of JP-8 that was applied to the skin (McDougal and Boeniger 2002):

$$K_p = \frac{J}{C_{JP-8}} \tag{4}$$

Our study design for humans is similar to *in vitro* studies that have used static diffusion cells. A chamber (i.e., donor cell) was used that sealed the exposure region. Blood samples were collected from the opposite arm to the one used for exposure (i.e., receptor cell). The main differences between our study and static diffusion-cell experiments were: (1) the duration of exposure was limited to 0.5 h, (2) real human skin was used, thus introducing variability in structure and content of the different layers of skin, (3) the volume of the blood could not be controlled but was inferred by allometric relationships, and (4) compounds underwent elimination from the central compartment (i.e., receptor cell). These differences will affect the estimates of K_p made *in vivo*. To distinguish K_p estimated in our study from K_p estimated *in vitro*, we will call it the "apparent K_p" from here on.

2.4 Results

2.4.1 Study volunteers

The average age of the volunteers was 27, which ranged from 21 to 37 years old. Seven of the study volunteers were Caucasians, one Asian, one African American, and one was mixed Asian-Caucasian. The mean body mass index (BMI) was 21 kg/m^2 and ranged from 19-25 kg/m^2. Further information about the study volunteers is reported in Table 2. All PBZ samples were below the limit of quantitation reported by Egeghy *et al*. (2003).

Table 2. Demographics of the study population.

Volunteer	Age	Gender	Ethnicity	Height (ft, in)	Weight (lbs)	*Volume of blood (L)	Main mode of transportation	Creams/lotions used
1	23	M	Caucasian	6' 0"	185	6271	bus and car	none
2	34	M	Asian	5'7"	123	4157	car	none
3	22	F	Black	5' 4"	116	3919	bus	lotion
4	24	F	Caucasian	5' 3"	125	4225	bus	none
5	28	M	Caucasian	6' 2"	160	5418	car	none
6	24	M	Caucasian	6' 3"	185	6271	car	none
7	37	M	Caucasian	5' 10"	140	4736	car/motorcycle	none
8	32	F	Caucasian	5' 8"	130	4396	car	Keri skin
9	24	F	Caucasian	5' 5"	120	4055	bus/car	Jason organic honey
10	21	F	Asian-American	5' 9"	155	5247	walk/car	Bath & Body works

*Volume of blood = 72.447 x (body weight in kg)$^{1.007}$ (Davies and Morris, 2003)

2.4.2 JP-8 characterization

The composition of JP-8 varies from batch to batch (McDougal *et al.* 2000). The weight percent of the aromatic and aliphatic hydrocarbons in the sample of JP-8 used in this study were 0.3% naphthalene (3.0 mg/ml), 0.3% 1-methyl naphthalene (2.5 mg/ml), 0.2% 2-methyl naphthalene (2.1 mg/ml), 3.3% decane (28.3 mg/ml), 12.8% undecane (111.2 mg/ml), and 11.8% dodecane (102.9 mg/ml). Compared to the sample analyzed by McDougal *et al.* (2000), this batch contained a higher

fraction of undecane (111.2 mg/ml *vs.* 48.4 mg/ml) and dodecane (102.9 mg/ml *vs.* 36.1 mg/ml), and a lower fraction of 1-methyl and 2-methyl naphthalene (4.6 mg/ml *vs.* 9.9 mg/ml).

2.4.3 Skin absorption

After the 0.5 h exposure to JP-8, the remaining jet fuel was wiped off the surface of the skin and successive tape strips were used to sample different depths of the stratum corneum. The mass per cm^2 of naphthalene, 1-methyl naphthalene, 2-methyl naphthalene, decane, undecane, and dodecane in each of the tape strips are reported in Table 3. The mass from each of the two exposure sites were combined to estimate the average total mass per cm^2 of exposure for each component of JP-8. The results show that JP-8 was absorbed into the skin during the 0.5 h exposure period as all compounds were quantifiable in the tape-strip samples. As expected, the mass per cm^2 for each chemical decreased rapidly with successive tape strips. The highest mass per cm^2 was found in the first tape strip. The rapid reduction in mass with depth is shown graphically in Figure 4. The aromatic compounds were quantifiable in all tape-strip samples. Similarly, undecane and dodecane were quantified in all tape-strip samples. Decane showed a very different pattern. Decane was not quantifiable after the 4th tape strip. Therefore, the plot in Figure 4 quickly reached an asymptotic value.

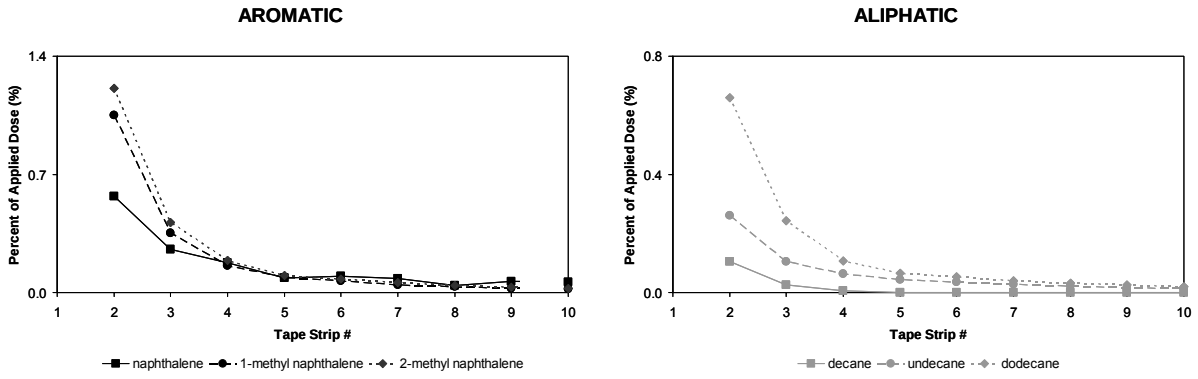

Figure 4. Percent of applied dose (mean) plots for aromatic and aliphatic hydrocarbons by tape-strip number. The first tape strip was not included in these plots because of potential residual contamination from the dose applied to the skin.

Table 3. Mass per area (μg/cm^2) of aromatic and aliphatic hydrocarbons in tape strips.

	Naphthalene		*1-Methyl Naphthalene*		*2-Methyl Naphthalene*	
Tape Strip	Mean	SD	Mean	SD	Mean	SD
1	216.1	126.5	304.4	101.6	283.3	91.4
2	17.1	10.3	26.3	20.8	25.4	19.6
3	7.6	3.7	8.9	6.7	8.7	7.0
4	5.3	5.0	4.0	2.6	4.0	2.4
5	2.6	1.0	2.2	1.1	2.1	1.1
6	3.0	3.4	1.7	0.8	1.7	0.8
7	2.5	3.4	1.1	0.8	1.2	0.7
8	1.3	0.7	0.9	0.6	0.9	0.6
9	2.0	3.3	0.6	0.6	0.7	0.5
10	1.8	3.2	0.5	0.4	0.5	0.3
	Decane		*Undecane*		*Dodecane*	
Tape Strip	Mean	SD	Mean	SD	Mean	SD
1	237.0	213.2	4032.7	2233.7	7277.0	1971.2
2	29.7	29.9	291.0	237.4	678.7	587.0
3	7.3	6.7	115.9	43.3	249.5	192.2
4	1.4	4.6	71.1	26.9	110.5	54.2
5	ND	-	47.3	17.1	67.4	26.6
6	ND	-	39.5	11.5	54.2	16.4
7	ND	-	29.8	9.3	40.8	9.6
8	ND	-	24.8	6.7	33.2	8.3
9	ND	-	18.1	4.4	26.7	5.5
10	ND	-	15.1	3.5	20.5	3.7

SD = Standard Deviation
ND = None Detected

2.4.4 Skin penetration

Figure 5 shows the cumulative mass of compound in blood per cm^2 of exposed area *vs.* time plot for one volunteer. We observed that the flux of the aliphatic components was greater than the flux of the aromatics because the concentration of the aliphatics in JP-8 was more than an order of

magnitude greater than the concentration of the aromatics. The slopes of the curve for aromatic compounds began to decrease at 120 min but did not reach zero. For undecane and dodecane, the cumulative blood mass per cm^2 continued to increase throughout the 4 h observation period. Across compounds, the linear portion of the graph occurred between 0 and 60 min with no evidence of a lag-time; therefore, these time points were used for estimating the apparent K_p. Individual estimates of the apparent K_p from all volunteers are summarized in Table 4. The apparent K_p was calculated for each volunteer and component of JP-8, assuming the absorbed compounds were restricted to the blood compartment in the body. The mean apparent K_p in decreasing order is naphthalene > 1-methyl naphthalene = 2-methyl naphthalene > decane > dodecane > undecane. A Student's *t*-test for comparison of the apparent K_p estimates for 1-methyl naphthalene and 2-methyl naphthalene showed no statistically significant difference ($p > 0.05$).

Table 4. Apparent permeability coefficients (cm/h) of aromatic and aliphatic hydrocarbons for each study volunteer.

Volunteer	Naphthalene	1-methyl Naphthalene	2-methyl Naphthalene	Decane	Undecane	Dodecane
1	1.6E-04	1.3E-05	5.3E-05	8.5E-06	2.1E-07	1.3E-06
2	3.4E-05	2.8E-05	3.1E-05	8.6E-06	3.6E-07	1.5E-06
3	3.2E-05	3.1E-05	3.0E-05	7.6E-06	2.3E-07	3.0E-06
4	3.7E-05	2.7E-05	3.2E-05	1.2E-05	2.5E-07	2.0E-06
5	5.4E-05	2.8E-05	2.9E-05	3.3E-06	6.7E-07	1.3E-06
6	5.7E-05	3.3E-05	3.0E-05	8.0E-06	4.8E-07	1.5E-06
7	4.1E-05	3.1E-05	3.0E-05	7.1E-06	3.3E-07	1.5E-06
8	4.1E-05	2.9E-05	3.1E-05	5.6E-06	4.1E-07	1.3E-06
9	3.3E-05	3.1E-05	3.0E-05	2.2E-06	7.6E-07	1.1E-06
10	4.2E-05	3.5E-05	2.8E-05	2.0E-06	8.3E-07	1.2E-06
mean	5.3E-05	2.9E-05	3.2E-05	6.5E-06	4.5E-07	1.6E-06
SD	3.8E-05	5.9E-06	7.4E-06	3.3E-06	2.3E-07	5.6E-07
minimum	3.2E-05	1.3E-05	2.8E-05	2.0E-06	2.1E-07	1.1E-06
maximum	1.6E-04	3.5E-05	5.3E-05	1.2E-05	8.3E-07	3.0E-06

SD = Standard Deviation

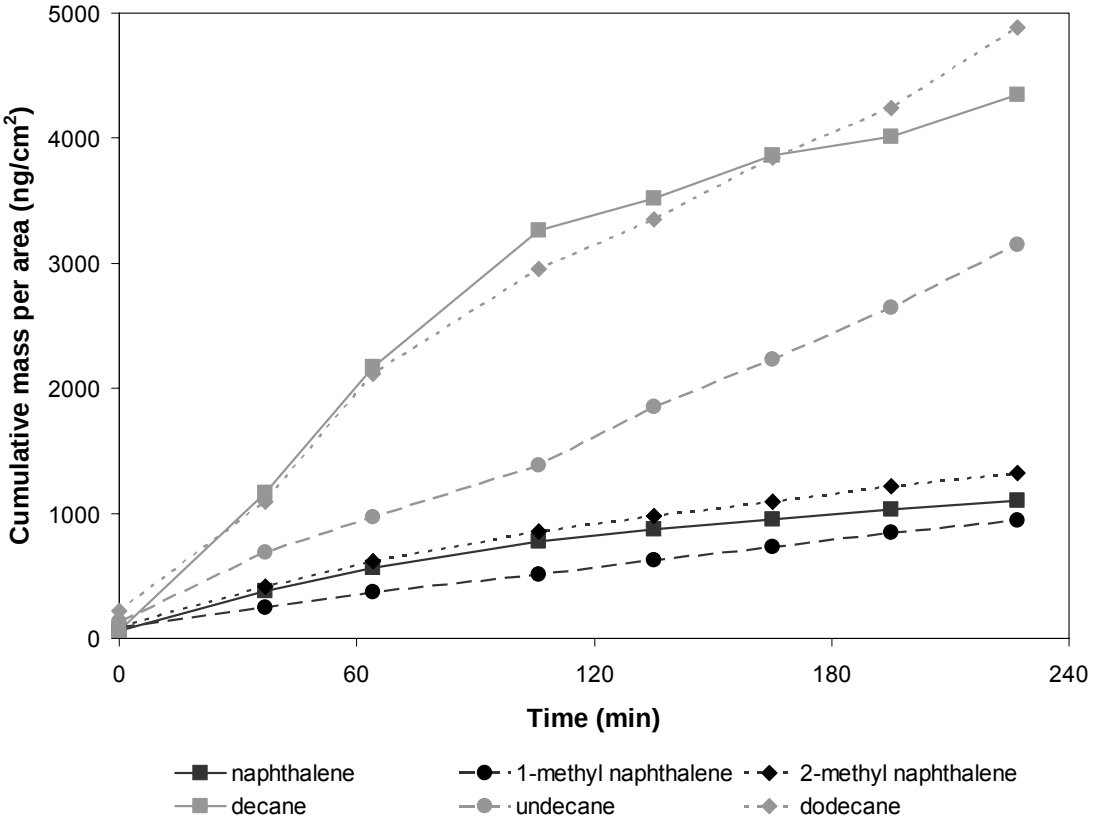

Figure 5. The time courses of the cumulative mass of aromatic and aliphatic hydrocarbons in blood per cm^2 of exposed skin area for one study volunteer. The slope (i.e., flux) was divided by the concentration of the specific chemical in JP-8 to estimate the apparent permeability coefficient. The apparent permeability coefficient was estimated using the first three data points for each chemical.

2.5 Discussion

Chemicals placed on the skin undergo absorption into the stratum corneum and evaporation from the surface of the skin. After absorption, the chemicals may be stored in deeper layers of the stratum corneum or in the viable epidermis, or they may penetrate into the dermis for eventual movement into the systemic circulation. Some absorbed compound may also transfer back to the skin surface and evaporate into the surrounding air. While instruments and techniques (e.g., washing, wiping, tape-stripping, biological monitoring) exist for measuring dermal exposures, the amount of uptake into the human body and the dose available for systemic circulation are not well understood and are often inferred from *in vitro* and *in vivo* studies using animal models. The current study was conducted to

determine whether the process of absorption and penetration across the human skin can be described in humans using a non-invasive tape-strip method combined with trace analytical techniques.

The skin is composed of two main layers: (1) the epidermis, which provides much of the barrier function and (2) the dermis, which is a highly vascularized layer containing fibrous proteins, blood vessels, nerves, lymphatics, and epidermal appendages (Montagna and Parakkal 1974). The epidermis consists of the hydrophobic layer called the stratum corneum and the hydrophilic layer called the viable epidermis. Measurement of the amount of chemical on (or in, which is intended here) the surface layer of the skin will give an indication of how rapidly the mass of chemical is reduced from this layer. Successive tape-strip samples give an indication of the depth of absorption as well as some indication of the rate of absorption (Loffler *et al.* 2004; Reddy *et al.* 2002; Surber *et al.* 1999). In our study, tape-stripping was conducted to better understand the absorption of JP-8 components into the skin. Our results suggest that there is absorption of both aromatic and aliphatic components of JP-8, as components were detected as deep as the 10^{th} tape-strip sample.

It is well known that the mass of stratum corneum removed decreases with successive tape-strip samples collected at the same site (Jacobi *et al.* 2005). Hence in our study, the decreasing mass of the chemical measured per tape strip may be the result of the decreasing mass of stratum corneum removed with increasing number of tape strips. In this study, we found that the mass of the chemical on the last tape strip was less than 1% of the mass measured on the first tape strip, suggesting that there is little mass of the chemical left in deeper layers of the stratum corneum. The mass of stratum corneum harvested using tape strips does not decrease as appreciably (Jacobi *et al.* 2005). Therefore, we conclude that, because we detected very little chemical in the deeper layers of the stratum corneum, the residence time in the stratum corneum was not very long.

McDougal *et al.* (2000) also quantified the amount of JP-8 components remaining in the skin after the diffusion-cell experiment was completed. They were able to measure only 6 components (nonane, decane, undecane, dodecane, tridecane, and tetradecane). These compounds are aliphatic with high octanol:water partition coefficients. In a separate experiment, they measured the presence of dibromomethane (a volatile compound) and found that evaporative loss from skin was negligible

based on a mass balance study. They suggested that evaporative losses could not be the reason for not being able to detect the aromatic components in the skin. It is possible that the straight chain compounds may be stored in deep layers of the skin prior to becoming available for systemic circulation. This is consistent with the results from our study. We noticed that, for some volunteers, the blood concentration for aliphatic compounds continued to increase after the 2nd blood sample was collected; this was not observed for aromatic compounds. Further, decane could not be quantified beyond the 4th tape strip, suggesting a short residence time in the stratum corneum. These results suggest that aliphatic compounds may be stored in deeper skin layers.

Our results were comparable to results from *in vitro* studies that measured the permeability coefficients of aromatic and aliphatic components of JP-8. Aromatic compounds were estimated to have apparent K_p values an order of magnitude larger than aliphatic compounds. Further, naphthalene was estimated to have the largest apparent K_p. The relative order of apparent K_p values in terms of magnitude were similar to the results reported by McDougal *et al.* (2000). The only exception was undecane, which had the smallest apparent K_p. Our results are also similar to Muhammad *et al.* (2004) who reported K_p estimates for naphthalene and dodecane of 2.1×10^{-4} cm/h and 2.5×10^{-6} cm/h, respectively. These estimates may be more comparable to our study because they used pig skin, which is a more widely accepted model for human skin.

Our apparent K_p values are smaller by an order of magnitude than K_p values estimated using diffusion cells. The most likely reason for this difference is our assumption that all absorbed fuel components are retained in the blood compartment. More accurate estimates will be possible using a pharmacokinetic model that describes the absorption, distribution and elimination of these components in the body. Nonetheless, some differences might be expected between human and other species. Rat skin has been suggested to be more permeable than human skin (McDougal *et al.* 2000). Pig skin, although a well-accepted model for studying human dermal absorption and penetration (Wester *et al.* 1998), overestimates the permeation of compounds across human skin. This was demonstrated in a study of caffeine and testosterone across human epidermal sheets, pig skin, and the reconstructed skin EpiDerm™ and SkinEthic® (Schreiber *et al.* 2005). In addition, although pig skin is a better model of human skin than rat skin, its physiology is equivalent to that of a

young child (Bronaugh and Maibach 1999). Reconstituted skin models, although an appealing alternative, are not regarded as useful for *in vitro* penetration studies mainly due to weak barrier properties when compared to fresh human skin, and equivalent or inferior to mouse, rat, and pig skin (Schmook *et al.* 2001). While a smaller value of K_p in humans versus these other model systems is not unexpected, the 10-fold difference is certainly an overestimate of the species differences in this parameter.

Principles from Fick's Law of Diffusion can be used to estimate the total amount of chemical that might penetrate across a permeable membrane. Fick's Law of Diffusion states that the flux across a membrane is proportional to the concentration gradient across that membrane. From this Law, one can derive the following expression to estimate the internal dose (M) of a chemical (McDougal and Boeniger 2002):

$$M = K_p \times C_{JP\text{-}8} \times A \times t \qquad (5)$$

where A is the area of exposure and t is the duration of exposure. The amount of chemical that might penetrate the skin for an exposure scenario of 1 h on both hands (840 cm^2) can be estimated with this equation. To illustrate, we use K_p values determined from rat skin, pig skin, and our study to estimate the internal dose of naphthalene: M_{rat} = 1.29 mg, M_{pig} = 0.53 mg, and M_{human} = 0.13 mg. The K_p from rat skin overestimates human internal dose by a factor of 10, and the K_p from pig skin by a factor of 4. An individual who is exposed on the hands only must be exposed to JP-8 for 10 hours in order to have the same internal dose estimated using the rat K_p.

In summary, our study demonstrates that it is possible to quantify the absorption and penetration of individual components of JP-8 across human skin *in vivo*. Our results are similar to *in vitro* studies that use diffusion cells and pig skin. Our tape-strip data showed evidence of absorption of naphthalene, 1-methyl naphthalene, 2-methyl naphthalene, decane, undecane, and dodecane, although decane seemed to disappear faster from the surface of the stratum corneum. We estimated that aromatic components of JP-8 penetrate faster than the aliphatic components. We showed that the flux of the aliphatic components is greater than the flux of the aromatic components because the

concentration of the aliphatics in JP-8 is more than an order of magnitude greater than the concentration of the aromatics. Our overall estimates of the apparent K_p were smaller than the *in vitro* estimates. Consequently, our study shows that permeability coefficients estimated *in vitro* may overestimate the internal dose of various components of JP-8. The results of our study need to be interpreted with caution because *in vitro* systems do not account for clearance mechanisms, i.e., processes such as uptake into peripheral tissues, binding to proteins, metabolism, and exhalation are not incorporated in diffusion-cell experiments. Future work will incorporate these clearance mechanisms into a mathematical model of the skin to quantify the rates of absorption, distribution, and elimination of JP-8 components from exposures on the human skin.

CHAPTER 3

A DERMATOTOXICOKINETIC MODEL OF HUMAN EXPOSURES TO JET FUEL

David Kim, Melvin E. Andersen, and Leena A. Nylander-French

(Submitted for publication)

3.1 Abstract

Workers, both in the military and the commercial airline industry, are exposed to jet fuel by inhalation and dermal contact. We present a dermatotoxicokinetic (DTK) model that quantifies the absorption, distribution, and elimination of aromatic and aliphatic components of jet fuel following dermal exposures in humans. Kinetic data were obtained from 10 healthy volunteers following a single dose of JP-8 to the forearm over a surface area of 20 cm^2. Blood samples were taken before exposure (t = 0 h), after exposure (t = 0.5 h), and every 0.5 h for up to 4 h past exposure. The DTK model that best fit the data included 5 compartments. The skin was described as two compartments: (1) the stratum corneum and (2) the viable epidermis. Addition of a storage compartment improved the model fit of the data. The DTK model was used to predict blood concentrations of the components of JP-8 based on dermal exposure measurements made in occupational exposure settings in order to better understand the toxicokinetic behavior of these compounds. Monte Carlo simulations of dermal exposure and cumulative internal dose demonstrated no overlap among the low-, medium-, and high-exposure groups. The DTK model provides a quantitative understanding of

the relationship between the mass of JP-8 components in the stratum corneum and the concentrations of each component in the systemic circulation. The model may be used for the development of a toxicokinetic modeling strategy for multi-route exposure to jet fuel.

3.2 Introduction

Occupational and environmental exposure assessments aim to quantify the uptake of toxicants through inhalation, ingestion, and dermal contact with environmental media (e.g., air, soil, water). Historically, inhalation exposures have been the focus of occupational and environmental exposure assessments. For the most part, the dermal route has been neglected, making it difficult to assess its importance relative to other routes of exposure. However, recent interest in dermal exposure assessment has been spawned by the decreasing trend in inhalation exposures to chemicals in the workplace (Sartorelli 2002; Schneider *et al.* 2000; Semple 2004; Semple 2005).

Current dermal exposure assessment strategies make use of three types of sampling techniques based on surrogate skin, removal, or a fluorescent tracer (Fenske 1993; Nylander-French 2003). One of the more promising methods is tape stripping (a removal technique), which is a method of direct sampling of the amount of chemical in the stratum corneum (Chao *et al.* 2005; Chao *et al.* 2006; Chao and Nylander-French 2004; Fent *et al.* in press; Jacobi *et al.* 2005; Nylander-French 2000; Surber *et al.* 1999). In tape stripping, part of the stratum corneum is removed and the rate and extent of dermal absorption is quantified. Tape stripping has been used in bioequivalence studies of therapeutic agents (Loden *et al.* 2004; Pershing *et al.* 2002; Pershing *et al.* 2003; Shah 2001) and for measurement of dermal exposures to jet fuel in occupational exposure settings (Chao *et al.* 2005; Chao *et al.* 2006).

The tape-strip sampling technique has not been fully utilized partly due to inconsistent standardization. For example, normalization of the mass measured on tape strips is done by dividing the mass of chemicals on tape strips by the mass of stratum corneum removed (Reddy *et al.* 2002) or by the keratin content (Chao and Nylander-French 2004). A standard approach for reporting tape-strip data has not yet been determined. In addition, there is insufficient evidence that tape-strip measurements from different exposure groups (i.e., high-, medium-, or low-exposure) are

representative of exposure based on internal dose metrics (e.g., blood and urine biological markers of exposure). A paucity of studies have demonstrated an association between dermal exposures measured using the tape-strip technique and urinary metabolite levels in humans under occupational exposure conditions (Chao *et al.* 2006). Clearly, demonstrating that tape-strip measurements are predictive of internal dose can be of benefit to exposure assessment and epidemiological studies.

Quantification of the absorption, distribution, metabolism, and elimination of chemicals that may come into contact with the skin is necessary for assessing exposures and human health risks associated with occupational and environmental exposures to chemicals. Membrane models have been used to quantify the toxicokinetic behavior of chemicals in the skin (Pirot *et al.* 1997; Reddy *et al.* 2002). In membrane models, skin is defined as a homogeneous membrane and the diffusion across the membrane is described by Fick's first law of diffusion:

$$J = -D \frac{\partial C}{\partial x} \quad (6)$$

where J is the flux of material across the membrane (mg/cm^2/hr), D is the diffusion coefficient (cm^2/h), ∂C is the concentration gradient across the membrane (mg/cm^3), and ∂x is the thickness of the membrane (cm). The main limitation to applying membrane models to tape-strip sampled data is that the mathematical treatment is difficult and cumbersome. Alternatively, compartmental models have been developed to quantitatively describe the dermal absorption and penetration of chemicals (Guy *et al.* 1985; Qiao *et al.* 2000; Shatkin and Brown 1991; Williams and Riviere 1995). However, a compartmental model of the skin that relates tape-strip measurements to internal dose has not been reported. Though compartmental models are not strictly representative of a complex tissue like the skin, they are easier to implement and can be combined with systemic compartmental models for quantitation of the toxicokinetic behavior of chemicals following dermal exposures.

In this study, we evaluated four different compartmental models of dermal exposure to jet-propulsion fuel 8 (JP-8). JP-8 is a fuel used extensively in military vehicles by member states of NATO (Subcommittee on Jet-Propulsion Fuel 8 2003). Dermal exposure to JP-8, which occurs

occupationally, may contribute to systemic levels of various aromatic and aliphatic hydrocarbon components (Chao *et al.* 2006; Serdar *et al.* 2004). We report in this paper data-based compartmental models (Andersen 1991). Data-based compartmental models of the skin have been referred to as dermatotoxicokinetic (DTK) models (Qiao *et al.* 2000); for consistency, we will also use this terminology. The main objective of our study was to construct a DTK model of the skin that quantitatively characterized and predicted the toxicokinetic behavior of JP-8 following controlled dermal exposures. A second objective was to examine the effect of dermal exposure variability on blood concentrations of JP-8 components. The following chemical components of JP-8 were examined: naphthalene, 1-methyl naphthalene, 2-methyl naphthalene, decane, undecane, and dodecane. Data derived from tape-strip and blood samples that were collected from dermal only exposed human volunteers provided the basis for model development. The results of our study are intended to facilitate the development of a modeling strategy for multi-route exposures to jet fuel.

3.3 Methods

3.3.1 Study population

Ten volunteers (five female and five male) were recruited for this study. The average age of the volunteers was 27 and ranged from 21 to 37 years. Seven of the study volunteers were Caucasian. One volunteer was Asian, another African American, and one was mixed Asian-Caucasian. The mean body mass index (BMI) was 21 kg/m^2 and ranged from 19-25 kg/m^2. Approval for this study was obtained from the Institutional Review Board on Research Involving Human Subjects (School of Public Health, The University of North Carolina at Chapel Hill, Chapel Hill, NC).

3.3.2 Experimental design

Exposures were conducted inside a chamber with dimensions of 20.3 cm width $\times$ 20.3 cm length $\times$ 18.8 cm height and a total volume of 7706 cm^3 (Chao and Nylander-French 2004). The volunteer's forearm was placed palm up inside the exposure chamber, and two aluminum application wells (dimensions 2.5 cm $\times$ 4.0 cm = 10 cm^2 per well) were pressed against the skin to prevent JP-8 from spreading during the experiment. A total of 1 ml of neat JP-8 was applied to the skin. The exposure

chamber was sealed for the duration of the 0.5 h experiment. At the end of the 0.5 h exposure period, the exposure sites were wiped with gauze pads and tape stripped up to 10 times. Tape strips were placed in 10 ml of acetone containing 1 µg/ml of internal standards (naphthalene-d_8 and dodecane-d_{26}). All tape-strip samples were stored in 20 ml vials (I-CHEM, Rockwood, TN) and refrigerated at 4°C. Blood samples were drawn from the unexposed arm at baseline, 0.5 h, 1 h, 1.5 h, 2 h, 2.5 h, 3 h, and 3.5 h and collected in 6 ml test tubes containing sodium heparin (Vacutainer, Franklin Lakes, NJ). The blood samples were transferred to 15 ml centrifuge tubes (Fisherbrand, Pittsburgh, PA) and stored at -80°C.

3.3.3 Chemical analysis

Tape-strip samples were analyzed by gas chromatography-mass spectrometry (GC-MS). A Thermoquest Trace GC (Thermo Electron Corporation, Austin, TX) coupled with a Combi Pal autosampler (CTC Analytics, Zwingen, Switzerland) and a Finnigan Polaris Q quadrupole ion trap MS (Thermo Electron Corporation, Austin, TX) in electron ionization mode, was used for the chemical analysis. Separation of the sample was done with a fused-silica capillary column, 30 m $\times$ 0.25 mm internal diameter, coated with a mixture of 5% diphenyl:95% dimethyl polysiloxane (0.25 µm film thickness, RTX-5MS, Restek Corporation, Bellefonte, PA). The oven temperature for analysis was 40°C (3 min) and then 10°C/min to 290°C (10 min). One µl of sample was directly injected into the inlet. The ions used for quantitation were m/z 128 (naphthalene), 142 (1-methyl and 2-methyl naphthalene), 136 (naphthalene-d_8), 71 (n-decane, n-undecane, n-dodecane), and 98 (dodecane-d_{26}).

Blood samples were analyzed using head-space solid-phase microextraction (HS-SPME) and the GC-MS system described above. Modifications were made from published methods (Cardinali *et al.* 2000; Waidyanatha *et al.* 2003). Whole blood (1 ml) was added to a 10 ml headspace vial with crimp top (Microliter, Suwanee, GA) containing 3 ml of deionized water, 2 g of NaCl, and 2 µl of 5 ng/ml internal standard. The vial was put into an aluminum block (CTC Analytics, Zwingen, Switzerland) for heating and agitating at 45ºC and 250 rpm. After 1 min, a 100 µm polydimethyl-siloxame (PDMS) fiber (Supelco, Bellefonte, PA) was inserted into the head-space of the vial for 20 min. The needle

containing the SPME fiber was withdrawn and introduced into the inlet of the GC for 20 min. The inlet temperature was set at 230°C; an IceBlue septum (Restek, Bellefonte, PA) and a liner with an internal diameter of 0.8 mm (SGE, Austin, TX) were used. All other GC-MS conditions were the same as for the analysis of tape-strip samples.

3.3.4 Basic DTK model

The initial DTK model (model A) developed to study the disposition of naphthalene, 1-methyl naphthalene, 2-methyl naphthalene, decane, undecane, and dodecane is linear with four first-order rate constants and three compartments representing the surface, skin, and blood (Figure 6). Diffusion of chemicals across the stratum corneum is described by k_0. Thus, the rate of input to skin is k_0 times the amount (defined as DERMDOSE) of the chemical applied to the skin:

$$\text{rate of input} = k_0 \times \text{DERMDOSE} \tag{7}$$

In compartmental models, the time course behavior of chemicals in each compartment is described by mass-balance differential equations (MBDE). The rate constant for input of chemical in blood is k_1, and the rate constant for efflux of chemical in the skin is k_2. The MBDE that describes the rate of change of the amount of chemical in skin is:

$$\frac{dAS}{dt} = k_0 DERMDOSE - k_1 AS + k_2 AB \tag{8}$$

where AS and AB are the amounts of chemical in the skin and blood respectively. Lastly, k_3 is the elimination rate constant. The MBDE for blood becomes:

$$\frac{dAB}{dt} = k_1 AS - (k_2 + k_3) AB \tag{9}$$

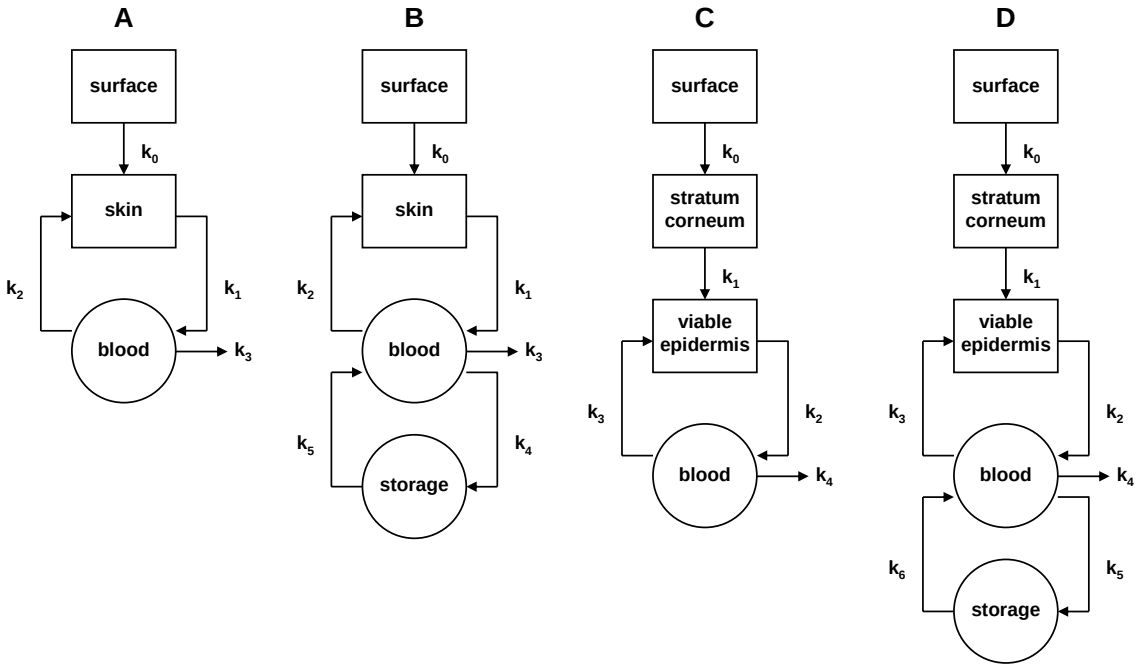

Figure 6. Schematic of DTK models following exposures to JP-8 components: naphthalene, 1-methyl naphthalene, 2-methyl naphthalene, decane, undecane, and dodecane. Models A and B describe the skin as one compartment. In models C and D, the skin is split into two compartments representing the stratum corneum and the viable epidermis. A compartment for storage of chemicals is included in models B and D.

3.3.5 Refined DTK model

The epidermis, which performs much of the barrier function of skin, is made up of two very different layers: the stratum corneum (SC) and the viable epidermis (VE). The SC consists of dead cells in a hydrophobic environment. The VE, on the other hand, is comprised of viable cells in a hydrophilic environment. Based on these biological differences between the two main protective layers of the skin, two-compartment DTK models are more realistic and may predict the toxicokinetic behavior of chemicals better than one-compartment models. This has been demonstrated successfully for dermal exposures to chemicals in an aqueous vehicle (Shatkin and Brown 1991). In our study, two different two-compartment DTK models were evaluated (models C and D). In both models, the diffusion of chemicals across the SC is described by k_0 and diffusion across the VE is described by k_1.

Furthermore, because the aromatic and aliphatic hydrocarbons naphthalene, 1-methyl naphthalene, 2-methyl naphthalene, decane, undecane, and dodecane are lipophilic compounds, they are stored in fat tissues throughout the body. The fat:blood partition coefficient for naphthalene is 160 (Willems *et al.* 2001) and 25 for decane (Perleberg *et al.* 2004). To account for the storage of JP-8 components in fat, the basic DTK model was altered to include a storage compartment and distribution rate constants k_4 (model B) and k_5 (model D) and redistribution rate constants k_5 (model B) and k_6 (model D).

Table 5. Initial values of rate constants. Initial values were estimated by averaging values reported in the literature (Guy *et al.* 1985; Qiao *et al.* 2000; Williams and Riviere 1995). All rate constants have the units min^{-1}.

model	k_0	k_1	k_2	k_3	k_4	k_5	k_6
A	0.003	1	1	0.0029			
B	0.003	1	1	0.0029	0.04	0.04	
C	0.003	0.04	1	1	0.0029		
D	0.003	0.04	1	1	0.0029	0.04	0.04

Table 6. Experimental dose to the skin (i.e., DERMDOSE) measured in the first tape strips of 10 study volunteers. DERMDOSE was set to zero at the end of the exposure period.

compound	mean ($\mu g/cm^2$)	SD* ($\mu g/cm^2$)	ratio**
naphthalene	216	127	1
1-methyl naphthalene	304	102	1.4
2-methyl naphthalene	283	91	1.3
decane	237	213	1.1
undecane	4033	2234	18.7
dodecane	7277	1971	33.7

* SD = standard deviation.

** The ratio is calculated as $\frac{\text{DERMDOSE}_{\text{chemical}}}{\text{DERMDOSE}_{\text{naphthalene}}}$.

3.3.6 Toxicokinetic analysis

The DTK models were formulated by simultaneously fitting the tape-strip and blood data. Parameters were optimized using the method of simulated annealing (Xcellon 2004). Simulated annealing is a global optimization method that optimizes parameter values without being influenced by the initial values. This optimization protocol is more robust than others (Goffe *et al.* 1994; Levitt 2002). However, a major limitation of simulated annealing is the longer computational time required. Default settings for simulated annealing were adjusted to include fewer maximum iterations (1000) and maximum function evaluations (5000) in order to decrease the optimization time. Initial values of rate constants (Table 5) were obtained by averaging literature values (Guy *et al.* 1985; Qiao *et al.* 2000; Williams and Riviere 1995). The first tape strip from each study participant was treated as the dose to the skin (Table 6). The baseline blood concentration was not subtracted from blood concentrations at t > 0 min but included as the initial concentration in the blood compartment because the volunteers may have had recent environmental exposures to similar compounds. Consequently, baseline concentration may not be an accurate (or true) baseline since the baseline concentrations may decrease after breathing cleaner indoor air. The volume of blood (V_b) was estimated using allometric relationships (Davies and Morris 1993). The equation is $V_b = 72.447 \times (\text{body weight in kg})^{1.007}$ and was used to calculate the mass of chemicals in the blood. The baseline amount in the skin (AS_0) compartment was calculated using the following algebraic expression:

$$AS_0 = \frac{k_0 DERMDOSE + k_2 AB_0}{k_1} \tag{10}$$

where AB_0 is the initial amount of chemical in blood. The initial amount in the peripheral compartment was calculated from:

for model B: $$AP_0 = \frac{k_4}{k_5} AB_0 \tag{11}$$

and for model D: $$AP_0 = \frac{k_5}{k_6} AB_0 \tag{12}$$

In models C and D, the initial amount in the SC was set to zero and the initial amount in the VE (AD_0) was calculated as:

$$AD_0 = \frac{k_3}{k_2} AB_0 \tag{13}$$

Rate constants were optimized for each study participant and results were summarized using descriptive statistics. The performance of the model fit to experimental data was evaluated using a combination of visual inspection and statistical evaluation (Andersen *et al.* 2001).

Simulations of occupational exposure scenarios were performed using the final model. The exposure scenarios were based on a field study that measured dermal exposures to naphthalene in the US Air Force personnel (Chao *et al.* 2005). Naphthalene was used as a surrogate for JP-8 exposure because it (1) is abundant in JP-8, (2) is readily absorbed into the blood, and (3) is only a minor component in confounding sources of exposure, such as cigarette smoke and gasoline exhaust (Rustemeier *et al.* 2002; Serdar *et al.* 2003). The first set of simulations involved predicting the concentration-time profile for a specific field exposure scenario. An average whole body (surface area = 2 m^2) dermal exposure level of 2018 ng/m^2 was used as the input in the simulations. The duration of exposure was 240 minutes. The dose to the skin was set to that of naphthalene, and exposure concentrations for other compounds were estimated using the ratios reported in Table 6. After the exposure was complete, the dose was set to zero and the simulation was continued for up to 8 h.

In the second set of simulations, a Monte Carlo method was used to examine the impact of exposure variability on cumulative internal dose. The geometric mean and standard deviation of the whole-body dermal exposure to naphthalene were 344 $\pm$ 4 ng/m^2 for the low-exposure group, 483 $\pm$ 4 ng/m^2 for the medium-exposure group, and 4188 $\pm$ 10 ng/m^2 for the high-exposure group. These values were used to specify the input distribution functions for the simulations. The distribution of the input parameters was log-normal and the number of simulations was set at 100. The model output

was cumulative internal dose ($DOSE_c$), i.e., the area under the blood concentration-time curve. $DOSE_c$ was calculated by integrating the blood concentration for the duration of the simulation:

$$DOSE_c = \int_{t_0}^{t_1} C_b(t)\, dt \qquad (14)$$

where t_0 was the time at the start of the simulation, t_1 was the time at the end of the simulation, and $C_b(t)$ was the concentration of the chemical in blood.

3.4 Results

3.4.1 Model selection: visual inspection

Simulations of the blood concentrations of naphthalene, 1-methyl naphthalene, 2-methyl naphthalene, decane, undecane, and dodecane were compared to experimentally measured blood concentrations in individual study volunteers. One of the volunteers was a 23-year old Caucasian male with a BMI of 25 kg/m^2 (Figure 7). For this individual, the maximum concentrations (C_{max}) in blood occurred shortly after the end of exposure ($t_{max} \approx 30$ min) for all chemicals but dodecane, which occurred at $t_{max} \approx 60$ min. The peak concentrations were 0.8 ng/ml, 0.5 ng/ml, 1 ng/ml, 3.5 ng/ml, 1.8 ng/ml, and 3.3 ng/ml for naphthalene, 1-methyl naphthalene, 2-methyl naphthalene, decane, undecane, and dodecane respectively. C_{max} was sustained for up to t = 100 min for decane and dodecane. The blood concentrations of all chemicals at t > 0 min did not return to baseline levels. The models B and D seemed to fit naphthalene and 1-methyl naphthalene data the best; all models fit the 2-methyl naphthalene time course equally well. For the aliphatic components, no model stood out as being superior to others, although model A seemed to fit the dodecane data the best. None of the models were able to predict the sustained blood concentration observed in the dodecane time course.

The simulations and the observed data for the individual discussed above were compared to results from a different individual (Figure 8). This individual was a 24-year old Caucasian female with a BMI of 22 kg/m^2. The toxicokinetic behavior of aromatic and aliphatic hydrocarbons was very different for this volunteer. The peak concentrations occurred at $t_{max} \approx 60$ min for naphthalene (C_{max} =

0.3 ng/ml), at $t_{max} \approx 100$ min for 1-methyl naphthalene (C_{max} = 0.3 ng/ml), and at $t_{max} \approx 60$ min for 2-methyl naphthalene (C_{max} = 0.3 ng/ml); peak concentrations for all aliphatic components occurred at $t_{max} \approx 30$ min. The C_{max} were 2.5 ng/ml, 1.2 ng/ml, and 3.5 ng/ml for decane, undecane, and dodecane respectively. Concentrations in blood at t > 0 min did not reach baseline levels for aromatic components; however, concentrations at t > 0 min did reach baseline concentrations for the aliphatic components. Model C seemed to fit the naphthalene data the best. Models A, C, and D fit 2-methyl naphthalene data equally well. Model fits to 1-methyl naphthalene data were poor. For the aliphatic components, model D fit most datasets; however, the peak concentration for decane was not predicted by any of the models.

3.4.2 Model selection: statistical evaluation

In addition to the visual inspection of model predictions and time-course data, a likelihood ratio (LR) test was used to provide a statistically rigorous comparison of the models (Andersen *et al.* 2001; Pinheiro and Bates 2000). One model is said to be nested within another model if it represents a special case of that model. If L_2 is the maximum likelihood of the model with additional parameters, and L_1 is the maximum likelihood of the model with fewer parameters, then $L_2 > L_1$ and, correspondingly, $\log L_2 > \log L_1$. The LR test statistic is:

$$\text{LR test statistic} = 2 \times (\log L_2 - \log L_1) \quad (15)$$

The LR test statistic is compared to a $\chi^2_{f,\alpha}$ distribution with f degrees of freedom. The p-value is compared to α, which is the significance level for accepting or rejecting the null hypothesis. All models were compared to model A at a significance level of $\alpha = 0.1$. With the addition of a storage compartment (model B), two additional degrees of freedom were introduced (k_4 and k_5). Splitting the skin compartment into the SC and VE (model C) introduced 1 more degree of freedom (k_1). Model D introduced three more degrees of freedom as a result of splitting the skin and addition of a storage compartment (k_1, k_5, and k_6). Overall, model B resulted in significantly improved fits to the data for

15% of the study volunteers. When models C and D were compared to model A, 25% and 40% of the volunteers had improved fits, respectively.

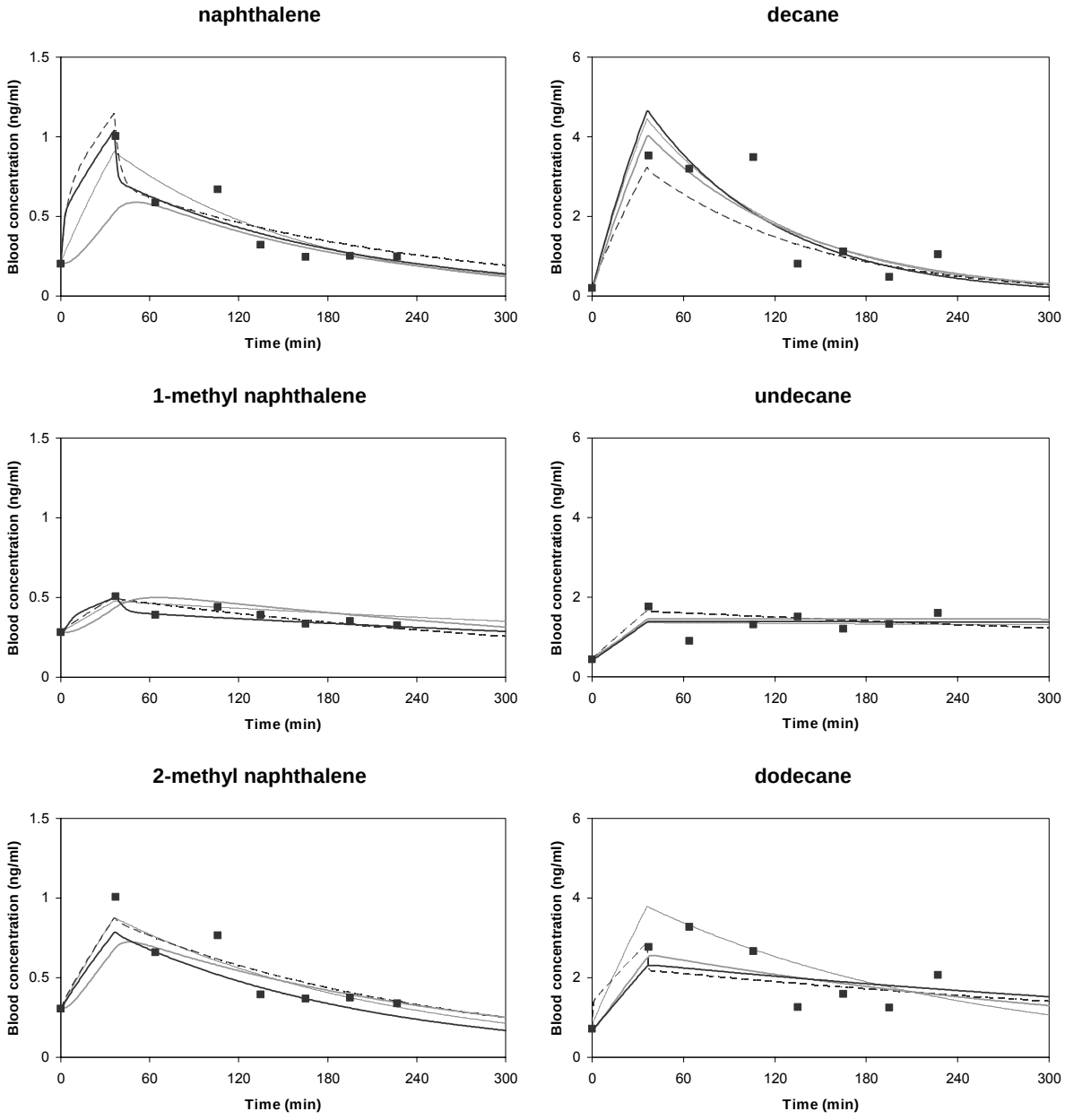

Figure 7. Time-course plots of fitted and observed blood concentrations of aromatic components of JP-8 for study volunteer 1. Shown are observed data (■), model A (----), model B (- - -), model C (——), and model D (——).

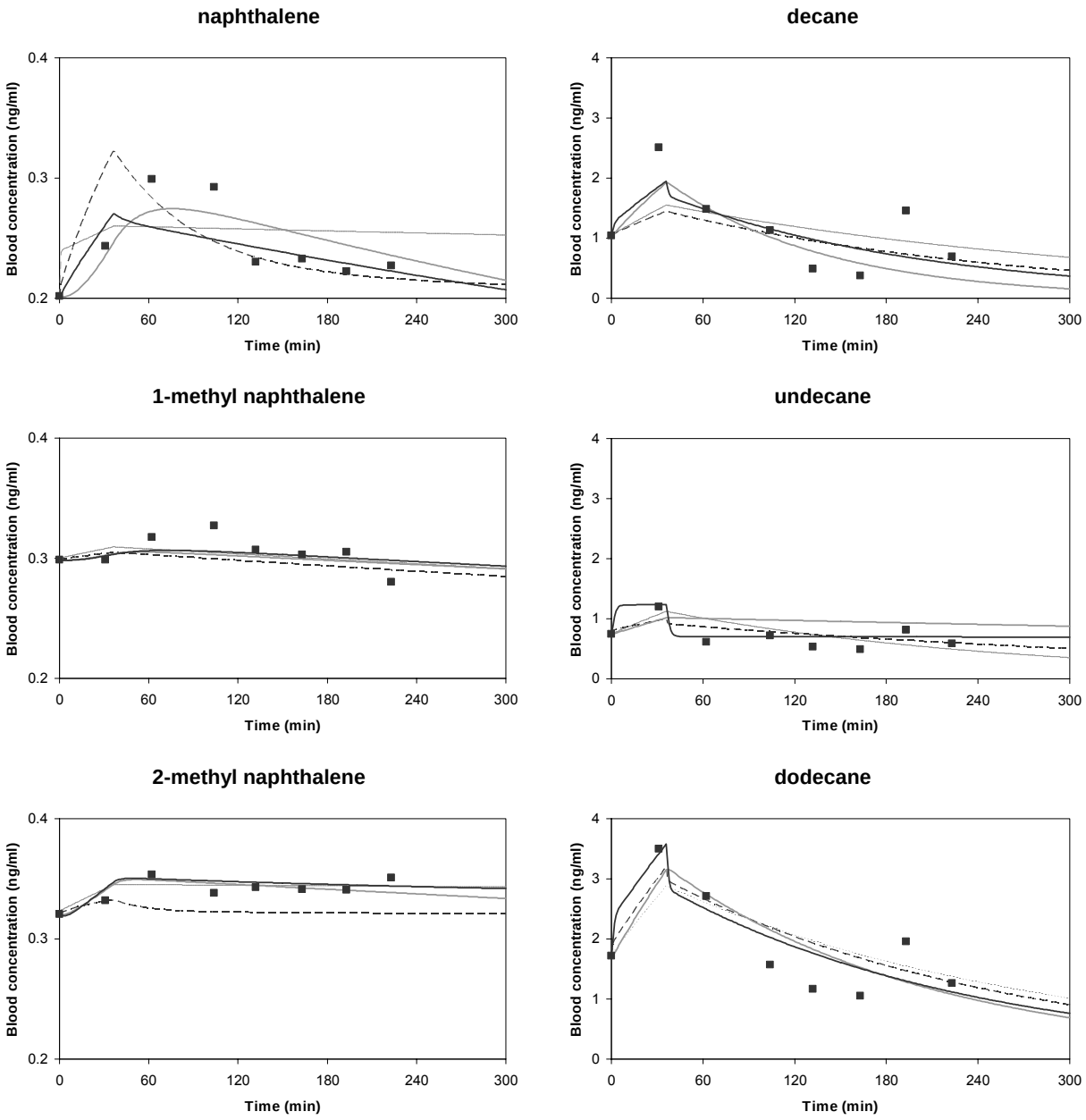

Figure 8. Time-course plots of fitted and observed blood concentrations of aromatic components of JP-8 for study volunteer 2. Shown are observed data (■), model A (----), model B (- - -), model C (—), and model D (—). The y-axis is adjusted (range 0.2 ng/ml to 0.4 ng/ml) for better visualization of model predictions and data for aromatic compounds.

Based on both visual inspection and statistical evaluation of the models, model D was selected as the model that best fit the kinetic data. The optimized rate constants for aromatic and aliphatic components are reported in Table 7. Some interesting patterns were observed. First, k_0 is 4 orders of magnitude smaller than k_1. This was expected since the SC is the rate limiting barrier to hydrophobic compounds, which are not as limited by the VE. Second, the distribution rate constant k_5 is larger than the redistribution rate constant k_6, which is consistent with the expected properties of the storage compartment. Finally, the elimination rate constant k_4 is consistently larger for aliphatic components.

Table 7. Optimized rate constants for model D. The average rate constants from all subjects are shown. The method of simulated annealing was used to optimize each rate constant. The units for all rate constants are min^{-1}.

	Naphthalene		1-Methyl Naphthalene		2-Methyl Naphthalene	
	mean	SD	mean	SD	mean	SD
k_0	4.1×10^{-4}	8.4×10^{-4}	7.8×10^{-5}	5.8×10^{-5}	2.5×10^{-4}	4.2×10^{-4}
k_1	1.9	1.6	1.0	1.5	1.2	0.9
k_2	35	30	10	19	30	33
k_3	43	26	29	24	42	34
k_4	0.04	0.04	0.04	0.04	0.04	0.04
k_5	1.4	1.0	1.9	1.0	0.8	0.6
k_6	0.10	0.07	0.13	0.10	0.11	0.12
	Decane		Undecane		dodecane	
	mean	SD	mean	SD	mean	SD
k_0	6.9×10^{-4}	7.6×10^{-4}	1.6×10^{-4}	3.3×10^{-4}	7.9×10^{-5}	1.3×10^{-4}
k_1	1.9	0.9	1.9	1.2	1.9	1.3
k_2	42	28	59	39	48	38
k_3	51	31	62	35	55	29
k_4	0.13	0.05	0.09	0.05	0.10	0.07
k_5	1.6	0.9	1.8	1.1	2.0	0.7
k_6	0.15	0.10	0.07	0.09	0.07	0.06

SD = Standard Deviation

3.4.3 Simulations of dermal exposures to JP-8

Simulations of whole body dermal exposure to JP-8 were conducted to examine the toxicokinetic behavior of aromatic and aliphatic components of JP-8 under an occupational exposure setting (Figure 9). The parameters for the simulations were an exposure duration of 240 minutes (4 hours) and dermal exposure to 2018 ng/m^2 of naphthalene for a 70 kg person. After the end of 240 min exposure, the simulations were extended for an additional 4 hours. Since dermal exposures to other components were not measured by Chao *et al*. (2005), exposures to 1-methyl naphthalene, 2-methyl naphthalene, decane, undecane, and dodecane were estimated using the ratios reported in Table 6. The model-predicted C_{max} were 3.6×10^{-3} ng/ml, 8.6×10^{-4} ng/ml, 3.9×10^{-3} ng/ml, 4.1×10^{-3} ng/ml, 1.4×10^{-2} ng/ml, and 1.1×10^{-2} ng/ml for naphthalene, 1-methyl naphthalene, 2-methyl naphthalene, decane, undecane, and dodecane, respectively. All peak concentrations occurred at t_{max} = 240 min. The model predictions of blood concentration of all components drop sharply at the end of the exposure. The concentrations at the end of the simulation were 54%, 58%, 37%, 10%, 44%, and 44% of C_{max} for naphthalene, 1-methyl naphthalene, 2-methyl naphthalene, decane, undecane, and dodecane respectively.

The mass of aromatic and aliphatic components of JP-8 in the SC, VE, and storage compartments were predicted to characterize the toxicokinetic behavior of these compounds (Figure 10). In these simulations, naphthalene and decane were treated as chemical tracers for the aromatic and aliphatic hydrocarbons, respectively. Predictions were made for the same simulation conditions as described above. The SC achieved a steady state while the other compartments did not. In the storage compartment, the ratio of mass at t = 8 h to the mass at t_{max} is 56% and 10% for aromatic and aliphatic components, respectively. Conversely, the ratios are 53% and 9% for aromatic and aliphatic components in the VE, respectively, and 0% for both aromatic and aliphatic components in the SC.

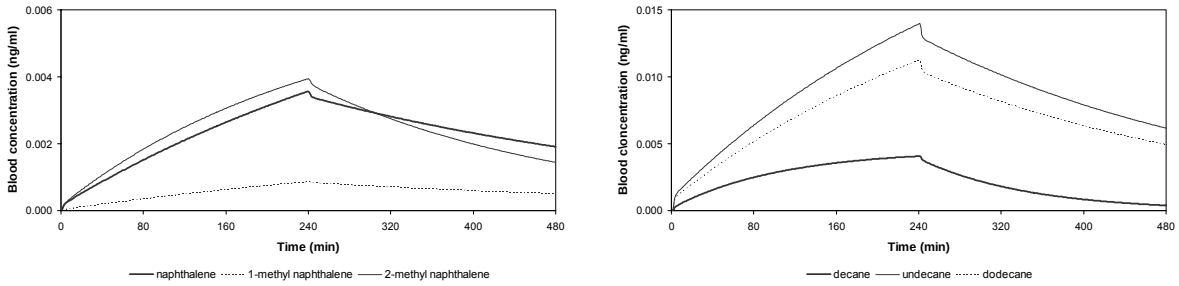

Figure 9. Simulated blood concentration profiles of aromatic and aliphatic components from dermal exposure to JP-8. Predictions were made using model D. The mean exposure to naphthalene was 2018 ng/m^2. The simulation was for a 70 kg person exposed over a whole body surface area of 2 m^2. Simulations were run for one full 8 h work day with an exposure duration of 240 min. The concentration of 1-methyl naphthalene, 2-methyl naphthalene, decane, undecane, and dodecane were estimated using the ratios from Table 2.

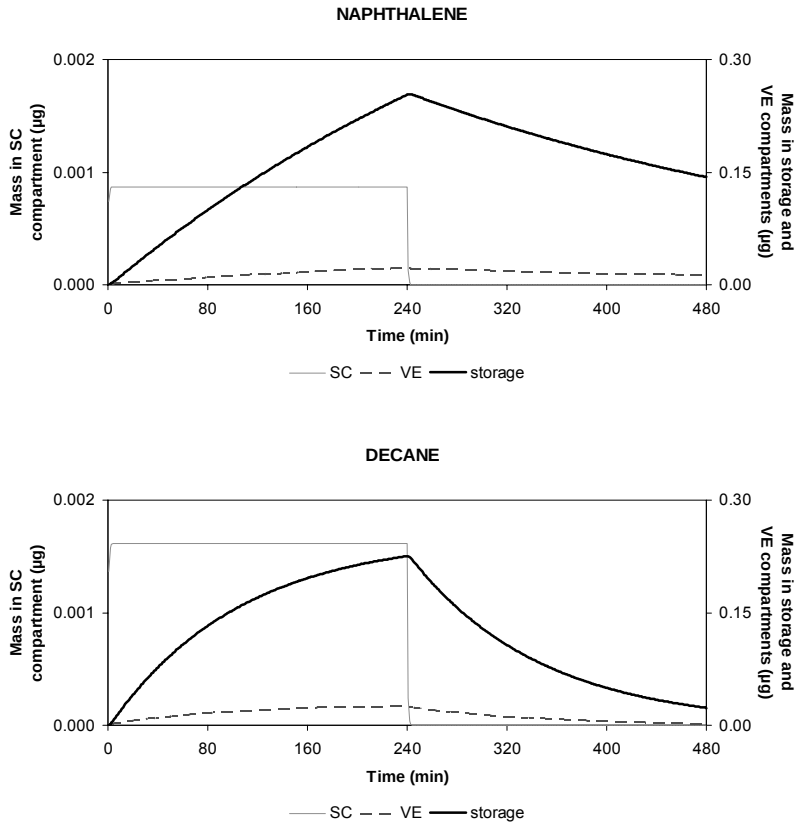

Figure 10. Simulation results of the mass of aromatic (i.e., naphthalene) and aliphatic (i.e., decane) components of JP-8 in the stratum corneum (SC), viable epidermis (VE) and the storage compartment. Predictions were made using model D. Dermal exposures to naphthalene and decane were set at 2.0 µg/m^2 and 2.2 µg/m^2 respectively. The duration of dermal exposure was 4 h and the simulations were carried out to 8 h.

3.4.4 Dermal Exposure variability

Monte Carlo methods were used to examine the distribution of the cumulative internal dose ($DOSE_c$) for naphthalene in blood resulting from variability of dermal exposure levels in the low-, medium-, and high-exposure groups. The input parameters were the geometric mean and standard deviation of the whole-body dermal exposure to naphthalene. These were 344 $\pm$ 4 ng/m^2 for the low-exposure group, 483 $\pm$ 4 ng/m^2 for the medium-exposure group, and 4188 $\pm$ 10 ng/m^2 for the high-exposure group. The distribution of the input parameters was specified as log-normal and 100 iterations were performed (Table 8). The $DOSE_c$ for naphthalene at all exposure levels was normally distributed and did not intersect one another. Further simulations of daily 4 h exposure to low, medium, and high levels of naphthalene were conducted to examine the time course profiles of naphthalene in blood from repeated exposures (Figure 11). The $DOSE_c$ for low, medium, and high dermal exposures are 1.6 ng·h/ml, 2.3 ng·h/ml, and 19.6 ng·h/ml, respectively.

Table 8. Results of Monte Carlo analysis of whole body dermal exposure to naphthalene in JP-8. The dermal exposure distribution was specified as log-normal and 100 simulations were run. Model D was used for these simulations. Exposure concentrations were obtained from Chao *et al.* (2005). Reported is geometric mean $\pm$ SD.

Exposure level	Dermal exposure to naphthalene (ng/m^2)	AUC (ng·min/ml)	Exposure level
low	344 $\pm$ 4	1.61 $\pm$ 0.02	low
medium	483 $\pm$ 4	2.26 $\pm$ 0.02	medium
high	4188 $\pm$ 10	19.56 $\pm$ 0.05	high

AUC = area under the curve

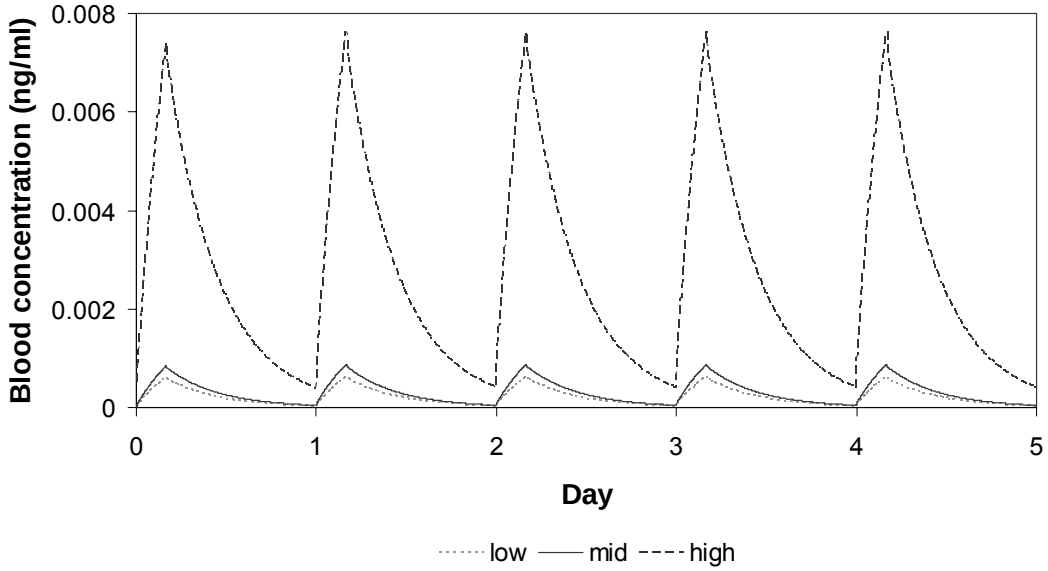

Figure 11. Simulations of the blood concentrations of naphthalene resulting from dermal exposures to JP-8. Predictions were made using model D. The length of each simulation was 5 days and the duration of exposures was for 4 hours each day. The $DOSE_c$ for low, medium, and high dermal exposures are 1.6 ng·h/ml, 2.3 ng·h/ml, and 19.6 ng·h/ml, respectively.

3.5 Discussion

Chemicals deposited on the skin can evaporate from the surface, be absorbed into deeper layers of the skin, be metabolized, or penetrate the skin for distribution to other tissues. Understanding the fate of chemicals deposited on the skin is an important step in assessing the associated risks. Therefore, the current study presents a DTK model that can be used to quantify the toxicokinetic behavior of chemicals following dermal exposure to a complex chemical mixture such as JP-8. This study represents the first attempt at deriving toxicokinetic parameters for dermal exposure to JP-8 in humans.

In the current study, a two-compartment model of the skin was developed and parameters estimated for dermal exposure to JP-8. We found that, although the one-compartment models fit some observed data, a two-compartment model of the skin fit the data better from all 10 study volunteers. In our model, the two compartments represented the SC and VE, thus representing a more biologically plausible description of the skin. Physiologically, the SC and VE have very different

physical characteristics, primarily in that the SC is *hydrophobic* and the VE is *hydrophilic*. Our estimates of k_0 and k_1 supported the two-compartment model structure; k_0 was 4 orders of magnitude less than k_1, suggesting slower diffusion across the SC than the VE. This was not unexpected since the SC is rate-limiting for the absorption of chemicals into deeper skin layers, and for penetration of chemicals into the blood. It is well known that non-polar chemicals with small molecular weights move across the SC by passive diffusion through a lipid matrix between protein filaments. The VE, however, consists of an aqueous medium with proteins that may be involved in metabolism and active transport of compounds into the systemic circulation. The rate of transport across the VE is dependent on blood flow, interstitial fluid movement, and interaction with VE constituents. Conversely, the rate of transport of a chemical across the SC is dependent on the thickness of the SC, the concentration gradient, level of hydration, and the diffusion coefficient of the compound.

The penetration of chemicals across the skin is quantified experimentally using diffusion cells and dermatomed skin from rats and pigs (McDougal *et al.* 2000; McDougal and Robinson 2002; Muhammad *et al.* 2004; Sartorelli *et al.* 1998). In these experiments, the chemical of interest is applied to a donor cell and the receptor compartment is sampled at different time points. The cumulative quantity of chemical collected in the receptor compartment is plotted as a function of time. The flux value is obtained from the slope of the cumulative amount of chemical permeated *vs*. time plot. Apparent permeability coefficient (K_p) values are computed using the following expression (McDougal and Boeniger 2002):

$$J = K_p \times C \tag{16}$$

where J is the flux (mass/area/time) and C is the concentration of chemical in the donor cell (mass/volume). Flux values are determined *in vitro* typically under steady-state conditions, i.e. when the concentration of chemical in the donor compartment is constant over time (Bronaugh and Maibach 1999; McDougal and Boeniger 2002); however, steady-state conditions are difficult to maintain experimentally *in vivo*. Previously, the flux value was estimated for aromatic and aliphatic components of JP-8 in humans from the slope of the linear portion of the cumulative mass of

chemical in blood per cm^2 *vs.* time curve (Kim *et al.* 2006). K_p was calculated using equation 16. This calculation did not take into account the mass in the storage compartment and the mass cleared from the blood, and therefore, underestimated K_p. Here, we have revised our previous estimates of K_p using the final DTK model. The rate of input in this DTK model is equivalent to the product of the permeability coefficient (K_p), the exposed surface area (A_{exp}), and the concentration of the chemical component in JP-8 ($C_{JP\text{-}8}$) (McCarley and Bunge 2001; McDougal and Boeniger 2002):

$$\text{rate of input} = k_0 \times \text{DERMDOSE} = K_p \times A_{exp} \times C_{JP\text{-}8} \quad (17)$$

Equation 17 can be rearranged to solve for K_p:

$$K_p = \frac{k_0 \times \text{DERMDOSE}}{A_{exp} \times C_{JP-8}} \quad (18)$$

Using equation 18, we calculated K_p values of 1.8×10^{-3} cm/h, 1.3×10^{-3} cm/h, 3.5×10^{-4} cm/h, 3.5×10^{-4} cm/h, and 3.3×10^{-3} cm/h for naphthalene, 1- and 2-methyl naphthalene, decane, undecane, and dodecane, respectively. The revised estimates of K_p were more than an order of magnitude larger than the values reported previously (Kim *et al.* 2006) but within an order of magnitude reported by McDougal *et al.* (2000). These results suggest that reasonable estimates of the permeability coefficient for aromatic and aliphatic components of JP-8 may be derived from *in vitro* studies.

Although the stratum corneum is the main rate-limiting barrier for the penetration of chemicals, the viable epidermis can also affect the amount of parent compound available for systemic circulation by binding chemicals and/or metabolizing them to a more water-soluble form. Although we did not include skin metabolism in our DTK model, we quantified the disposition of chemicals in the VE. The net rate of change of the amount of chemical in the VE depends on the rate of input from the SC, rate of efflux to the systemic circulation, and rate of input from the systemic circulation. Therefore, the MBDE for the VE is:

$$\frac{dAE}{dt} = k_1 AS - k_2 AE + k_3 AB \quad (19)$$

where AE is the amount of chemical in the VE. The rate constants k_2 and k_3 in equation 19 have been represented in terms of the physicochemical and physiological properties of the skin (McCarley and Bunge 2001). The rate constant k_2 has been expressed as $Q_{ve}/(V_{ve} \times P_{ve:b})$ where Q_{ve} is the volumetric flow rate to the exposed area of skin, V_{ve} is the volume of the exposed VE, and $P_{ve:b}$ is the solubility of the chemical in the blood relative to the VE, i.e., VE:blood partition coefficient. The rate constant k_3 is represented as Q_{ve}/V_b. Rearranging, $P_{ve:b}$ therefore equals $(V_b/V_{ve}) \times (k_3/k_2)$. Using this expression, we estimated an average $P_{ve:b}$ of 5 for aromatic compounds and 3 for aliphatic compounds. The $P_{ve:b}$ for 1-methyl naphthalene was larger than other components of JP-8; when this value was taken out of the calculation, we estimated a $P_{ve:b}$ of 3 also for the aromatic components. Our estimates were similar to $P_{ve:b}$ reported in the literature. McCarley and Bunge (2001) calculated $P_{ve:b}$ using the following equation:

$$P_{ve:b} = \frac{(1 - f_{fat,ve}) + f_{fat,ve} K_{ow}}{(1 - f_{fat,b}) + f_{fat,b} K_{ow}} \quad (20)$$

where $f_{fat,ve}$ and $f_{fat,b}$ are the fractions of fat in the VE and blood respectively, and K_{ow} is the octanol:water partition coefficient. Using equation 15, $f_{fat,ve}$ = 0.02, and $f_{fat,b}$ = 0.007, the predicted value of $P_{ve:b}$ was 3 for all aromatic and aliphatic hydrocarbons examined in our study. The consistency between estimating $P_{ve:b}$ using equation 15 and the values that we report in our study give confidence to our findings.

Another major change we made to the basic DTK model was the addition of a storage compartment. JP-8 is a mixture of lipophilic hydrocarbons, which suggests that sequestration of JP-8 components in fat stores throughout the body is very likely. Chemicals are stored in fat by dissolution in neutral fats, which constitute from about 20 – 50% of the body weight (Klaassen 1996). Thus, considerable amounts of chemicals with high fat:blood partition coefficients will be stored in body fat.

Also, blood proteins such as albumin can bind with chemicals and serve as a depot protein. Further, the liver and kidneys both have a high capacity for metabolism and/or binding chemicals before elimination by active transport (Klaassen 1996). Few DTK models have included a storage compartment for toxicants. Qiao *et al*. (2000) included a storage compartment to quantify the toxicokinetic behavior of *p*-nitrophenol in swine using a 12-compartment model. They found that the peripheral compartment was able to store a constant amount of *p*-nitrophenol, and the excess was redistributed to the systemic circulation for elimination. In our study, simulations of dermal exposure to JP-8 showed that the storage capacity of the SC compared to the VE is small, while as expected, the storage compartment is a larger reservoir for exogenous chemicals.

For the six aromatic and aliphatic components of JP-8 that we examined in our study, there are three significant clearance pathways: metabolism, exhalation, and urination. Urinary clearance is not considered to be a major pathway for chemicals with high K_{ow} since they will be reabsorbed efficiently through the tubular cells of the nephron back into the systemic circulation. The metabolic clearance of all the components of JP-8, mostly from the liver, is not well understood. The metabolism of naphthalene, however, has been studied extensively (ATSDR 1995; Buckpitt and Bahnson 1986; US EPA 1998). Phase I metabolism of naphthalene involves oxygenation by the cytochrome P450 monooxygenases (e.g., CYP 1A1) to naphthalene-1,2-oxide. This epoxide rearranges to 1- or 2-naphthol or undergoes phase II reactions to form more water-soluble compounds for eventual urinary clearance. The metabolism of aliphatic components, such as dodecane, is not well understood, but they are thought to undergo oxidation reaction to a ketone through an intermediate hydroxylation step (Subcommittee on Jet-Propulsion Fuel 8 2003). Clearance by exhalation is the other major loss mechanism for volatile organics. Pulmonary clearance can be approximated by cardiac output times the ratio $1 / (1+P_{b:a})$ where $P_{b:a}$ is the blood:air partition coefficient (Andersen *et al.* 2001). For naphthalene ($P_{b:a} \approx 571$), pulmonary clearance is 0.2% of cardiac output whereas for decane ($P_{b:a} \approx 5$) it is 16%. The difference in pulmonary clearance between the aromatic and aliphatic components may explain the difference in estimates of k_4 between aliphatic ($k_4 = 0.11$ min^{-1}) and aromatic ($k_4 = 0.04$ min^{-1}) components of JP-8.

We constructed and evaluated a DTK model based on empirical data that may be used to quantify the absorption, distribution, and elimination of aromatic and aliphatic compounds following dermal exposure to JP-8. The final optimized model was used to simulate the time-course of naphthalene and other components of JP-8 using information collected in an occupational exposure assessment study (Chao *et al.* 2005; Chao *et al.* 2006). We observed that the predicted cumulative internal dose was distinctly different among low-, medium-, and high-exposure groups. This supports the hypothesis that dermal exposure measurements made by tape-strip sampling may be used in exposure assessment studies. We note that biological variability will introduce more variation into the distribution of $DOSE_c$. In our study, we could not examine inter- and/or intra-individual variation in the disposition of JP-8 components due to the limited sample size. Further study is required to better estimate inter- and intra-individual variability in exposure measurements for different work processes. We have described here a DTK model that will be useful for the development of a toxicokinetic modeling strategy for multi-route exposures to jet fuel in humans.

CHAPTER 4

HUMAN DERMAL AND INHALATION EXPOSURES TO JET FUEL CAN BE PREDICTED USING A PBTK MODEL

David Kim, Melvin E. Andersen, Yi-Chun E. Chao, Peter P. Egeghy, Stephen M. Rappaport, and Leena A. Nylander-French

(Manuscript)

4.1 Abstract

Occupational exposure studies have measured dermal and inhalation exposures to jet-propulsion fuel type 8 (JP-8); however, a quantitative understanding of the contribution of external exposure to internal dose is lacking for occupational and environmental exposure scenarios. We constructed a physiologically based toxicokinetic (PBTK) model, which accurately describes the disposition of naphthalene, a prominent aromatic constituent of JP-8, in humans. We then estimated the relative contributions of dermal and inhalation exposures to the systemic levels of naphthalene. The PBTK model consisted of five compartments representing the stratum corneum, viable epidermis, blood, fat, and other tissues. The parameters were optimized using exclusively human exposure and biological monitoring data. The optimized values of parameters for naphthalene were (1) blood:air partition coefficient = 27.1, (2) fat:blood partition coefficient = 40.4, (3) permeability coefficient for the stratum corneum = 5.2×10^{-5} cm/h, (4) stratum corneum:viable epidermis partition coefficient = 12.7, and (5)

permeability coefficient for the viable epidermis = 2.0 cm/h. The estimated permeability coefficient was comparable to the values estimated from *in vitro* studies. Based on simulations of worker's exposures to JP-8 during aircraft fuel-cell maintenance operations, the median relative contribution of dermal exposure to the internal dose of naphthalene was 1.7% (10^{th} percentile = 0.3% and 90^{th} percentile = 6.9%). PBTK modeling allowed contributions of the systemic dose of naphthalene, an important JP-8 constituent, to be partitioned between dermal and inhalation routes of exposure. The model also pointed to the need for further exposure assessment to provide data with which to better characterize the toxicokinetic behavior of JP-8 components following occupational and environmental exposures.

4.2 Introduction

The single largest source of chemical exposure on military bases of the North Atlantic Treaty Organization (NATO) is jet-propulsion fuel 8 (JP-8), which is the preferred fuel for both aircraft and military vehicles in NATO countries. JP-8 is composed of many aromatic hydrocarbons, including benzene and naphthalene, and aliphatic hydrocarbons such as nonane and decane (McDougal *et al.* 2000). Exposures to JP-8 can occur during spills, transportation and storage of the fuel, as well as fueling, general maintenance and operation of aircraft and military vehicles, fueling of military tent heaters, and cleaning and degreasing of parts with the fuel.

Since JP-8 can enter the body via both inhalation and dermal contact, the assessment of occupational exposures to fuel constituents can be difficult. Personal sampling of JP-8 vapors provides information about levels in the breathing zone but not from dermal contact. Likewise sampling the exposed skin provides information about dermal contact but not inhalation. The collection of end-exhaled breath concentrations, on the other hand, provides an integrated estimate of uptake via both inhalation and dermal contact (Egeghy *et al.* 2003; Pleil *et al.* 2000) but cannot determine the relative contributions of the two exposures routes to the internal dose. Through statistical evaluation of levels of naphthalene in air, breath and skin, measured in Air Force personnel during fuel maintenance procedures, Chao *et al.* (2006) demonstrated that both inhalation and dermal exposures to JP-8 contributed to the internal dose. However, given the use of respiratory protection

in that population, it was difficult to determine the relative contributions of dermal and inhalation exposures to the systemic levels of JP-8 components.

Physiologically based toxicokinetic (PBTK) modeling is an effective tool for quantifying the absorption, distribution, metabolism, and elimination of chemicals. PBTK models have been developed for various components of JP-8, notably naphthalene and decane (Perleberg *et al.* 2004; Quick and Shuler 1999; Willems *et al.* 2001) The model developed by Quick and Shuler (1999) focused upon the disposition of naphthalene in five compartments representing the lungs, liver, fat, rapidly perfused tissues, and slowly perfused tissues and relied upon *in vitro* data to calibrate kinetic constants. Willems *et al*. (2001) refined the Quick and Shuler (1999) model by using kinetic constants derived from *in vivo* data from laboratory animal experiments performed by the National Toxicology Program. They observed that a diffusion-limited PBTK model was necessary to characterize the toxicokinetic behavior of naphthalene in rats and mice. Perleberg *et al*. (2004) developed a PBTK model using decane as a chemical marker of JP-8. Data for calibration and validation of this model was derived from an animal study where rats were exposed for 4 h to decane vapor at three different concentrations: 1200 ppm, 781 ppm, or 273 ppm. Their final model consisted of flow-limited compartments for liver and lung, and diffusion-limited compartments for the brain, bone marrow, fat, skin, and spleen. The model was used to adequately predict the time course of decane in tissue and blood from low-level exposures to decane vapor.

Since the PBTK models mentioned above did not examine the uptake via dermal exposure, we developed a PBTK model, which included both inhalation and dermal sources of exposure. Naphthalene was chosen as the surrogate for JP-8 exposure because it is abundant in JP-8, is readily absorbed into blood, and is only a minor component in confounding sources of exposure, such as cigarette smoke and gasoline exhaust (Rustemeier *et al.* 2002; Serdar *et al.* 2003). The model was calibrated with concentrations of naphthalene measured in the skin, in the personal breathing zone air, and in the end-exhaled breath samples of US Air Force personnel (Chao *et al.* 2005; Egeghy *et al.* 2003) and in a study of controlled dermal exposure in humans (Kim *et al.* 2006).

4.3 Methods

4.3.1 Laboratory study of dermal exposure to JP-8

A laboratory study was conducted to quantify the dermal absorption and penetration of JP-8 components across human skin *in vivo* (Kim *et al.* 2006). Ten volunteers (five females and five males) were recruited for this study. Briefly, exposures were conducted in an exposure chamber (20.3 cm width × 20.3 cm length × 18.8 cm height and a total volume of 7706 cm^3). One forearm was placed palm up inside the exposure chamber, and two aluminum application wells were pressed against the skin and sealed for the duration of the experiment (0.5 h). At the end of the 0.5 h exposure period, the exposed sites were tape-stripped 10 times with adhesive tape strips (Cover-Roll™ tape; Beiersdorf, Germany). Blood samples were drawn from the unexposed arm at baseline, 0.5, 1, 1.5, 2, 2.5, 3, and 3.5 h. Both tape-strip and blood samples were analyzed by gas chromatography mass spectrometry (GC-MS). The time course of naphthalene in blood for all study volunteers showed considerable inter-individual variability. For example, the time course for a 23-year-old Caucasian male with a body mass index (BMI) of 25 kg/m^2 was very different from a 24-year-old Caucasian female with a BMI of 22 kg/m^2. For the male volunteer, the maximum concentrations in blood (C_{max}) occurred shortly after the end of exposure ($t_{max} \approx 30$ min) with a value of 0.8 ng/ml. The C_{max} for the female volunteer occurred at $t_{max} \approx 60$ min with a value of 0.3 ng/ml. In either case, the concentrations in blood at $t > 0$ min did not reach baseline levels.

4.3.2 Field study of dermal and inhalation exposures to JP-8

Exposure data was obtained from the assessment of dermal and inhalation exposures to JP-8 in the personnel at six US Air Force bases in the continental US (Chao *et al.* 2005; Egeghy *et al.* 2003). The duration of exposure was approximately 4 h. The concentration of naphthalene in the personal breathing zone air (referred to as air concentration from here on) was measured using passive monitors (Egeghy *et al.* 2003). End-exhaled breath samples were collected pre- and post-exposure (Egeghy *et al.* 2003). Both air and breath samples were analyzed by gas chromatography with photoionization detection. Dermal samples were collected post-exposure using adhesive tape strips with dimensions of 2.5 cm × 4.0 cm (surface area 10 cm^2) from exposed body regions including the

forehead, neck, shoulders, arms, hands, legs, knees, feet, and buttocks (Chao *et al.* 2005). All tape-strip samples were extracted with acetone and analyzed by gas chromatography-mass spectrometry.

The median air concentrations of naphthalene in air samples were 1.9 μg/m^3 (range: <1.0 - 16.9 μg/m^3), 29.8 μg/m^3 (range: <1.0 - 932 μg/m^3), and 867 μg/m^3 (range: 12.8 - 3910 μg/m^3) for the low-, medium-, and high-exposure groups, respectively (Egeghy *et al.* 2003). The median pre-exposure breath levels of naphthalene were <0.5 μg/m^3 (range: <0.5 – 36.3 μg/m^3), <0.5 μg/m^3 (range: <0.5 - 16.1μg/m^3), and <0.5 μg/m^3 (range: <0.5 - 6.1 μg/m^3) for the low-, medium-, and high-exposure groups. The median post-exposure breath levels were 0.73 μg/m^3 (range: <0.5 - 6.9 μg/m^3), 0.93 μg/m^3 (range: <0.5 - 13.0 μg/m^3), and 1.83 μg/m^3 (range: <0.5 - 15.8 μg/m^3) for the low-, medium-, and high-exposure groups, respectively. The corresponding median concentrations of dermal samples were 344 ng/m^2 (range: 159 - 54 200 ng/m^2), 483 ng/m^2 (range: 150 - 13 200 ng/m^2), and 4188 ng/m^2 (range: 100 - 4 880 000 ng/m^2) in the low-, medium-, and high-exposure groups (Chao *et al.* 2005).

4.3.3 Description of the PBTK model

A dermatotoxicokinetic (DTK) model, which was previously developed for describing the disposition of aromatic and aliphatic components of JP-8 following controlled dermal exposure (Kim *et al.* submitted), formed the basis of the PBTK model (Figure 12). The DTK model consisted of five compartments representing the surface, stratum corneum, viable epidermis, blood, and storage tissues. The parameters for the DTK model were estimated by fitting the model to the data. The major difference between the DTK and the PBTK model structures is that the storage compartment was split into fat and all other tissues. The rationale behind defining the storage compartment in this fashion was based on the high fat:blood partition coefficient ($P_{f:b}$) of naphthalene (160), which is more than five times the partition coefficient of the other tissues (Fiserova-Bergerova 1983). Further additions to the PBTK model included pulmonary uptake and clearance. All compartments in the PBTK model corresponded to the actual anatomy and physiology of humans. The skin compartments were composed of the skin directly under the exposed area. All tissues were perfusion limited and well-mixed. Absorbed naphthalene was distributed to other tissue compartments at a rate equal to

the blood flow rate to that tissue. Naphthalene was stored in the fat and other tissue compartments based on the physiological parameters of that compartment, i.e., tissue:blood partition coefficient, tissue volume, and blood perfusion rate.

Most physiologically based compartmental models separate the arterial blood from the central venous blood. Data based compartmental models treat the blood as one compartment. Also in data based compartmental models, the peripheral compartments represent organs or tissues that, being poorly perfused with blood, are in slower equilibrium distribution with blood. Blood samples were collected from the antecubital vein in the study by Kim *et al*. (2006). The antecubital vein drains blood from the hand and the superficial layers of the forearm. The concentration of solute in the antecubital vein is different from the concentrations of solute in the arterial and central venous blood (Levitt 2004). However, the blood in the antecubital vein is in rapid equilibrium with arterial and central venous blood relative to the fat and other tissue compartments. Therefore, we treated the arterial and central vein as a single compartment, and approximated the concentration of naphthalene in the central (i.e., blood) compartment using measurements made from the antecubital vein.

Two routes of exposure were modeled: dermal and inhalation. Pulmonary uptake is equal to the ventilation rate (QP) times the concentration of naphthalene in the personal breathing zone (C_{PBZ}):

$$\text{Pulmonary uptake} = QP \times C_{PBZ} \tag{21}$$

In equation 21, rapid equilibration of naphthalene takes place across the alveolar lining, and neither storage nor metabolism in the lungs appreciably affects the uptake of naphthalene into the systemic circulation. Since arterial, lung, and venous blood are treated as a combined blood compartment, the rate of absorption is equal to pulmonary uptake. Dermal absorption and penetration is modeled as a one-directional diffusive process according to Fick's first law of diffusion. As such, the diffusion of naphthalene across the stratum corneum (SC) and the viable epidermis (VE) are quantified using permeability coefficients, the area of exposure, and the thickness of the membrane (McCarley and Bunge 2001; McDougal and Boeniger 2002). The rate of efflux from the SC to the VE is dependent on the solubility of naphthalene in the SC relative to the VE. Therefore, the rate of efflux of

naphthalene from the SC to the VE is equal to $K_{pv} \times A_{exp} \times CD/PD$, where K_{pv} is the permeability coefficient across the VE, CD is the concentration in the SC, A_{exp} is the exposed surface area, and $P_{sc:ve}$ is the SC:VE partition coefficient. The mass balance differential equation (MBDE) for the SC is:

$$\frac{dAD}{dt} = K_{uptake}\, DERMDOSE - \frac{K_{pv}}{P_{sc:ve}} A_{exp}\, CD \tag{22}$$

where K_{uptake} is the input rate constant and DERMDOSE is the dose to the skin. The rate of input from blood to VE is the cutaneous blood flow rate (QE) times the concentration of naphthalene in blood (CB), and the rate of efflux from the VE to blood is controlled by QE and the solubility of naphthalene in the blood ($P_{ve:b}$). The MBDE for the amount of naphthalene in the VE is:

$$\frac{dAE}{dt} = \frac{K_{pv}}{P_{sc:ve}} A_{exp}\, CD + QE\left(CB - \frac{CE}{P_{ve:b}} \right) \tag{23}$$

where AE is the amount and CE is the concentration of naphthalene in the VE.

Elimination of naphthalene proceeds by two significant mechanisms: exhalation and metabolism. The concentration of naphthalene in end-exhaled air is equal to the blood concentration divided by the blood:air partition coefficient ($P_{b:a}$). Pulmonary clearance of naphthalene is the ventilation rate (QP) divided by $P_{b:a}$. Metabolism of naphthalene occurs in the liver by a single metabolic pathway following first-order kinetics. The initial step in naphthalene metabolism is the formation of naphthalene-1,2-oxide by cytochrome P450 monooxygenases (ATSDR 1995). Liver clearance (Cl_L) is:

$$Cl_L = QL\left(\frac{V_{max}/K_M}{V_{max}/K_M + QL} \right) \tag{24}$$

where V_{max} (mg/min) is the maximum rate of metabolism, K_M (mg/L) is the Michaelis-Menten constant, and QL the blood flow rate to the liver (L/min). The ratio of liver clearance to liver blood flow is the extraction ratio (E_L) where E_L is:

$$E_L = \frac{V_{max} / K_M}{V_{max} / K_M + QL} \tag{25}$$

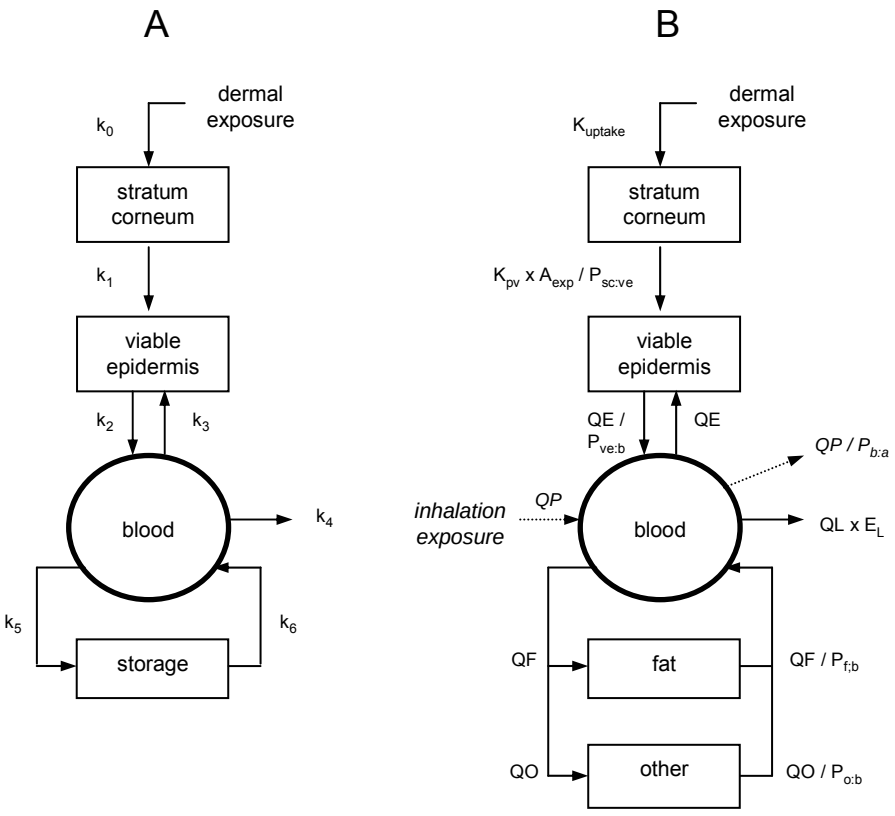

Figure 12. Schematic of the (A) dermatotoxicokinetic (DTK) and (B) physiologically based toxicokinetic (PBTK) models for the study of naphthalene toxicokinetics. Pulmonary uptake of naphthalene in the personal breathing zone and pulmonary clearance from the blood compartment are added to the DTK model.

Table 9. Naphthalene PBTK model parameters.

Parameter	Symbol	Units	Value	Notes and References
Body weight	BW	kg	61	Kim *et al*. (in press)
Height	HT	cm	174	Kim *et al*. (in press)
Body mass index	BMI	kg/m^2	20	$BMI = BW / HT^2$
Organ volumes				
Blood[a]	V_b	L	4.5	$BW = (72.447/1000) \times BW^{1.007}$
Stratum corneum	V_{sc}	L	2×10^{-5}	$VD = A_{exp} \times Td$
Viable epidermis[b]	V_{ve}	L	1.9×10^{-3}	$VE = VEC \times BW - VD$
Fat[c]	V_f	L	5.5	$VF = BW \times (\ln BMI - 126.2)/100$
Other tissue	V_o	L	51.0	VO = BW – (VB+VD+VE+VF)
Ventilation rate	QPC	$L/h/BW^{0.75}$	15	Brown *et al*. (1997)
Cardiac output	QCC	$L/h/BW^{0.75}$	15	Brown *et al*. (1997)
Regional blood flow				
to skin[d]	QE	L/h	1.7×10^{-2}	$QE = QEC \times (A_{exp}/SURFA)$
to fat	QF	L/h	16.4	$QF = QFC \times QC$
to other tissues	QO	L/h	311.0	QO = QC – (QE+QF)
Metabolic clearance parameters				
ratio of V_{max}:K_M	V_{max}/K_M	L/h	698	Willems *et al*. (2001)
blood flow to liver	QL	L/h	75.3	$QL = QLC \times QC$
Partition coefficients				
blood:air	$P_{b:a}$	-	27.1	estimated
stratum corneum:viable epidermis	$P_{sc:ve}$	-	12.7	estimated
VE:blood	$P_{ve:b}$	-	2.8	McCarley and Bunge (2001)
fat:blood	$P_{f:b}$	-	40.4	estimated
other tissue:blood	$P_{o:b}$	-	4.2	estimated
Skin permeation parameters				
area of exposure	A_{exp}	cm^2	20	Dimensions of the tape strip
total body surface area[e]	SURFA	cm^2	19238	$(BW^{0.45}) \times (HT^{0.725}) \times 71.84$
permeability coefficient for stratum corneum	K_{ps}	cm/h	5.2×10^{-4}	estimated
permeability coefficient for viable epidermis	K_{pv}	cm/h	2.0	estimated

[a] Davies and Morris (1993)

[b] The volume of the viable epidermis is calculated as the volume of the exposed skin minus the volume of the stratum corneum under the exposed area. The fraction of body weight in skin (VEC) is from Brown *et al*. (1997)

[c] The fraction of body weight in fat = ln BMI – 126.2 (Mills 2005).

[d] The fractions of cardiac output to skin (QEC) and to liver (QLC) were obtained from Brown *et al*. (1997).

[e] Total body surface area (Haycock *et al.* 1978).

4.3.4 Model parameters

All physiological parameters (cardiac output, ventilation rate, blood flow rate to the tissues, and tissue volumes) for humans were obtained from the literature (Table 9) (Brown *et al.* 1997). Tissue partition coefficients were predicted from the octanol-water partition coefficients and regression models for different tissues (Abraham *et al.* 1985; Fiserova-Bergerova *et al.* 1984; Hansch *et al.* 1995; Willems *et al.* 2001). The maximum rate of naphthalene metabolism (V_{max}) and Michaelis-Menten constant (K_M) have been estimated for rats and mice (Willems *et al.* 2001). In our study, the rate of metabolism was assumed to follow first-order kinetics, given the relatively low naphthalene concentrations measured in post-exposure breath samples (Egeghy *et al.* 2003).

4.3.5 Parameter estimation

Based upon preliminary sensitivity analyses, the blood:air partition coefficient ($P_{b:a}$) was most sensitive for predicting breath concentrations. The $P_{b:a}$ value of 571 for naphthalene reported by Willems *et al*. (2001) is unusually large. For comparison, the $P_{b:a}$ for some aromatic and aliphatic components of JP-8 are 8.8 for benzene (Thrall *et al.* 2002), 13.9 for toluene (Thrall *et al.* 2002), 6.9 for decane (Smith *et al.* 2005), and 30.3 for dodecane (Smith *et al.* 2005). Similarly, the fat:blood partition coefficient ($P_{f:a}$) was reported high (160.4) by Willems *et al*. (2001). The reported $P_{f:a}$ for benzene is 55 (Travis *et al.* 1990) and 25 for decane (Perleberg *et al.* 2004). Field exposure data for Air Force personnel with only inhalation exposure (i.e., no dermal exposure) to naphthalene were used for optimization of $P_{b:a}$. The optimized value of $P_{b:a}$ was then kept constant, and the parameters K_{uptake}, K_{pv}, $P_{sc:ve}$, $P_{f:a}$, and other tissue:blood partition coefficient ($P_{o:b}$) were adjusted to fit the blood time course data for each volunteer in the laboratory study. Initial values of all parameters were obtained from the literature (Guy and Potts 1992; McCarley and Bunge 2001; Qiao *et al.* 2000; Willems *et al.* 2001; Williams and Riviere 1995). The Nelder-Mead algorithm was used to optimize parameters, with tolerance set at 1×10^{-5} (Xcellon 2004). Relatively large ranges were allowed in the optimization step because little is known about them for naphthalene for humans under *in vivo* conditions.

4.3.6 Model validation

A subset of the Air Force data was set aside for validation of the optimized model. This dataset included personnel who had both dermal and inhalation exposure to JP-8. The concentrations of naphthalene in the air and dermal samples and the duration of exposure were used as input terms for the model. Predicted end-exhaled breath concentrations were compared to measured levels of end-exhaled breaths.

For the medium- and high-exposure groups, end-exhaled breath samples were collected immediately at the end of the work and, sometime later, at a central testing site (CTS). Three US Air Force personnel were selected from the medium- and high-exposure groups, combined, who represented the 10^{th}, 50^{th}, and 90^{th} percentiles based on the end-exhaled breath measurements. The medium- and high-exposure groups included individuals who came in regular contact with jet fuel. In addition, the high-exposure group consisted of fuel-cell maintenance workers who entered fuel tanks during their work. Therefore, the concentration of naphthalene in the air was much higher in the immediate work environment for these two exposure groups compared to the low-exposure group, which had no direct contact with JP-8 and, therefore, represented background exposures to naphthalene. The air concentration of naphthalene was reported for the duration of the sampling period, which included travel time to the CTS (approximately 30 min). Thus, the air concentration at the work site was estimated as:

$$INHAL1_{est} = \frac{C_{PBZ} \times \Delta t_{total} - INHAL2_{est} \times \Delta t_{travel}}{\Delta t_{work}} \quad (26)$$

where $INHAL1_{est}$ is the concentration of naphthalene in the breathing zone during the work shift of Δt_{work} h, C_{PBZ} is the air concentration measured during the full sampling period of Δt_{total} h, $INHAL2_{est}$ is the background air concentration of naphthalene estimated for the low-exposed group, and Δt_{travel} is the time required to travel from the workplace to the CTS.

4.3.7 Sensitivity analysis

Sensitivity analyses were performed to evaluate the relative importance of model parameters on the concentrations of naphthalene in end-exhaled breath. Sensitivity coefficients were calculated using equation 27 (Evans and Andersen 2000).

$$\text{Sensitivity Coefficient} = \frac{\Delta m}{m} \times \frac{p}{\Delta p} \quad (27)$$

where m is the response variable (i.e., concentration of naphthalene in end-exhaled breath), Δm is the change in the response variable, p is the value of the parameter of interest (e.g., blood:air partition coefficient), and Δp is the change in the parameter value. Each parameter was changed 1% (i.e., $\Delta p \div p = 0.01$).

4.4 Results

4.4.1 Inhalation exposure toxicokinetics

The PBTK model was optimized for inhalation exposure using data from 76 Air Force personnel (19 females and 57 males) who did not have dermal contact with jet fuel. Only $P_{b:a}$ was adjusted to fit the end-exhaled breath concentrations of naphthalene in this low-exposure group. The median height and weight of the personnel were 175 cm and 76 kg, respectively. In the optimization procedure, the median air concentration of naphthalene was 2.0 μg/m^3 (range: 0.7 - 482 μg/m^3) and was held constant for the duration of exposure (median duration = 235 min). For each US Air Force subject, the pre-exposure concentration of naphthalene in the end-exhaled breath was subtracted from the post-exposure measurements. The median end-exhaled breath level of naphthalene was 0.2 μg/m^3 (range: 0 - 12.4 μg/m^3). The optimized value of $P_{b:a}$ was 27.1.

4.4.2 Dermal exposure toxicokinetics

The average height and weight of the subjects to which JP-8 was dermally administered was 174 cm and 61 kg, respectively (BMI = 21 kg/m^2). Time-course plots showed considerable variability

among the study volunteers (Figure 14). The mean and standard deviation (SD) of the peak concentration of naphthalene in blood was 0.18 ± 0.22 ng/ml and occurred at 62 ± 16 min. The time course for subject No. 1 was very different from that of the other volunteers. The peak concentration for this volunteer was 0.80 ng/ml and occurred at 37 min. Model predictions of the blood concentration of naphthalene are also shown for each volunteer (Figure 14) using optimized parameter values. The skin parameters (K_{uptake}, K_{pv}, and $P_{sc:ve}$) and the partition coefficients $P_{f:b}$ and $P_{o:b}$ were adjusted to fit the blood time course data for dermal exposures only. The rate of input from dermal exposure is equivalent to the product of the permeability coefficient for the SC (K_{ps}), the exposed surface area (A_{exp}), and the concentration of the naphthalene in JP-8 (C_{JP-8}) (McCarley and Bunge 2001; McDougal and Boeniger 2002):

$$\text{rate of input} = K_{uptake} \times \text{DERMDOSE} = K_{ps} \times A_{exp} \times C_{JP-8} \tag{28}$$

Equation 28 can be rearranged to solve for the stratum corneum permeability coefficient K_{ps} as follows:

$$K_{ps} = \frac{K_{uptake} \times \text{DERMDOSE}}{A_{exp} \times C_{JP-8}} \tag{29}$$

The optimized value of K_{uptake} is 0.027 ± 0.053 h^{-1} (mean ± SD), and for K_{ps} it is $5.2\times10^{-5} \pm 5.0\times10^{-5}$ cm/h (mean ± SD) (Table 10). The effective permeability coefficient (K_{eff}) for the epidermis is 5.2×10^{-5} cm/h.

Table 10. Optimized values of the skin parameters K_{uptake}, K_{pv}, $P_{sc:ve}$, $P_{f:b}$, and $P_{o:b}$. K_{ps} was calculated using equation 29. The parameters were optimized for each of the 10 study volunteers.

Volunteer	$K_{uptake}\times10^{-3}$ (h^{-1})	$K_{ps}\times10^{-5}$ (cm/h)	K_{pv} (cm/h)	$P_{sc:ve}$	$P_{f:b}$	$P_{o:b}$
1	176.8	17.4	0.0058	1.0	4.4	0.6
2	3.4	0.8	9.1	4.8	1.3	2.0
3	7.8	4.6	0.0059	4.3	75.0	6.2
4	16.8	2.5	0.010	3.8	12.0	2.5
5	7.3	5.1	0.020	5.9	3.9	2.0
6	17.2	8.8	0.024	14.7	10.0	5.9
7	10.2	5.6	0.00092	0.5	49.8	3.0
8	20.0	4.4	0.26	78.5	61.6	17.3
9	7.5	1.3	1.3	13.7	6.1	1.3
10	3.1	1.1	9.1	0.2	180	1.1
mean	27.0	5.2	2.0	12.7	40.4	4.2
SD	53.0	5.0	3.8	23.7	56.1	5.0

SD, standard deviation;

K_{ps}, the permeability coefficient for the stratum corneum;

K_{pv}, the permeability coefficient for the viable epidermis;

K_{uptake}, the rate constant for uptake into the stratum corneum;

$P_{sc:ve}$, the stratum corneum:viable epidermis partition coefficient;

$P_{f:b}$, the fat:blood partion coefficient;

$P_{o:b}$, the other tissue:blood partition coefficient;

DERMDOSE, dose to the skin;

A_{exp}, exposed surface area;

C_{JP-8}, JP-8 concentration in the tape-strips.

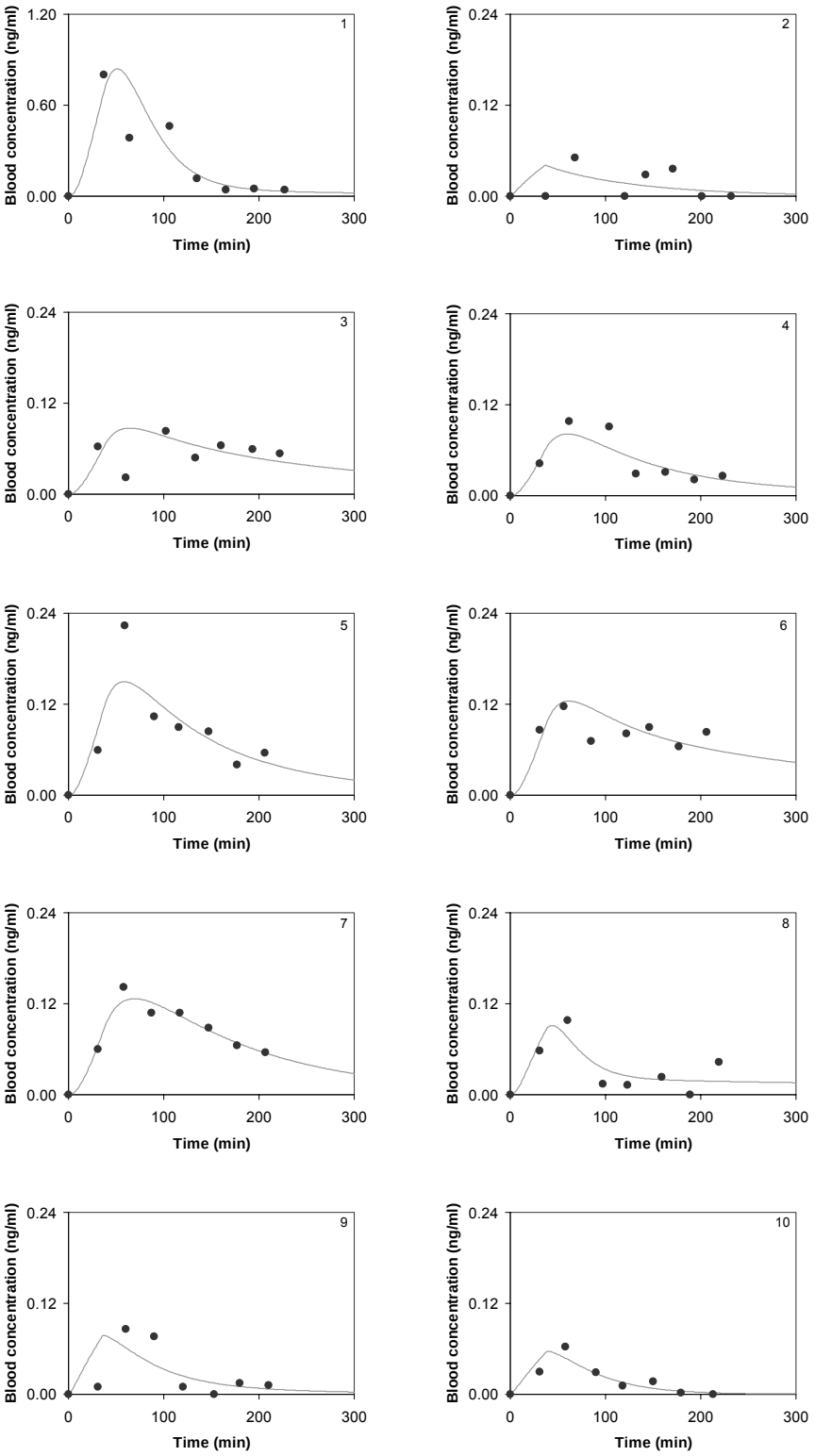

Figure 13. Plots comparing the PBTK model simulations to experimentally measured naphthalene concentrations in blood from 10 study volunteers who were dermally exposed to JP-8 on the volar forearm.

4.4.3 Predictions of end-exhaled breath concentrations

Model predictions of the end-exhaled breath concentration of naphthalene were compared to field measurements among three Air Force personnel who represented the 10^{th}, 50^{th}, and 90^{th} percentiles based on the end-exhaled breath concentrations. These three US Air Force personnel were in the high-exposure group; thus, they spent time in a fuel tank during their work shift. The input parameters and values for each US Air Force personnel are reported in Table 11. The PBTK model consistently over-predicted the end-exhaled breath concentrations at the end of work for all three US Air Force personnel (Figure 14). This could be attributed to the use of supplied-air respirators. Therefore, the air concentration of naphthalene during work (i.e., $INHAL1_{est}$) was adjusted (i.e., $INHAL1_{adj}$) to better estimate the true inhalation exposure (Figure 14). The values of $INHAL1_{adj}$ are reported in Table 12.

Table 11. Input parameters and values for prediction of end-exhaled breath concentrations of naphthalene in US Air Force personnel who represented the 10^{th}, 50^{th}, and 90^{th} percentiles based on end-exhaled breath measurements.

Variable	10^{th} percentile	50^{th} percentile	90^{th} percentile
height (cm)	175	188	168
body weight (kg)	81	109	73
$INHAL1_{est}$ (μg/m^3)	499	322	3640
$INHAL2_{est}$ (μg/m^3)	2.0	2.0	2.0
DERMDOSE (μg/cm^2)	3.9×10^{-5}	5.5×10^{-4}	9.2×10^{-3}
Duration of exposure (min)	224	322	260

$INHAL1_{est}$, the estimated air concentration of naphthalene during work;
$INHAL2_{est}$, the background air concentration of naphthalene;
DERMDOSE, dose to the skin.

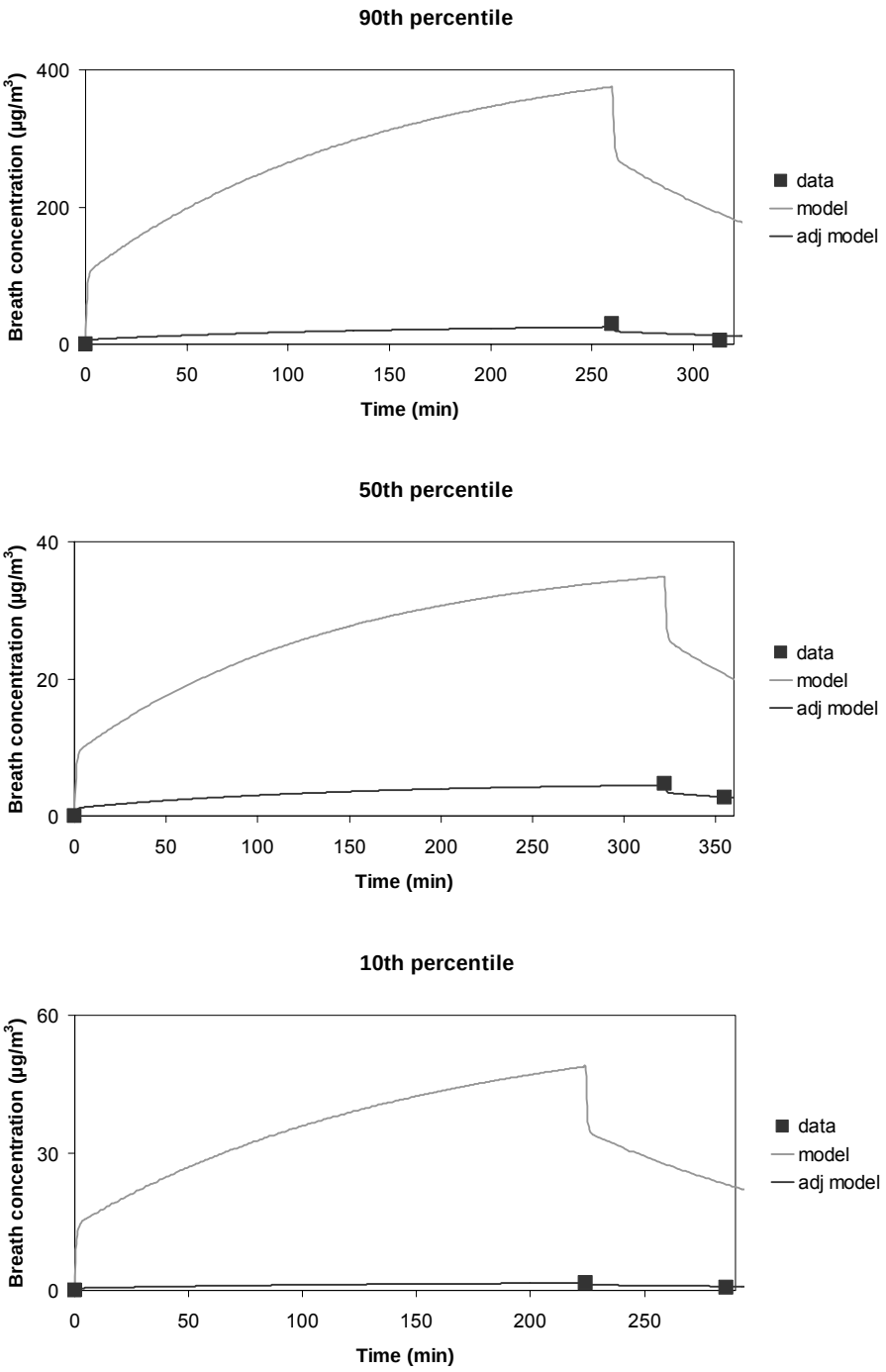

Figure 14. Model simulations and end-exhaled breath concentrations for the US Air Force personnel who were exposed to JP-8 via inhalation and dermal routes. Breath samples were collected immediately at the end of the work shift and at a central testing site (CTS). Shown are the measured and predicted values for three US Air Force personnel who represented the 10^{th}, 50^{th}, and 90^{th} percentiles of measured end-exhaled breath concentrations. Simulations are also shown after adjusting the air concentration of naphthalene during work to better estimate the true inhalation exposure (adj model).

4.4.4 Sensitivity analysis

Normalized sensitivity coefficients (mean) were calculated separately for exposure and physiological parameters in the medium- and high-exposure groups. The response variable in both sets of calculations was the concentration of naphthalene in the end-exhaled breath. For exposure variables, the resulting sensitivity coefficients were positive (Figure 15). The end-exhaled breath concentrations were most sensitive to the estimated air concentration of naphthalene during work ($INHAL1_{est}$). The sensitivity coefficient for $INHAL1_{est}$ was 1.0 for both the medium- and high-exposure groups. End-exhaled breath concentrations were not sensitive to the variables DERMDOSE and A_{exp}. In the PBTK model, the end-exhaled breath concentration of naphthalene was most sensitive to cardiac output (-0.7), ventilation rate (1.0), and the blood:air partition coefficient (-0.9) (Figure 16). The sensitivity coefficients for other parameters were less than |0.2|.

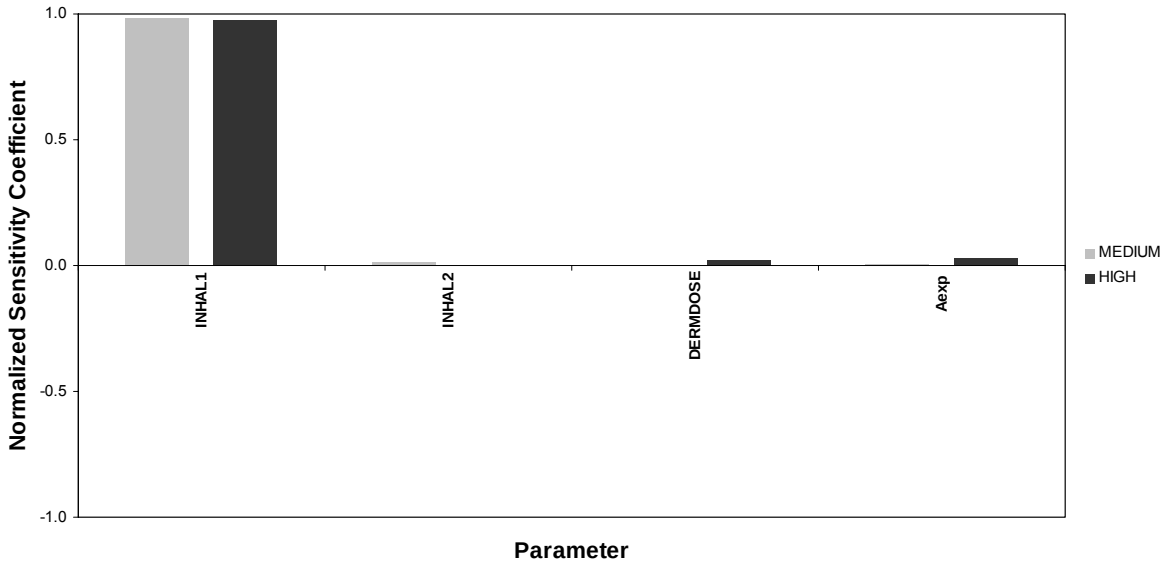

Figure 15. Normalized sensitivity coefficients for the end-exhaled breath concentrations in the medium- and high-exposure groups. The parameters $INHAL1_{est}$ and $INHAL2_{est}$ are the naphthalene air concentrations ($\mu g/m^3$) during work and during travel to the central testing site, respectively. DERMDOSE is the mass (µg) of naphthalene in the tape strips and A_{exp} is the area of the exposed site (cm^2). Parameters were adjusted at the 1% level.

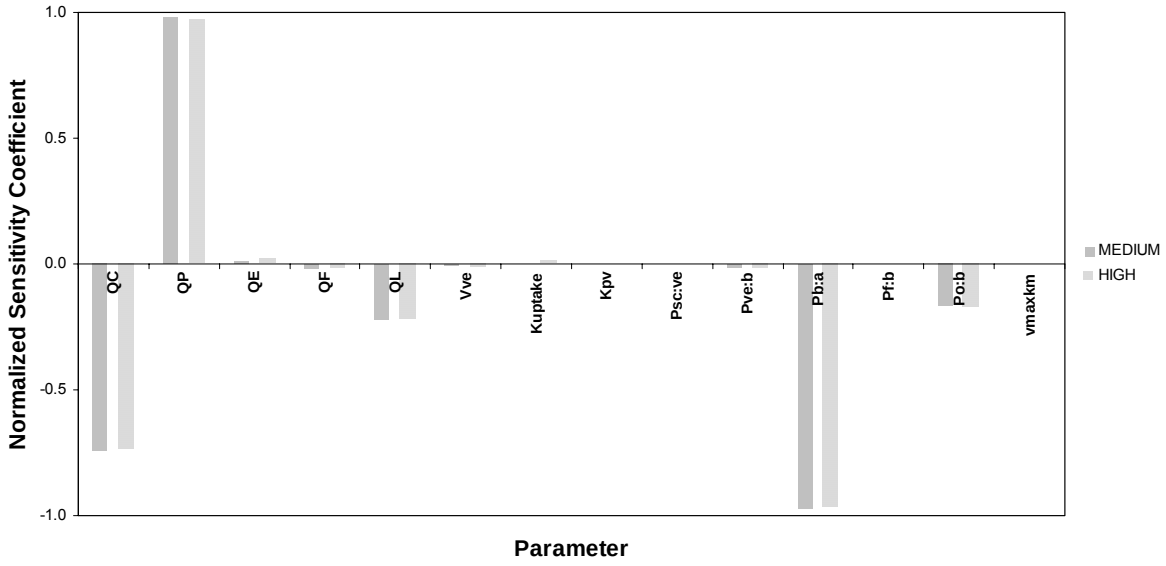

Figure 16. Normalized sensitivity coefficients for the end-exhaled breath concentrations in the medium- and high-exposure groups. Physiological and biochemical parameters were adjusted at the 1% level. Explanation of abbreviations can be found in Table 9.

4.4.5 Comparison of dermal and inhalation exposure routes

Simulations were conducted for three US Air Force personnel to compare the contribution of dermal exposure to the end-exhaled breath concentrations relative to inhalation exposure (Table 12). These three individuals were all fuel-cell maintenance workers. The area under the end-exhaled breath concentration-time curve (AUC_{ex}) was calculated for dermal exposures using the following equation:

$$AUC_{ex} = \int_{t_0}^{t_1} C_{ex}(t)\, dt \qquad (30)$$

where C_{ex} is the concentration of naphthalene in the end-exhaled breath and t_1 is the time at the end of the exposure. The values of AUC_{ex} for dermal exposures were 0.8, 18.6, and 310 μg·min/m^3 for the 10^{th}, 50^{th}, and 90^{th} percentiles, respectively. Dermal exposures were set to zero and the naphthalene air concentration was adjusted to obtain the same value of AUC_{ex}. The predicted air

concentrations ($INHAL1_{pred}$) were 0.05 μg/m^3, 0.71 μg/m^3, and 15.7 μg/m^3, respectively. These values are 0.3%, 1.7%, and 6.9% of the air concentrations of naphthalene for the individuals whose breath measurements represented the 10th, 50th, and 90th percentiles, respectively.

Table 12. Estimated contribution of dermal exposure to the end-exhaled breath concentrations of naphthalene relative to inhalation exposure. This analysis was based on three US Air Force personnel whose end-exhaled breath concentrations represented the 10th, 50th, and 90th percentiles. The ratio of $INHAL1_{pred}$ to $INHAL1_{adj}$ is a measure of the relative percent contribution of dermal exposure to the internal dose.

Percentile	Breath (μg/m^3)	AUC_{ex} (μg·min/m^3)	$INHAL1_{adj}$ (μg/m^3)	$INHAL1_{pred}$ (μg/m^3)	Ratio (%)
10%	1.7	0.8	16.4	5.0×10^{-2}	0.3
50%	4.7	18.6	40.8	0.7	1.7
90%	29.4	310	227	15.7	6.9

AUC_{ex}, area under the breath concentration-time plot for dermal exposures only;
$INHAL1_{adj}$ is the adjusted value of $INHAL1_{est}$, and better represented the inhalation exposures of fuel-cell maintenance personnel who wore respirators during work inside fuel tanks;
$INHAL1_{pred}$ was determined by varying the air concentration of naphthalene to obtain the same value of AUC_{ex}.

4.5 Discussion

The PBTK model was developed to predict end-exhaled breath concentrations of naphthalene following dermal and inhalation exposure to JP-8. Our model consisted of five compartments representing the stratum corneum, viable epidermis, blood, fat, and other tissues, and contains fewer parameters than previously published physiologically based compartmental models of naphthalene (Quick and Shuler 1999; Willems *et al.* 2001). The fat was considered separate from the other tissues because the time constant for fat (13.5 h) was larger than the time constant for other tissues (0.7 h). However, the other tissue compartment was included in the model because the skin compartment consisted of the skin directly under the exposed area. The remaining skin was included in the other tissue compartment.

Adjustments had to be made to the blood:air and fat:blood partition coefficients for the PBTK model predictions to fit the experimental and occupational exposure data. For many chemicals, the partition coefficients are not known. In such cases, quantitative structure-activity relationship (QSAR) models may be used to predict the necessary partition coefficients; however, the predictions are limited to chemicals with physicochemical properties that lie within the calibration dataset (Beliveau *et al.* 2003). In our study, we calibrated the values of $P_{b:a}$ and $P_{f:b}$, which were predicted by Willems *et al*. (2001) using QSAR models, against human exposure data. We estimated a $P_{b:a}$ value of 27.1 for naphthalene, which is more realistic than the value of 571 reported by Willems *et al*. (2001). Also, we estimated a $P_{f:b}$ value of 40.4 for naphthalene, which is more plausible given that the $P_{f:b}$ for benzene is 55 and 25 for decane. $P_{b:a}$ and $P_{f:b}$ were identified as sensitive parameters in the model, and optimization of these parameter values was necessary for accurate prediction of the kinetic behavior of naphthalene.

The optimized PBTK model was used to predict end-exhaled breath measurements collected in the workplace from US Air Force personnel exposed via inhalation and dermal contact. The three US Air Force personnel who were selected based on their end-exhaled breath concentration representing the 10^{th}, 50^{th}, and 90^{th} percentiles were all in the high-exposure group. We observed that the median contribution of dermal exposure to the internal dose of naphthalene was relatively small (1.7%). However, in the US Air Force personnel who represented the 90^{th} percentile, the relative contribution of dermal exposure to the internal dose was 6.9%. The high-exposure group consisted of fuel-cell maintenance workers. These workers wore personal protective equipment, which included forced supply-air respirators, while working in the fuel tank. The use of dermal protective equipment can further decrease the internal dose of naphthalene in the fuel-cell maintenance workers.

The PBTK model was used to calculate the permeability coefficient (K_p) for naphthalene in humans *in vivo*. Previously, the K_p had been calculated using Fick's law of diffusion. A K_p value of 5.1×10^{-4} cm/h was estimated *in vitro* (McDougal *et al.* 2000). This *in vitro* K_p value was compared to a K_p value that was estimated by calculating the flux value for aromatic and aliphatic components of JP-8 in humans from the slope of the linear portion of the cumulative mass of chemical in blood per cm^2 *vs.* time curve (Kim *et al.* 2006). We calculated an apparent K_p of 5.3×10^{-5} cm/h, which is approximately

an order of magnitude different from the rat K_p. This K_p calculation was revised using a DTK model and equation 29. A larger K_p value was estimated (1.8×10^{-3} cm/h), which was more similar to the K_p estimated *in vitro* by McDougal *et al.* (McDougal *et al.* 2000). The limitation of using a data based compartmental model is that the parameter values are not constrained by the actual anatomy and physiology of the human body, and the biochemistry of naphthalene *in vivo*. We incorporated such constraints into our PBTK model and revised our calculation of K_p for naphthalene. We estimated a K_{ps} value of 5.2×10^{-5} cm/h and a K_{pv} value of 2.0 cm/h. The value of K_{eff}, which is the overall permeability coefficient for chemicals crossing the skin (McCarley and Bunge 2001), is 5.2×10^{-5} cm/h. The estimated value of K_{eff} is the same as K_{ps}.

K_{eff} is about an order of magnitude smaller than the K_p reported by McDougal *et al*. (2000). A ten-fold difference in the value of the permeability coefficient was not unexpected because rat skin is more permeable than human skin (McDougal *et al.* 2000). Molecular diffusion is the dominant mechanism that governs the permeation of naphthalene across the skin. For diffusion, the flux (and K_p) is inversely proportional to the thickness of the diffusion distance, as stated by Fick's first law of diffusion. Therefore, doubling the thickness of the skin will result in halving the K_p. McDougal *et al*. (2000) estimated K_p across rat skin of thickness 560 μm. The human skin thickness ranges from 500 μm to 4000 μm; therefore, the human K_p value is expected to be between 6.4×10^{-5} cm/h and 5.7×10^{-4} cm/h. Our estimate of the effective permeability coefficient for naphthalene represents the lower limit of this range. However, we observed a considerable amount of variation in the values of K_{eff}. Further study of the sources of the observed variation in permeability coefficient values is needed.

The approach taken in this study represents a useful technique for modeling and assessing the contribution of dermal and inhalation exposures to the systemic levels of naphthalene. This PBTK model has reduced the uncertainty in modeling JP-8 exposures because fewer parameters were required to predict the time-course of naphthalene. However, our model has also identified some data gaps. First, inhalation exposures should be measured over shorter time intervals. Sensitivity analysis of exposure parameters for the medium- and high-exposure groups demonstrated that end-exhaled breath levels of naphthalene were most sensitive to the air concentration of naphthalene during work. In our study, we used time-weighted average concentrations (over approximately 4 h),

which did not capture exposures to high levels of naphthalene from local sources. Therefore, shorter time-resolved data may be used to better explain the transient nature of inhalation exposures to JP-8. Second, the blood:air partition coefficient for naphthalene should be determined experimentally, for example, using the vial-equilibration technique (Sato and Nakajima 1979). The sensitivity analysis showed that the concentration of naphthalene in the end-exhaled breath was highly sensitive to $P_{b:a}$. Therefore, accurate measurement of the $P_{b:a}$ value will reduce some of the uncertainty in the model. The $P_{b:a}$ values for other JP-8 components should also be determined experimentally since human $P_{b:a}$ values are unavailable for many of these aromatic and aliphatic hydrocarbons. Finally, occupational and environmental exposure studies of other components of JP-8 are needed to gain a more complete picture of JP-8 exposures. Currently, occupational exposure studies have focused on single chemical components of JP-8. The results of multi-chemical exposure assessment studies may be compared to results from single-chemical studies, and add to our understanding of the absorption, distribution, metabolism, and elimination of complex chemical mixtures.

In conclusion, the PBTK model was used to quantify the contribution of dermal exposures to the systemic levels of naphthalene. We estimated a permeability coefficient that was 10-fold lower than estimates made *in vitro*. However, we observed a wide range of permeability coefficient values and, thus, recommend further study of the sources of inter- and intra-individual variation. Overall, we have used a combination of exposure assessment, biological monitoring, and toxicokinetic modeling tools to integrate external exposure and biomarker data into a single description of the toxicokinetic behavior of naphthalene. We constructed a PBTK model of dermal and inhalation exposure to jet fuel that required estimation of fewer parameters than previously published PBTK models of naphthalene. This PBTK model, which included two major exposure routes relevant to occupational and environmental exposure scenarios, may be used for integrating animal and human observational studies into an improved understanding of human health risks.

CHAPTER 5

DISCUSSION AND CONCLUSIONS

The series of papers in this dissertation have presented three distinct contributions to the scientific literature. The first paper presented the overall study design and the results from a human volunteer study of dermal exposure to JP-8. The second paper presented four dermatotoxicokinetic models of aromatic and aliphatic hydrocarbons. Each of these models was used to predict the time course of naphthalene, 1-methyl naphthalene, 2-methyl naphthalene, decane, undecane, and dodecane. Dermal exposure measurements from US Air Force personnel and Monte Carlo analyses were conducted to examine the distribution of the cumulative internal dose for the six JP-8 components. In the third paper, the structure of the DTK model was used to construct a PBTK model that integrated both the dermal and inhalation routes of exposure. This PBTK model was used to predict occupational exposure to JP-8 in USAF personnel, and to quantify the contribution of dermal exposure to the internal dose of naphthalene. The most significant results that have furthered our understanding of how chemicals are absorbed into the skin and taken up into the systemic circulation are discussed in this chapter.

5.1 Absorption and penetration of JP-8 across skin

In chapter 2, the controlled dermal exposure study of JP-8 was described in detail. The findings from this human volunteer study have made several contributions to our knowledge of dermal exposures to complex chemical mixtures. Chemicals deposited on the skin can evaporate from the

surface, be absorbed into deeper layers of the skin, be metabolized, or penetrate the skin for distribution to other tissues. Most pharmacokinetic and toxicokinetic studies of topically applied chemicals are performed *in vitro*. However, these models are not necessarily predictive of the disposition of chemicals in humans. Extrapolation of results from animal studies to humans is affected by a considerable amount of uncertainty. The human volunteer study had several design characteristics that were similar to *in vitro* studies: (1) JP-8 was applied to the surface of the skin, (2) the amount that penetrated the skin was determined at specific time points, and (3) the mass of chemical absorbed by the skin was quantified. This study provided an opportunity to directly compare the absorption and penetration of JP-8 components between animals *in vitro* and humans *in vivo*.

The patterns of dermal absorption and penetration of six JP-8 components were consistent between *in vitro* and *in vivo* studies. First, the tape-strip data showed evidence of absorption of naphthalene, 1-methyl naphthalene, 2-methyl naphthalene, decane, undecane, and dodecane. Second, aromatic compounds had apparent K_p values that were an order of magnitude larger than aliphatic compounds. Third, naphthalene had the largest apparent K_p. The rank order of the apparent K_p values were similar to results from McDougal *et al*. (2000). A significant difference was that the human permeability coefficient was 10-fold lower than estimates made *in vitro*; however, a wide range of K_p values was estimated. Therefore, further study of the sources of inter- and intra-individual variation in human K_p values is recommended. Overall, what can be concluded from these comparisons is that *in vitro* studies may be used to predict dermal absorption and penetration of JP-8 components in humans. However, these *in vitro* studies are limited to initial assessments of the absorption and penetration of chemicals across human skin because they do not capture the inter-individual variability observed in human populations.

5.2 Dermatotoxicokinetic model of the skin

In chapter 3, four dermatotoxicokinetic models of human exposure to JP-8 were presented. Two major contributions to the scientific literature were made: (1) toxicokinetic parameters were obtained for dermal exposures in humans, and (2) a mathematical model of the skin was developed that could be used to facilitate a modeling strategy for dermal exposures to complex chemical mixtures. The

best description of the skin was a two-compartment model where the first compartment represented the stratum corneum and the second compartment represented the viable epidermis. This structure represented a more plausible description of the skin since the stratum corneum and the viable epidermis have very different anatomical and biochemical characteristics.

The optimal DTK model was used to simulate the time-course of naphthalene and other components of JP-8 using information collected from an occupational exposure assessment study (Chao *et al.* 2005). The predicted internal dose was distinctly different among the low-, medium-, and high-exposure groups. Therefore, these simulations supported the use of the tape-strip technique to measure dermal exposures to complex chemical mixtures in exposure assessment studies.

5.3 PBTK model of occupational exposure to JP-8

Building upon the structure of the optimal DTK model, a PBTK model was constructed and used to quantify the relationship between environmental exposures and the internal dose of naphthalene (Chapter 4). This model represented the first attempt at incorporating both the dermal and inhalation routes of exposure into a single description of the kinetic behavior of naphthalene in humans. The PBTK model consisted of 5 compartments representing the stratum corneum, viable epidermis, blood, fat, and other tissues. Model parameters were calibrated against data from an occupational exposure and a laboratory study. The optimized values of parameters were blood:air partition coefficient = 27.1, fat:blood partition coefficient = 40.4, permeability coefficient for the stratum corneum = 5.2×10^{-5} cm/h, stratum corneum:viable epidermis partition coefficient = 12.7, and permeability coefficient for the viable epidermis = 2.0 cm/h. Adjustments to the blood:air partition and fat:blood partition coefficients had to be made to fit the time course data for naphthalene in blood. The adjusted values of the partition coefficients were more realistic than the literature values (Willems *et al.* 2001) when compared to the partition coefficients for similar compounds.

The major scientific contribution of the PBTK model was that it had been constructed using data from (1) an observational study of occupational exposures and (2) a human volunteer study where exposures were controlled. The optimized PBTK model was used to reveal some of the errors related to environmental sampling. This PBTK modeling approach represented a shift from model

development using laboratory animals towards model application in humans, as demonstrated by the simulations of occupational exposures to JP-8. The simulations showed that the median contribution of dermal exposure to the internal dose of naphthalene was 1.7% (10^{th} percentile = 0.3% and 90^{th} percentile = 6.9 %). These findings suggest that implementation of dermal exposure controls that target the dermal route will further decrease the internal dose of naphthalene in fuel-cell maintenance workers. Overall, the third paper presented a novel application of PBTK models. Given the use of personal protective equipment, prior statistical evaluations had found it difficult to determine the relative contributions of dermal and inhalation exposures to the systemic levels of JP-8 components. In this study, PBTK modeling human exposures to JP-8 using diverse data sets revealed the quantitative relationship between external exposure measurements and the internal dose of naphthalene. The approach taken in this study has, therefore, added to the current understanding of the toxicokinetic behavior of naphthalene, and has pointed to a novel way of assessing human exposures to chemical mixtures.

5.4 Summary of scientific contributions

This investigation has provided three significant scientific contributions to the study of dermal exposures to complex chemical mixtures. The controlled dermal exposure study was the first published work that gave some insight into the dermal absorption and penetration of JP-8 components in humans. Further, this investigation provided an opportunity to compare *in vivo* estimates of the permeability coefficient to those made *in vitro* using rat skin and Franz diffusion cells. The second significant addition was the development of a dermatotoxicokinetic model for JP-8 exposures in humans. This model represented the first attempt at estimating rate constants that were directly relevant for humans. The model was used to demonstrate the differences in internal dose for dermal exposures in the low-, medium-, and high-exposure categories. The final scientific contribution was the development of a human PBTK model that included both the dermal and inhalation routes of exposure. This PBTK model was constructed using a combination of exposure assessment, biological monitoring, and toxicokinetic modeling tools. The uniqueness of this PBTK model was that it was calibrated and validated exclusively with human exposure and biomarker data.

Therefore, the optimal model could be used to predict occupational exposures without the uncertainty associated with extrapolating from animal studies. Future studies may adopt this modeling strategy for assessing the risks associated with exposures to complex chemical mixtures in human populations.

5.5 Limitations and suggestions for future research

There were several limitations to this study. First, there was a paucity of exposure data that could be used to explain the exposure-internal dose relationship for work-related activities. The occupational exposure data consisted of time-weighted average inhalation exposure data and sparse end-exhaled breath measurements. Since the half-life of naphthalene is approximately 22 min (Egeghy *et al.* 2003), the time-weighted average exposure data (e.g., over a 4 h work-shift) make it difficult to quantify the exposure-internal dose relationships for complex exposure patterns. Second, exposure measurements for specific tasks were not available. Therefore, it was difficult to reconstruct the exposure scenario that corresponded to the end-exhaled breath measurements. Detailed information about the times at which exposures occurred and the exposure levels during those time periods are necessary for improving the inputs to the PBTK model. Third, partition coefficients were not available for naphthalene but had to be estimated using the time course data for naphthalene. However, the time course of naphthalene in blood and in breath is a composite behavior governed by fundamental physiological and biochemical processes. Thus, partition coefficients should be determined separately using (for example) a vial-equilibration technique.

This investigation has generated new ideas for future research that address some of the aforementioned limitations. In particular, the PBTK model has provided insight into the expansion of the current model, specifically in making it more useful for human exposure and risk assessment. In order to improve understanding of the kinetic behavior of compounds that are sequestered in deeper layers of the skin, experiments are needed to measure chemicals that evaporate from the surface of the skin after exposure has stopped. This experiment will answer questions about the possibility of reverse-diffusion (i.e., from deeper skin layers to the surface rather than toward the systemic circulation). Studies that measure the rates of metabolism in the skin are also needed to understand

the effect of metabolism on the disposition of chemicals in the skin and in the systemic circulation. In both data-based and physiologically-based compartmental models, the diffusion of chemicals across the stratum corneum was modeled as a one-directional diffusive process. Therefore, compartmental models should be compared to membrane models of the skin to validate this assumption. Further occupational exposure studies are needed to better understand dermal exposures to JP-8 during specific work tasks. Measurements of the time-weighted average concentration of JP-8 components over the duration of a work-shift do not capture exposures to peak levels of naphthalene from local sources. Shorter time-resolved data can be used to better explain the transient nature of inhalation exposures to JP-8, and to elucidate the effect of short-term JP-8 exposures on the toxicokinetic behavior of naphthalene. Finally, future studies of JP-8 should measure not only one component but many JP-8 components to gain a more complete picture of JP-8 exposures. The results of these studies may then be compared to results from single-chemical studies, and add to our understanding of the absorption, distribution, metabolism, and elimination of complex chemical mixtures. Better understanding of the kinetic behavior of complex chemical mixtures can make plausible the findings from epidemiological investigations.

APPENDIX A:

PROTOCOLS FOR THE CONTROLLED DERMAL EXPOSURE STUDY

A. PROTOCOL FOR PREPARATION OF SAMPLING EQUIPMENT

MATERIALS (for 1 subject):

N.B. For storage of urine, blood, and internal standards, use the 10 or 20 ml vials with crimp-top because this seals better.

- Exposure chamber
- 9.5 mm Thermogreen septa LB-2 (2)
- 500 ul syringe with blunt end (2)
- Latex gloves (1 box)
- 50 ml Urine collections vials (16)
- 10 ml Blood sampling tubes (8)
- Crimper and De-crimper
- 10 ml Headspace vials (8)
- 20 ml Headspace vials (6)
- PTFE crimp-top caps (14)
- 50 ml conical vials (6)
- 15 ml conical vials (8)
- 20 ml Scintillation vials (15)
- 20 ml Pipette
- Automated pipetter
- 75 ml Glass bulb (12)
- Passive sampling tubes (20)
- JP-8 jet fuel
- 50 µl pipette with tips
- Internal standard (Naphthalene d_8 + Dodecane d_{26})
- Acetone (bottle and dispenser)
- DI water
- 4 beakers
- Labels
- Clipboard
- Pre-printed tables for each subject

SAMPLE LABELING

S AaBbCc

where S = sample type, Aa = Subject ID; Bb = Visit number; Cc = Sample number.

The sample type identifiers are U = urine, D = skin, B = blood, R = breath, C = chamber, P = personal breathing zone, T = boat, J = 0.5 ml of JP8

Time (24:00) and Date (year/month/day)

PREPARATION OF INTERNAL STANDARDS:

1. For urine and blood internal standards, do the following:
    a. Dissolve 0.1 g naphthalene d_8 in 20 ml of methanol. This is the stock solution. Label it as urine/blood naphthalene d_8 stock, record concentration, and date.
    b. Dissolve 0.1 g n-dodecane d_{26} in 20 ml of methanol. This is the stock solution. Label it as urine/blood n-dodecane d_8 stock, record concentration, and date.
    c. Aliquot 1 ml of each of the stock solutions into a 25 ml volumetric flask. Fill to 25 ml with methanol. Label as 1st dilution, record concentration, and date. Store the remaining solution in 20 ml HS vials with crimp-top.
    d. Aliquot 0.625 ml of the 1st dilution into a 25 ml volumetric flask. Fill to 25 ml with methanol. This is the internal standard.
    e. Transfer the internal standard to a 20 ml head-space vial with crimp-top. Label it as urine/blood internal standard, record concentration, and date.
    f. Store the stock and internal standard at -80 °C.

2. For dermal internal standard
    a. Dissolve 0.1 g naphthalene d_8 in 20 ml of acetone. This is the stock solution. Label it as dermal naphthalene d_8 stock, record concentration, and date.
    b. Dissolve 0.1 g naphthalene d_8 in 20 ml of acetone. This is the stock solution. Label it as dermal stock and date. Label it as dermal n-dodecane d_{26} stock, record concentration, and date.
    c. Aliquot 5 ml of the stock solution into a 25 ml volumetric flask. Fill to 25 ml with acetone. This is the internal standard.
    d. Transfer the internal standard to a 20 ml head-space vial with crimp-top. Label it as dermal internal standard, record concentration, and date.
    e. Store the internal standard at -80 °C.

B. PROTOCOL FOR SAMPLE COLLECTION (PRE-EXPOSURE)

All equipment for collection of samples must be prepared in advance. The following protocol is to be completed on the day before and prior to exposing the subject(s) in the chamber.

DAY BEFORE EXPOSURE:

1. Condition the passive sampling tubes in Dr. Rappaport's laboratory, first at 250°C and second at 225°C. Conditioned tubes are capped and stored at room temperature.

2. Prepare the breath sampling bulbs by rinsing with deionized water and acetone. Do not rinse the caps. Air dry at room temperature.

3. Make internal standards if necessary.

4. Bake out the vials and caps for storing blood and urine in the oven in the 4^{th} floor lab at 80 °C overnight.

5. Print out the labels with subject ID, visit number, sample number, and date.

6. Leave space in notebook for the following information: (1) date, start and stop times for exposure, and (2) tables for dermal, breath, blood, and urine samples. Construct tables in the lab notebook with the following headings: subject ID, visit number, sample number, date, and time.

7. Cut out 140 dermal tape strips

DAY OF EXPOSURE:

1. Cool down the blood and urine vials first thing in the morning inside the fume hood.

2. Replace thermogreen septa

3. Have air sampling tubes, 0.5 ml syringes, and dermal tape strips on the workbench near the exposure chamber.

4. Have internal standard, and HS vials in the fume hood for dermal, urine and blood sample collection.

5. Label sixty-two 20 ml scintillation vials and place 10 ml of acetone and 20 µl of internal standard (IS = naphthalene d_8 and dodecane d_{26}) in them.

6. Place 0.5 ml of the JP-8 fuel into one of the 20 ml scintillation vials containing 9.5 ml acetone and 20 µl internal standard. Label and store in -20°C.

7. Set aside two 20 ml scintillation vial for the JP-8 residue from the position holders. These vials should contain 9.5 ml of acetone and 20 µl of internal standard.

8. Greet the volunteer and take him/her to the waiting area. Store the volunteer's personal belongings and lunch in the student office.

9. Brief the volunteer on the day's events using the time chart. Record the subject's body weight, height, and fat content. Ask if he/she has any questions.

10. Have the volunteer provide a urine sample. Record the time in the lab notebook and on the pre-labeled sample vial. Transfer the urine sample to 2 pre-labeled 20 ml HS vials (urine is stored in duplicate). Store in -20ºC refrigerator.

11. Direct the volunteer to the exposure chamber and have him/her seated in a comfortable position.

12. Explain how the breath sample is to be given. Have the volunteer provide a breath sample. Record the time in the lab notebook and on the pre-labeled sample tube.

13. Ask the nurse to draw a blood sample from the volunteer. Record the time in the lab notebook and on the pre-labeled blood test tube. Transfer the blood sample to pre-labeled 10 ml HS vials. Store in -20ºC refrigerator.

C. PROTOCOL FOR SAMPLE COLLECTION (EXPOSURE)

The following steps are to be taken once pre-exposure samples (urine, breath, and blood) are collected and the volunteer is comfortably seated in the chair in preparation for the 30 minute exposure period.

1. Place a passive air monitor on the volunteer's lapel. Record the time in the lab notebook and on the sampling device.0

2. Insert the volunteer's arm into the exposure chamber. Seat the aluminum application chamber onto the volunteer's arm. Ensure the volunteer's comfort. Adjust the arms so that there is a tight seal on the forearm. Ensure that the subject has circulation to the fingertips.

3. Apply JP-8 to the volunteer's forearm. Record the time of the first application of JP-8 in the lab notebook. Also make note of which site JP-8 was applied first.

4. Place a Tenax sampling tube in opening end of the chamber. Tenax tubes are changed every 5 minutes. Record the start/stop times for each.

5. Collect breath samples at t = 5 min, 10 min, 15 min, 20 min, and 25 min. Record the times that the breath samples are collected in the lab notebook and on the pre-labeled sample tubes.

6. Collect blood samples half way through the 30 minute exposure (i.e. t = 15 min). Record the time that the blood is drawn in the lab notebook and on the blood test tube. Transfer the blood into pre-labeled 10 ml HS vials. Store the blood in the -20ºC refrigerator.

7. Immediately before the end of 30 minutes of exposure, collect breath and blood samples. Record the times that the breath and blood samples are collected in the lab notebook and on the pre-labeled sample tube and vial. Transfer 3 ml of blood into a pre-labeled 10 ml HS vial; transfer the remaining blood into 15 ml conical tubes. Store the blood in the -20ºC refrigerator.

8. Remove the final Tenax tube from the chamber at the end of the 30 minutes of exposure.

9. Extract the remaining JP-8 from the two sites of exposure and transfer into pre-labeled 20 ml scintillation vials that contain 20 ml of acetone and 20 µl of IS.

10. Carefully raise the application chamber and remove the volunteer's arm from the exposure chamber.

11. Wash the aluminum chambers with 10 ml of acetone for each site and collect in a large beaker. Transfer the contents of the beaker to the 20 ml scintillation vials used to extract dermal samples; insert 20 µl IS to this vial. Wash the exposure chamber with deionized water.

12. Apply tape to the exposed sites and record the time. Leave the tape on the skin for 2 min.

13. Slowly remove the tape at 45º from both sites on the forearm and place in corresponding pre-labeled 20 ml scintillation vials that contain 10 ml of acetone and 20 µl of IS. Record the time that the tapes are removed. Switch gloves and place new tape on both sites on the forearm. Record the time that the tapes are applied. Leave tape on the skin for 2 min.

14. Repeat step 12 until each site on the forearm has been tape stripped up to 30 times.

D. PROTOCOL FOR SAMPLE COLLECTION (POST-EXPOSURE)

The following steps are to be taken upon completion of tape stripping the skin.

1. Collect breath sample. Record the time that the breath sample is collected in the lab notebook and on the pre-labeled sample tube.

2. Collect blood sample. Record the time that the blood is drawn in the lab notebook and on the blood test tube. Transfer the blood into pre-labeled 10 ml HS vials. Store the blood in the -20ºC refrigerator.

3. Collect urine sample. Record the time in the lab notebook and on the pre-labeled sample vial. Transfer the urine sample to 4 pre-labeled 20 ml HS vials. Store the urine in the -20ºC refrigerator.

4. Assist the volunteer into the student office. Instruct the volunteer not to leave the student office except for snacks, beverages, lunch, or washroom breaks.

5. Repeat steps 1-3 hourly until four more breath, blood, and urine samples are collected.

6. At the end of the day, remove the passive air monitor from volunteer. Record the time in the lab notebook and on the sampling device.

7. Remove all other experimental objects from the volunteer (e.g. catheter).

8. Place passive sampling tubes inside the breath sampling bulbs for overnight extraction. Immediately cap the passive sampling tubes in the morning and store at room temperature.

9. Ensure that all blood, urine, breath, dermal, chamber air, personal breathing zone samples are correctly labeled and stored.

10. Ensure that all forms (consent and personal data) are completed and signed.

11. Set up an appointment for the 2^{nd} exposure. Inform the volunteer that they will be reminded 1 week and 1 day prior to the next appointment.

12. Give 10 urine containers in cooler with icepacks, and instruct the volunteer to collect urine at every void, labeling with time and data. Have the subject come in the next morning with cooler and icepacks.

13. Give reimbursement for their contribution to the study once all urine samples have been returned.

APPENDIX B:

DERMATOTOXICOKINETIC MODEL PROGRAM

```
PROGRAM: dtk.csl
! Developed for JP-8 skin exposure MODEL D
! by David Kim
! Department of Environmental Sciences and Engineering, School of Public Health
! The University of North Carolina at Chapel Hill
! Construction of this program began on Nov 29, 2005


INITIAL                                 ! Beginning of pre-execution section

CONSTANT    BW = 70                     ! Body weight of individuals (kg)
CONSTANT  AEXP = 20000                  ! Surface area of exposure (cm^2)
 VB = 72.447*(BW**1.007)                ! Volume of blood (ml)


!-------*****************************----------!
!-------     KINETIC CONSTANTS    -----------!
!-------*****************************----------!

constant        k0N = 4.10E-04
constant        k1N = 1.9
constant        k2N = 35
constant        k3N = 43
constant        k4N = 0.04
constant        k5N = 1.4
constant        k6N = 0.1

constant        k0N1m = 7.80E-05
constant        k1N1m = 1
constant        k2N1m = 10
constant        k3N1m = 29
constant        k4N1m = 0.04
constant        k5N1m = 1.9
constant        k6N1m = 0.13

constant        k0N2m = 2.50E-04
constant        k1N2m = 1.2
constant        k2N2m = 30
constant        k3N2m = 42
constant        k4N2m = 0.04
constant        k5N2m = 0.8
constant        k6N2m = 0.11

constant        k0C10 = 6.90E-04
constant        k1C10 = 1.9
constant        k2C10 = 42
constant        k3C10 = 51
constant        k4C10 = 0.13
constant        k5C10 = 1.6
constant        k6C10 = 0.15

constant        k0C11 = 1.60E-04
constant        k1C11 = 1.9
constant        k2C11 = 59
constant        k3C11 = 62
constant        k4C11 = 0.09
```

```
constant        k5C11 = 1.8
constant        k6C11 = 0.07

constant        k0C12 = 7.90E-05
constant        k1C12 = 1.9
constant        k2C12 = 48
constant        k3C12 = 55
constant        k4C12 = 0.1
constant        k5C12 = 2
constant        k6C12 = 0.07


!-------DOSING

CONSTANT CBinitN = 0                    ! Initial amount in blood
CONSTANT CBinitN1m = 0
CONSTANT CBinitN2m = 0
CONSTANT CBinitC10 = 0
CONSTANT CBinitC11 = 0
CONSTANT CBinitC12 = 0


CONSTANT   CJP8N = 344                  ! Concentration of JP8 component in first tape strip (ng/m2)
CONSTANT   CJP8N1m = 304
CONSTANT   CJP8N2m = 283
CONSTANT   CJP8C10 = 237
CONSTANT   CJP8C11 = 4033
CONSTANT   CJP8C12 = 7277


!-----CALCULATED PARAMETERS

 MJP8N = CJP8N*AEXP/10000000                    ! Mass applied (ug)
 MJP8N1m = CJP8N*1.4*AEXP/10000000
 MJP8N2m = CJP8N*1.3*AEXP/10000000
 MJP8C10 = CJP8N*1.1*AEXP/10000000
 MJP8C11 = CJP8N*18.7*AEXP/10000000
 MJP8C12 = CJP8N*33.7*AEXP/10000000

  ABinitN = VB*CBinitN/1000
  ADinitN = ABinitN*k4N/k3N
  APinitN = (k5N/k6N)*ABinitN

  ABinitN1m = VB*CBinitN1m/1000
  ADinitN1m = ABinitN1m*k4N1M/k3N1M
  APinitN1M = (k5N1M/k6N1M)*ABinitN1M

  ABinitN2m = VB*CBinitN2m/1000
  ADinitN2m = ABinitN2m*k4N2M/k3N2M
  APinitN2M = (k5N2M/k6N2M)*ABinitN2M

  ABinitC10 = VB*CBinitC10/1000
  ADinitC10 = ABinitC10*k4C10/k3C10
  APinitC10 = (k5C10/k6C10)*ABinitC10

  ABinitC11 = VB*CBinitC11/1000
```

```
  ADinitC11 = ABinitC11*k4C11/k3C11
  APinitC11 = (k5C11/k6C11)*ABinitC11

  ABinitC12 = VB*CBinitC12/1000
  ADinitC12 = ABinitC12*k4C12/k3C12
  APinitC12 = (k5C12/k6C12)*ABinitC12


!-------Simulation parameters

CONSTANT  TEXP = 240                    ! Duration of exposure (min)
CONSTANT  TSTOP = 7200                  ! Duration of simulation (min)
 POINTS = 7200                          ! Number of times data are logged
 CINT = TSTOP/POINTS                    ! Communication intervals

ALGORITHM IALG = 2                      ! Use Gear integration algorithm

END                                     ! End of initial section

!---------------------------------------------------------------------------------------------------------------

DYNAMIC  ! Beginning of execution section

DISCRETE CAT1                           !Schedule events to turn exposure on and off daily
   INTERVAL CAT = 1440.                 !Set interval larger than any TSTOP(to prevent multiple
exposure)
            DERMDOSEN = MJP8N
            DERMDOSEN1m = MJP8N1m
            DERMDOSEN2m = MJP8N2m
            DERMDOSEC10 = MJP8C10
            DERMDOSEC11 = MJP8C11
            DERMDOSEC12 = MJP8C12

   SCHEDULE CAT2 .AT. T + TEXP          !Schedule end of exposure
END                                     !End of CAT1

DISCRETE CAT2
      DERMDOSEN = 0.
      DERMDOSEN1m = 0.
      DERMDOSEN2m = 0.
      DERMDOSEC10 = 0.
      DERMDOSEC11 = 0.
      DERMDOSEC12 = 0.

END                                     !End of CAT2



!---------------------------------------------------------------------------------------------------------------
```

```
DERIVATIVE  ! Beginning of derivative definition block


!-------------------------------------NAPHTHALENE-----------------------------------------------------------

!-----AXN = Amount of exposure
            RAXN = k0N*DERMDOSEN
             AXN = INTEG(RAXN,0.0)

!-----ASN = Amount in skin (ug)
            RASN = k0N*DERMDOSEN - k1N*ASN
             ASN = INTEG(RASN,0.0)

!-----ADN = Amount in deep skin (ug)
           RADN = k1N*ASN - k2N*ADN + k3N*ABN
            ADN = INTEG(RADN,ADinitN)

!-----ABN = Amount in blood (ug)
            RABN = k2N*ADN - k3N*ABN - k4N*ABN - k5N*ABN + k6N*APN
             ABN = INTEG(RABN,ABinitN)
             CBN = ABN/VB
            CBVN = CBN*1000                          ! Units are ng/ml

            AUCN = INTEG(CBVN,0.0)

!-----APN = Amount in peripheral (ug)
            RAPN = k5N*ABN - k6N*APN
             APN = INTEG(RAPN,APinitN)

!-----ALN = Amount lost (ug)
            RALN = k4N*ABN
             ALN = INTEG(RALN,0.0)



!-------------------------------------1-METHYL  NAPHTHALENE-------------------------------------------------

!-----AXN1M = Amount of exposure
            RAXN1M = k0N1M*DERMDOSEN1M
             AXN1M = INTEG(RAXN1M,0.0)

!-----ASN1M = Amount in skin (ug)
            RASN1M = k0N1M*DERMDOSEN1M - k1N1M*ASN1M
             ASN1M = INTEG(RASN1M,0.0)

!-----ADN1M = Amount in deep skin (ug)
           RADN1M = k1N1M*ASN1M - k2N1M*ADN1M + k3N1M*ABN1M
            ADN1M = INTEG(RADN1M,ADinitN1M)

!-----ABN1M = Amount in blood (ug)
            RABN1M = k2N1M*ADN1M - k3N1M*ABN1M - k4N1M*ABN1M - k5N1M*ABN1M +
k6N1M*APN1M
             ABN1M = INTEG(RABN1M,ABinitN1M)
             CBN1M = ABN1M/VB
            CBVN1M = CBN1M*1000                          ! Units are ng/ml
```

```
            AUCN1M = INTEG(CBVN1M,0.0)

!-----APN1M = Amount in peripheral (ug)
            RAPN1M = k5N1M*ABN1M - k6N1M*APN1M
             APN1M = INTEG(RAPN1M,APinitN1M)

!-----ALN1M = Amount lost (ug)
            RALN1M = k4N1M*ABN1M
             ALN1M = INTEG(RALN1M,0.0)



!--------------------------------------2-METHYL NAPHTHALENE-----------------------------------------------------

!-----AXN2M = Amount of exposure
            RAXN2M = k0N2M*DERMDOSEN2M
             AXN2M = INTEG(RAXN2M,0.0)


!-----ASN2M = Amount in skin (ug)
            RASN2M = k0N2M*DERMDOSEN2M - k1N2M*ASN2M
             ASN2M = INTEG(RASN2M,0.0)

!-----ADN2M = Amount in deep skin (ug)
           RADN2M = k1N2M*ASN2M - k2N2M*ADN2M + k3N2M*ABN2M
            ADN2M = INTEG(RADN2M,ADinitN2M)

!-----ABN2M = Amount in blood (ug)
            RABN2M = k2N2M*ADN2M - k3N2M*ABN2M - k4N2M*ABN2M - k5N2M*ABN2M +
k6N2M*APN2M
             ABN2M = INTEG(RABN2M,ABinitN2M)
             CBN2M = ABN2M/VB
            CBVN2M = CBN2M*1000                              ! Units are ng/ml

            AUCN2M = INTEG(CBVN2M,0.0)

!-----APN2M = Amount in peripheral (ug)
            RAPN2M = k5N2M*ABN2M - k6N2M*APN2M
             APN2M = INTEG(RAPN2M,APinitN2M)

!-----ALN2M = Amount lost (ug)
            RALN2M = k4N2M*ABN2M
             ALN2M = INTEG(RALN2M,0.0)



!--------------------------------------DECANE-------------------------------------------------------------------

!-----AXC10 = Amount of exposure
            RAXC10 = k0C10*DERMDOSEC10
             AXC10 = INTEG(RAXC10,0.0)

!-----ASC10 = Amount in skin (ug)
            RASC10 = k0C10*DERMDOSEC10 - k1C10*ASC10
```

```
            ASC10 = INTEG(RASC10,0.0)


!-----ADC10 = Amount in deep skin (ug)
           RADC10 = k1C10*ASC10 - k2C10*ADC10 + k3C10*ABC10
            ADC10 = INTEG(RADC10,ADinitC10)

!-----ABC10 = Amount in blood (ug)
            RABC10 = k2C10*ADC10 - k3C10*ABC10 - k4C10*ABC10 - k5C10*ABC10 +
k6C10*APC10
            ABC10 = INTEG(RABC10,ABinitC10)
            CBC10 = ABC10/VB
            CBVC10 = CBC10*1000                          ! Units are ng/ml

            AUCC10 = INTEG(CBVC10,0.0)

!-----APC10 = Amount in peripheral (ug)
            RAPC10 = k5C10*ABC10 - k6C10*APC10
            APC10 = INTEG(RAPC10,APinitC10)

!-----ALC10 = Amount lost (ug)
            RALC10 = k4C10*ABC10
            ALC10 = INTEG(RALC10,0.0)



!-------------------------------------UNDECANE-----------------------------------------------------------

!-----AXC11 = Amount of exposure
            RAXC11 = k0C11*DERMDOSEC11
            AXC11 = INTEG(RAXC11,0.0)

!-----ASC11 = Amount in skin (ug)
            RASC11 = k0C11*DERMDOSEC11 - k1C11*ASC11
            ASC11 = INTEG(RASC11,0.0)

!-----ADC11 = Amount in deep skin (ug)
           RADC11 = k1C11*ASC11 - k2C11*ADC11 + k3C11*ABC11
            ADC11 = INTEG(RADC11,ADinitC11)

!-----ABC11 = Amount in blood (ug)
            RABC11 = k2C11*ADC11 - k3C11*ABC11 - k4C11*ABC11 - k5C11*ABC11 +
k6C11*APC11
            ABC11 = INTEG(RABC11,ABinitC11)
            CBC11 = ABC11/VB
            CBVC11 = CBC11*1000                          ! Units are ng/ml

            AUCC11 = INTEG(CBVC11,0.0)

!-----APC11 = Amount in peripheral (ug)
            RAPC11 = k5C11*ABC11 - k6C11*APC11
            APC11 = INTEG(RAPC11,APinitC11)

!-----ALC11 = Amount lost (ug)
            RALC11 = k4C11*ABC11
```

```
            ALC11 = INTEG(RALC11,0.0)


!---------------------------------------DODECANE-------------------------------------------------------------

!-----AXC12 = Amount of exposure
            RAXC12 = k0C12*DERMDOSEC12
             AXC12 = INTEG(RAXC12,0.0)

!-----ASC12 = Amount in skin (ug)
            RASC12 = k0C12*DERMDOSEC12 - k1C12*ASC12
             ASC12 = INTEG(RASC12,0.0)

!-----ADC12 = Amount in deep skin (ug)
           RADC12 = k1C12*ASC12 - k2C12*ADC12 + k3C12*ABC12
            ADC12 = INTEG(RADC12,ADinitC12)

!-----ABC12 = Amount in blood (ug)
            RABC12 = k2C12*ADC12 - k3C12*ABC12 - k4C12*ABC12 - k5C12*ABC12 +
k6C12*APC12
             ABC12 = INTEG(RABC12,ABinitC12)
             CBC12 = ABC12/VB
            CBVC12 = CBC12*1000                              ! Units are ng/ml

            AUCC12 = INTEG(CBVC12,0.0)

!-----APC12 = Amount in peripheral (ug)
            RAPC12 = k5C12*ABC12 - k6C12*APC12
             APC12 = INTEG(RAPC12,APinitC12)

!-----ALC12 = Amount lost (ug)
            RALC12 = k4C12*ABC12
             ALC12 = INTEG(RALC12,0.0)



!---------------------------------------MASS BALANCE---------------------------------------------------------

!-----Mass balance
  TMASSN = ASN + ADN + ABN + ALN + APN
  MASSBALANCEN = TDOSEN - TMASSN
  TDOSEN = AXN + ABinitN + ADinitN + APinitN

  TMASSN1m = ASN1m + ADN1m + ABN1m + ALN1m + APN1M
  MASSBALANCEN1m = TDOSEN1m - TMASSN1m
  TDOSEN1m = AXN1m + ABinitN1m + ADinitN1m + APinitN1M


  TMASSN2m = ASN2m + ADN2m + ABN2m + ALN2m + APN2M
  MASSBALANCEN2m = TDOSEN2m - TMASSN2m
  TDOSEN2m = AXN2m + ABinitN2m + ADinitN2m + APinitN2M

  TMASSC10 = ASC10 + ADC10 + ABC10 + ALC10 + APC10
  MASSBALANCEC10 = TDOSEC10 - TMASSC10
  TDOSEC10 = AXC10 + ABinitC10 + ADinitC10 + APinitC10
```

```
 TMASSC11 = ASC11 + ADC11 + ABC11 + ALC11 + APC11
 MASSBALANCEC11 = TDOSEC11 - TMASSC11
 TDOSEC11 = AXC11 + ABinitC11 + ADinitC11 + APinitC11

 TMASSC12 = ASC12 + ADC12 + ABC12 + ALC12 + APC12
 MASSBALANCEC12 = TDOSEC12 - TMASSC12
 TDOSEC12 = AXC12 + ABinitC12 + ADinitC12 + APinitC12



TERMT(T.GE.TSTOP)                    ! Condition for terminating simulation

END     ! End of derivative block
END     ! End of dynamic section
END     ! End of program
```

APPENDIX C:

PHYSIOLOGICALLY-BASED TOXICOKINETIC MODEL PROGRAM

```
PROGRAM: PBTKmanuscript3.CSL PHYSIOLOGICAL MODEL
! PBTK model for inhalation and dermal exposure to NAPHTHALENE
! Department of Environmental Sciences and Engineering, School of Public Health
! The University of North Carolina at Chapel Hill
! Constructed by David Kim beginning December 21, 2005

INITIAL

!Physiological Parameters ***********************************

CONSTANT       HT = 178                    ! Height (cm)
CONSTANT      BW = 78                      ! Body weight (kg)
CONSTANT    AEXP = 21845.6                 ! Surface area of exposure (cm^2)
CONSTANT     QCC = 15                      ! Cardiac output (L/hr-1kg)
CONSTANT     QPC = 15                      ! Alveolar ventilation (L/hr-1kg)
CONSTANT     QEC = 0.05                    ! Fractional blood flow to skin
CONSTANT     QFC = 0.05                    ! Fractional blood flow to fat
CONSTANT     QLC = 0.23                    ! Fractional blood flow to liver
CONSTANT     VEC = 0.03                    ! Fraction skin tissue


!Skin parameters ***************************************

CONSTANT     PERM1 = 0.00000045            ! Permeability coefficient through stratum corneum
(cm/min)
CONSTANT      PERM2 = 0.033                ! Permeability coefficient through viable
                                           epidermis (cm/min)
CONSTANT      PD = 12.7                    ! Partition coefficient of SC to VE
CONSTANT      PE = 2.8                     ! Skin/blood partition coefficient (VE to blood
                                           partition coefficient from McCarley and Bunge 2001)
CONSTANT     TD = 0.001                    ! Thickness of stratum corneum (cm)
CONSTANT     TE = 0.03                     ! Thickness of viable epidermis (cm)


!Chemical specific parameters *********************************

CONSTANT      PB = 54.7                    ! Blood/air partition coefficient
CONSTANT      PF = 40.4                    ! Fat/blood partition coefficient
CONSTANT       PO = 4.2                    ! Other/blood partition coefficient
CONSTANT      MW = 128                     ! Molecular weight (g/mol)


!Metabolism parameters****************************************

CONSTANT   vmaxkm = 698                    ! metabolic rate (L/min)


!Calculated parameters ***************************************
    HTM = HT/100                           ! Height (m)
     VB = (72.447/1000)*(BW**1.007)        ! Volume of blood (L)
    BMI = BW/(HTM**2)                      ! Body mass index (kg/m2)
    FAT = -126.2 + 45*log(BMI)             ! Fat percent (%)
  SURFA = (BW**0.45)*(HT**0.725)*71.84     ! Total body surface area (cm^2) by DuBois and
                                           DuBois (1916)

     k0 = PERM1/Td                         ! exposure to SC (1/min)
```

```
    k1 = (PERM2*AEXP/PD)/1000              ! SC to VE (L/min)

   VECX = VEC*(AEXP/SURFA)                 ! Fraction skin tissue exposed
         VFC = FAT/100                     ! Fraction fat tissue
          VD = AEXP*TD/1000                ! volume of SC (L)

    VE = VECX*BW - VD                      ! Volume of viable epidermis - L
         VF = VFC*BW                       ! Volume of fat - L
    VO = 0.91*BW - VE - VF - VD            ! Other tissue volume - L

         QC = (QCC*BW**0.75)/60            ! Cardiac output - L/min
    QP = (QPC*BW**0.75)/60                 ! Alveolar ventilation - L/min

        QECX = QEC*(AEXP/SURFA)            ! Fractional blood flow to exposed skin
    QE = QECX*QC                           ! Exposed skin blood flow - L/min
    QF = QFC*QC                            ! Fat blood flow - L/min
    QO = QC - QF - QE                      ! Other tissue blood flow - L/min
         QL = QLC*QC

  kmet1 = vmaxkm/(vmaxkm + QL)             ! extraction coefficient


!Parameters for simulation of experiment **********************

CONSTANT   INHALCONC1 = 182.6              ! Concentration in air (ug/m^3)
          INHALCIX1 = INHALCONC1/1000      ! Air concentration in ug/L

CONSTANT   INHALCONC2 = 12.3               ! Concentration in air (ug/m^3)
          INHALCIX2 = INHALCONC2/1000      ! Air concentration in ug/L

CONSTANT    DJP8 = 0.00008                 ! Mass per cm^2 of JP8 component on TS
                          MJP8 = DJP8*AEXP ! Mass of JP8 component on TS


!Timing commands *********************************************

CONSTANT  TEXP = 229                       ! Duration of exposure (min)
CONSTANT TSTOP = 300                       ! Duration of simulation (min)
 POINTS = 300                              ! Number of times data are logged
   CINT = TSTOP/POINTS                     ! Communication intervals

ALGORITHM IALG = 2                         ! Use Gear integration algorithm

END                                        ! End of initial section


DYNAMIC

!-----------------------------------------------------------

DISCRETE CAT1                              ! Schedule events to turn exposure on and off daily
   INTERVAL CAT = 10000.0                  ! Set interval larger than any TSTOP (to prevent
                                           multiple exposure)
          CI = INHALCIX1                   ! Start inhalation exposure
      DERMDOSE = MJP8
```

```
  SCHEDULE CAT2 .AT. T + TEXP              ! Schedule end of exposure
END                                        ! End of CAT1

DISCRETE CAT2
        CI = INHALCIX2                     ! End inhalation exposure
          DERMDOSE = 0.0                   ! End dermal exposure
END                                        ! End of CAT2

!-----------------------------------------------------


DERIVATIVE

!************************ NAPHTHALENE ****************************

        !AD = Amount in stratum corneum (ug)
        RAD = k0*DERMDOSE - k1*CD
        AD = INTEG(RAD,0.0)
        CD = AD/VD

        !AE = Amount in viable epidermis (ug)
        RAE = k1*CD + QE*(CV - CE/PE)
        AE = INTEG(RAE,0.0)
        CE = AE/VE

        !AF = Amount in fat tissue (ug)
        RAF = QF*(CV - CF/PF)
        AF = INTEG(RAF,0.0)
        CF = AF/VF

        !AO = Amount in other tissues (ug)
        RAO = QO*(CV - CO/PO)
        AO = INTEG(RAO,0.0)
        CO = AO/VO

        !CV = Venous blood concentration (ug/L)
        RAV = QP*CI + QE*CE/PE + QF*CF/PF + QO*CO/PO - QC*CV - QL*kmet1*CV - QP*CV/PB
        AV = INTEG(RAV,0.0)
        CV = AV/VB

        !AM = Amount metabolized (ug)
        RAM = QL*kmet1*CV
        AM = INTEG(RAM,0.0)

        !AX = Amount exhaled (ug)
        RAX = QP*CX
        AX = INTEG(RAX,0.0)
        CX = CV/PB                         ! units ug/L

        CEX = CX*1000                      ! units ug/m^3
        AUCEX = INTEG(CEX,0.0)

! MASS BALANCE NAPHTHALENE

RINHALINPUT = QP*CI
INHALINPUT = INTEG(RINHALINPUT,0.0)
```

```
RDERMALINPUT = k0*DERMDOSE
 DERMALINPUT = INTEG(RDERMALINPUT,0.0)

INPUT = INHALINPUT + DERMALINPUT

! TMASS for Mass Balance (ug)
  TMASS = AD + AE + AF + AO + AX + AM + AV

MASSBALANCE = INPUT - TMASS


TERMT(T.GE.TSTOP)

END      ! End of derivative
END      ! End of dynamic
END      ! End of program
```

REFERENCES

Abraham, M. H., Kamlet, M. J., Taft, R. W., Doherty, R. M., and Weathersby, P. K. (1985). Solubility properties in polymers and biological media. 2. The correlation and prediction of the solubilities of nonelectrolytes in biological tissues and fluids. *J Med Chem* **28**, 865-70.

Andersen, M. E. (1991). Physiological modelling of organic compounds. *Ann Occup Hyg* **35**, 309-21.

Andersen, M. E. (2003). Toxicokinetic modeling and its applications in chemical risk assessment. *Toxicol Lett* **138**, 9-27.

Andersen, M. E., Sarangapani, R., Reitz, R. H., Gallavan, R. H., Dobrev, I. D., and Plotzke, K. P. (2001). Physiological modeling reveals novel pharmacokinetic behavior for inhaled octamethylcyclotetrasiloxane in rats. *Toxicol Sci* **60**, 214-31.

ATSDR (1995). Toxicological profile for naphthalene, 1-methylnaphthalene, and 2-methylnaphthalene. U.S. Department of Health and Human Services, U.S. Public Health Service, Atlanta, GA.

Babu, R. J., Chatterjee, A., and Singh, M. (2004). Assessment of skin irritation and molecular responses in rat skin exposed to nonane, dodecane and tetradecane. *Toxicol Lett* **153**, 255-66.

Barratt, M. D. (1995). Quantitative structure-activity relationships for skin permeability. *Toxicol In Vitro* **9**, 27-37.

Basak, S. C., Mills, D., Hawkins, D. M., and El-Masri, H. A. (2003). Prediction of human blood:air partition coefficients: A comparison of structure-based and property-based methods. *Risk Analysis* **23**, 1173-1184.

Baynes, R. E., Brooks, J. D., Budsaba, K., Smith, C. E., and Riviere, J. E. (2001). Mixture effects of JP-8 additives on the dermal disposition of jet fuel components. *Toxicol Appl Pharmacol* **175**, 269-81.

Beliveau, M., Tardif, R., and Krishnan, K. (2003). Quantitative structure-property relationships for physiologically based pharmacokinetic modeling of volatile organic chemicals in rats. *Toxicol Appl Pharmacol* **189**, 221-232.

Borras-Blasco, J., Diez-Sales, O., Lopez, A., and Herraez-Dominguez, M. (2004). A mathematical approach to predicting the percutaneous absorption enhancing effect of sodium lauryl sulphate. *Int J Pharm* **269**, 121-9.

Bronaugh, R. L., and Franz, T. J. (1986). Vehicle effects on percutaneous absorption: in vivo and in vitro comparisons with human skin. *Br J Dermatol* **115**, 1-11.

Bronaugh, R. L., and Maibach, H. I. (1999). Percutaneous absorption drugs--cosmetics--mechanisms--methodology. Dekker, New York.

Brouwer, D. H., Boeniger, M. F., and van Hemmen, J. (2000). Hand wash and manual skin wipes. *Ann Occup Hyg* **44**, 501-10.

Brown, R. P., Delp, M. D., Lindstedt, S. L., Rhomberg, L. R., and Beliles, R. P. (1997). Physiological parameter values for physiologically based pharmacokinetic models. *Toxicol Ind Health* **13**, 407-484.

Buckpitt, A., and Bahnson, L. (1986). Naphthalene metabolism by human lung microsomal enzymes. *Toxicol* **41**, 333-341.

Cardinali, F. L., Ashley, D. L., Wooten, J. V., McCraw, J. M., and Lemire, S. W. (2000). The use of solid-phase microextraction in conjunction with a benchtop quadrupole mass spectrometer for the analysis of volatile organic compounds in human blood at the low parts-per-trillion level. *J Chromatogr Sci* **38**, 49-54.

Chao, Y. C., Gibson, R. L., and Nylander-French, L. A. (2005). Dermal exposure to jet fuel (JP-8) in US Air Force personnel. *Ann Occup Hyg* **49**, 639-45.

Chao, Y. C., Kupper, L. L., Serdar, B., Egeghy, P. P., Rappaport, S. M., and Nylander-French, L. A. (2006). Dermal Exposure to Jet Fuel JP-8 Significantly Contributes to the Production of Urinary Naphthols in Fuel-Cell Maintenance Workers. *Environ Health Perspect* **114**, 182-5.

Chao, Y. C., and Nylander-French, L. A. (2004). Determination of keratin protein in a tape-stripped skin sample from jet fuel exposed skin. *Ann Occup Hyg* **48**, 65-73.

Cherrie, J. W., Brouwer, D. H., Roff, M., Vermeulen, R., and Kromhout, H. (2000). Use of qualitative and quantitative fluorescence techniques to assess dermal exposure. *Ann Occup Hyg* **44**, 519-522.

Chilcott, R. P., Jenner, J., Hotchkiss, S. A., and Rice, P. (2001). In vitro skin absorption and decontamination of sulphur mustard: comparison of human and pig-ear skin. *J Appl Toxicol* **21**, 279-83.

Chou, C. C., Riviere, J. E., and Monteiro-Riviere, N. A. (2003). The cytotoxicity of jet fuel aromatic hydrocarbons and dose-related interleukin-8 release from human epidermal keratinocytes. *Arch Toxicol* **77**, 384-91.

Davies, B., and Morris, T. (1993). Physiological parameters in laboratory animals and humans. *Pharm Res* **10**, 1093-5.

Egeghy, P. P., Hauf-Cabalo, L., Gibson, R., and Rappaport, S. M. (2003). Benzene and naphthalene in air and breath as indicators of exposure to jet fuel. *Occup Environ Med* **60**, 969-76.

Elias, J. J. (1989). *The microscopic structure of the epidermis and its derivatives*. Marcel Dekker, Inc., New York.

Evans, M. V., and Andersen, M. E. (2000). Sensitivity analysis of a physiological model for 2,3,7,8-tetrachlorodibenzo-p-dioxin (TCDD): assessing the impact of specific model parameters on sequestration in liver and fat in the rat. *Toxicol Sci* **54**, 71-80.

Fenske, R. A. (1993). Dermal exposure assessment technique. *Ann Occup Hyg* **37**, 687-706.

Fent, K. W., Jayaraj, K., Gold, A., Ball, L. M., and Nylander-French, L. A. (in press). A tape-strip sampling method to measure dermal exposure to 1,6-hexamethylene diisocyanate. *Scand J Work Environ Health*.

Fiserova-Bergerova, V. (1983). *Modeling of inhalation exposures to vapors: uptake, distribution, and elimination*. CRC Press, Boca Raton, FL.

Fiserova-Bergerova, V., Tichy, M., and Di Carlo, F. J. (1984). Effects of biosolubility on pulmonary uptake and disposition of gases and vapors of lipophilic chemicals. *Drug Metab Rev* **15**, 1033-70.

Gioia, F., and Celleno, L. (2002). The dynamics of transepidermal water loss (TEWL) from hydrated skin. *Skin Res Technol* **8**, 178-86.

Goffe, W. L., Ferrier, G. D., and Rojers, J. (1994). Global optimization of statistical functions with simulated annealing. *J Econ* **60**, 65-99.

Guy, R. H., Hadgraft, J., and Maibach, H. I. (1985). Percutaneous absorption in man: a kinetic approach. *Toxicol Appl Pharmacol* **78**, 123-9.

Guy, R. H., and Potts, R. O. (1992). Structure-permeability relationships in percutaneous penetration. *J Pharm Sci* **81**, 603-604.

Hansch, C., Hoekman, D., Leo, A., Zhang, L., and Li, P. (1995). The expanding role of quantitative structure-activity relationships (QSAR) in toxicology. *Toxicol Lett* **79**, 45-53.

Harding, C. R. (2004). The stratum corneum: structure and function in health and disease. *Dermatol Ther* **17**, 6-15.

Hawkins, D. M., Basak, S. C., and Mills, D. (2004). QSARs for chemical mutagens from structure: ridge regression fitting and diagnostics. *Environ Toxicol Pharm* **16**, 37-44.

Haycock, G. B., Schwartz, G. J., and Wisotsky, D. H. (1978). Geometric method for measuring body surface area: a height-weight formula validated in infants, children, and adults. *J Pediatr* **93**, 62-6.

Jacobi, U., Weigmann, H. J., Ulrich, J., Sterry, W., and Lademann, J. (2005). Estimation of the relative stratum corneum amount removed by tape stripping. *Skin Res Technol* **11**, 91-6.

Kalinin, A., Marekov, L. N., and Steinert, P. M. (2001). Assembly of the epidermal cornified cell envelope. *J Cell Sci* **114**, 3069-3070.

Kanikkannan, N., Burton, S., Patel, R., Jackson, T., Shaik, M. S., and Singh, M. (2001a). Percutaneous permeation and skin irritation of JP-8+100 jet fuel in a porcine model. *Toxicol Lett* **119**, 133-42.

Kanikkannan, N., Patel, R., Jackson, T., Shaik, M. S., and Singh, M. (2001b). Percutaneous absorption and skin irritation of JP-8 (jet fuel). *Toxicol* **161**, 1-11.

Kim, D., Andersen, M. E., and Nylander-French, L. A. (2006). Dermal absorption and penetration of jet fuel components in humans. *Toxicol Lett*.

Kim, D., Andersen, M. E., and Nylander-French, L. A. (submitted). A dermatotoxicokinetic model of human exposures to jet fuel.

Klaassen, C. D. (1996). *Casarett and Doull's Toxicology: The Basic Science of Poisons*. McGraw-Hill, New York.

Larese Filon, F., Maina, G., Adami, G., Venier, M., Coceani, N., Bussani, R., Massiccio, M., Barbieri, P., and Spinelli, P. (2004). In vitro percutaneous absorption of cobalt. *Int Arch Occup Environ Health* **77**, 85-9.

Levitt, D. G. (2002). PKQuest: a general physiologically based pharmacokinetic model. Introduction and application to propranolol. *BMC Clin Pharmacol* **2**, 5.

Levitt, D. G. (2004). Physiologically based pharmacokinetic modeling of arterial - antecubital vein concentration difference. *BMC Clin Pharmacol* **4**, 2.

Lien, E. J., and Gao, H. (1995). QSAR analysis of skin permeability of various drugs in man as compared to *in vivo* and *in vitro* studies in rodents. *Pharm Sci* **4**, 562-265.

Loden, M., Akerstrom, U., Lindahl, K., and Berne, B. (2004). Bioequivalence determination of topical ketoprofen using a dermatopharmacokinetic approach and excised skin penetration. *Int J Pharm* **284**, 23-30.

Loffler, H., Dreher, F., and Maibach, H. I. (2004). Stratum corneum adhesive tape stripping: influence of anatomical site, application pressure, duration and removal. *Br J Dermatol* **151**, 746-52.

Madison, K. C. (2003). Barrier function of the skin: "la raison d'etre" of the epidermis. *J Invest Dermatol* **121**, 231-41.

Marks, R. (2004). The stratum corneum barrier: the final frontier. *J Nutr* **134**, 2017S-2021S.

McCarley, K. D., and Bunge, A. L. (2001). Pharmacokinetic models of dermal absorption. *J Pharm Sci* **90**, 1699-1719.

McDougal, J. N., and Boeniger, M. F. (2002). Methods for assessing risks of dermal exposures in the workplace. *Crit Rev Toxicol* **32**, 291-327.

McDougal, J. N., Pollard, D. L., Weisman, W., Garrett, C. M., and Miller, T. E. (2000). Assessment of skin absorption and penetration of JP-8 jet fuel and its components. *Toxicol Sci* **55**, 247-55.

McDougal, J. N., and Robinson, P. J. (2002). Assessment of dermal absorption and penetration of components of a fuel mixture (JP-8). *Sci Tot Environ* **288**, 23-30.

McDougal, J. N., and Rogers, J. V. (2004). Local and systemic toxicity of JP-8 from cutaneous exposures. *Toxicol Lett* **149**, 301-8.

Mills, T. C. (2005). Predicting body fat using data on the BMI. *Journal of Statistics Education* **13**, 1-13.

Montagna, W., and Parakkal, P. F. (1974). *The structure and function of skin*. Academic Press, Inc., New York.

Moss, G. P., Dearden, J. C., Patel, H., and Cronin, M. T. (2002). Quantitative structure-permeability relationships (QSPRs) for percutaneous absorption. *Toxicol In Vitro* **16**, 299-317.

Muhammad, F., Brooks, J. D., and Riviere, J. E. (2004). Compartive mixture effects of JP-8(100) additives on the dermal absorption and disposition of jet fuel hydrocarbons in different membrane model systems. *Toxicol Lett* **150**, 351-365.

Mukhtar, H. (1992). *Pharmacology of the skin*. CRC Press, Boca Raton.

Nylander-French, L. A. (2000). A tape-stripping method for measuring dermal exposure to multifunctional acrylates. *Ann Occup Hyg* **44**, 645-51.

Nylander-French, L. A. (2003). Occupational dermal exposure assessment. In Patty's Industrial Hygiene (R. Harrison, ed.) John Wiley & Sons, Inc., New York.

Parent, M. E., Hua, Y., and Siemiatycki, J. (2000). Occupational risk factors for renal cell carcinoma in Montreal. *Am J Ind Med* **38**, 609-18.

Perleberg, U. R., Keys, D. A., and Fisher, J. W. (2004). Development of a physiologically based pharmacokinetic model for decane, a constituent of jet propellant-8. *Inhal Toxicol* **16**, 771-783.

Pershing, L. K., Bakhtian, S., Poncelet, C. E., Corlett, J. L., and Shah, V. P. (2002). Comparison of skin stripping, in vitro release, and skin blanching response methods to measure dose response and similarity of triamcinolone acetonide cream strengths from two manufactured sources. *J Pharm Sci* **91**, 1312-23.

Pershing, L. K., Nelson, J. L., Corlett, J. L., Shrivastava, S. P., Hare, D. B., and Shah, V. P. (2003). Assessment of dermatopharmacokinetic approach in the bioequivalence determination of topical tretinoin gel products. *J Am Acad Dermatol* **48**, 740-51.

Pillai, O., Hamad, M. O., Crooks, P. A., and Stinchcomb, A. L. (2004). Physicochemical evaluation, in vitro human skin diffusion, and concurrent biotransformation of 3-O-alkyl carbonate prodrugs of naltrexone. *Pharm Res* **21**, 1146-52.

Pinheiro, J. C., and Bates, D. M. (2000). *Mixed-Effects Models in S and S-Plus*. Springer-Verlag Inc, New York.

Pirot, F., Kalia, Y. N., Stinchcomb, A. L., Keating, G., Bunge, A., and Guy, R. H. (1997). Characterization of the permeability barrier of human skin in vivo. *Proc Natl Acad Sci USA* **94**, 1562-7.

Pleil, J., Smith, L. B., and Zelnick, S. D. (2000). Personal exposure to JP-8 jet fuel vapors and exhaust at air force bases. *Environ Health Perspect* **108**, 183-192.

Poet, T. S., and McDougal, J. N. (2002). Skin absorption and human risk assessment. *Chem Biol Interact* **140**, 19-34.

Qiao, G. L., Chang, S. K., Brooks, J. D., and Riviere, J. E. (2000). Dermatoxicokinetic modeling of p-nitrophenol and its conjugation metabolite in swine following topical and intravenous administration. *Toxicol Sci* **54**, 284-94.

Quick, D. J., and Shuler, M. L. (1999). Use of in vitro data for construction of a physiologically based pharmacokinetic model for naphthalene in rats and mice to probe species differences. *Biotech Prog* **15**, 540-555.

Reddy, M. B., Stinchcomb, A. L., Guy, R. H., and Bunge, A. L. (2002). Determining dermal absorption parameters in vivo from tape strip data. *Pharm Res* **19**, 292-8.

Reddy, M. B., Yang, R. S., Clewell, H. J., and Andersen, M. E. (2005). *Physiologically Based Pharmacokinetic Modeling*. John Wiley & Sons, Inc., Hoboken, NJ.

Rhodes, A. G., LeMasters, G. K., Lockey, J. E., Smith, J. W., Yiin, J. H., Egeghy, P., and Gibson, R. (2003). The effects of jet fuel on immune cells of fuel system maintenance workers. *J Occup Environ Med* **45**, 79-86.

Ross, E. A., Savage, K. A., Utley, L. J., and Tebbett, I. R. (2004). Insect repellant interactions: sunscreens enhance deet (N,N-diethyl-m-toluamide) absorption. *Drug Metab Dispos* **32**, 783-5.

Rougier, A., Lotte, C., and Maibach, H. I. (1987). In vivo percutaneous penetration of some organic compounds related to anatomic site in humans: predictive assessment by the stripping method. *J Pharm Sci* **76**, 451-4.

Rustemeier, K., Stabbert, R., Haussmann, H. J., Roemer, E., and Carmines, E. L. (2002). Evaluation of the potential effects of ingredients added to cigarettes. Part 2: chemical composition of mainstream smoke. *Food Chem Toxicol* **40**, 93-104.

Sartorelli, P. (2002). Dermal exposure assessment in occupational medicine. *Occup Med (Lond)* **52**, 151-6.

Sartorelli, P., Aprea, C., Cenni, A., Novelli, M. T., Orsi, D., Palmi, S., and Matteucci, G. (1998). Prediction of percutaneous absorption from physicochemical data: a model based on data of in vitro experiments. *Ann Occup Hyg* **42**, 267-76.

Sato, A., and Nakajima, T. (1979). Partition coefficients of some aromatic hydrocarbons and ketones in water, blood and oil. *Br J Ind Med* **36**, 231-234.

Schmook, F. P., Meingassner, J. G., and Billich, A. (2001). Comparison of human skin or epidermis models with human and animal skin in in-vitro percutaneous absorption. *Int J Pharm* **215**, 51-6.

Schneider, T., Cherrie, J. W., Vermeulen, R., and Kromhout, H. (2000). Dermal exposure assessment. *Ann Occup Hyg* **44**, 493-9.

Schneider, T., Vermeulen, R., Brouwer, D. H., Cherrie, J. W., Kromhout, H., and Fogh, C. L. (1999). Conceptual model for assessment of dermal exposure. *Occup Environ Med* **56**, 765-73.

Schreiber, S., Mahmoud, A., Vuia, A., Rubbelke, M. K., Schmidt, E., Schaller, M., Kandarova, H., Haberland, A., Schafer, U. F., Bock, U., Korting, H. C., Liebsch, M., and Schafer-Korting, M. (2005). Reconstructed epidermis versus human and animal skin in skin absorption studies. *Toxicol In Vitro* **19**, 813-22.

Semple, S. (2004). Dermal exposure to chemicals in the workplace: just how important in skin absorption? *Occup Environ Med* **61**, 376-382.

Semple, S. (2005). Assessing occupational and environmental exposure. *Occup Med (Lond)* **55**, 419-24.

Serdar, B., Egeghy, P. P., Gibson, R., and Rappaport, S. M. (2004). Dose-dependent production of urinary naphthols among workers exposed to jet fuel (JP-8). *Am J Ind Med* **46**, 234-44.

Serdar, B., Egeghy, P. P., Waidyanatha, S., Gibson, R., and Rappaport, S. M. (2003). Urinary biomarkers of exposure to jet fuel (JP-8). *Environ Health Perspect* **111**, 1760-4.

Shah, V. P. (2001). Progress in methodologies for evaluating bioequivalence of topical formulations. *Am J Clin Dermatol* **2**, 275-80.

Shah, V. P., Flynn, G. L., Yacobi, A., Maibach, H. I., Bon, C., Fleischer, N. M., Franz, T. J., Kaplan, S. A., Kawamoto, J., Lesko, L. J., Marty, J. P., Pershing, L. K., Schaefer, H., Sequeira, J. A., Shrivastava, S. P., Wilkin, J., and Williams, R. L. (1998). Bioequivalence of topical dermatological dosage forms--methods of evaluation of bioequivalence. *Pharm Res* **15**, 167-71.

Shatkin, J. A., and Brown, H. S. (1991). Pharmacokinetics of the dermal route of exposure to volatile organic chemicals in water: a computer simulation model. *Environ Res* **56**, 90-108.

Siemiatycki, J., Dewar, R., Nadon, L., Gerin, M., Richardson, L., and Wacholder, S. (1987). Associations between several sites of cancer and twelve petroleum-derived liquids. Results from a case-referent study in Montreal. *Scand J Work Environ Health* **13**, 493-504.

Singh, S., Zhao, K., and Singh, J. (2003). In vivo percutaneous absorption, skin barrier perturbation, and irritation from JP-8 jet fuel components. *Drug Chem Toxicol* **26**, 135-46.

Smith, A. Q., Campbell, J. L., Keys, D. A., and Fisher, J. W. (2005). Rat tissue and blood partition coefficients for n-alkanes (C8 to C12). *Int J Toxicol* **24**, 35-41.

Smith, L. B., Bhattacharya, A., Lemasters, G., Succop, P., Puhala, E., Medvedovic, M., and Joyce, J. (1997). Effect of chronic low-level exposure to jet fuel on postural balance of US Air Force personnel. *J Occup Environ Med* **39**, 623-32.

Subcommittee on Jet-Propulsion Fuel 8 (2003). *Toxicologic assessment of Jet-Propulsion Fuel 8*. The National Academies Press, Washington, D.C.

Surber, C., Schward, F. P., and Fmith, E. W. (1999). Tape stripping technique. In Percutaneous Absorption - Drug - Cosmetics - Mechanisms - Methodology (H. Bronough and H. I. Maibach, eds.), pp. 395-409. Marcel Dekker, New York.

Thrall, K. D., Gies, R. A., Muniz, J., Woodstock, A. D., and Higgins, G. (2002). Route-of-entry and brain tissue partition coefficients for common superfund contaminants. *J Toxicol Environ Health A* **65**, 2075-86.

Travis, C. C., Quillen, J. L., and Arms, A. D. (1990). Pharmacokinetics of benzene. *Toxicol Appl Pharmacol* **102**, 400-420.

US EPA (1998). Toxicological review of naphthalene. U.S. Environmental Protection Agency, Washington, D.C.

Venier, M., Adami, G., Larese, F., Maina, G., and Renzi, N. (2004). Percutaneous absorption of 5 glycol ethers through human skin in vitro. *Toxicol In Vitro* **18**, 665-71.

Wagner, H., Kostka, K. H., Lehr, C. M., and Schaefer, U. F. (2000). Drug distribution in human skin using two different in vitro test systems: comparison with in vivo data. *Pharm Res* **17**, 1475-81.

Waidyanatha, S., Zheng, Y., and Rappaport, S. M. (2003). Determination of polycyclic aromatic hydrocarbons in urine of coke oven workers by headspace solid phase microextraction and gas chromatography-mass spectrometry. *Chem Biol Interact* **145**, 165-74.

West, D. P., Halket, J. M., Harvey, D. R., Hadgraft, J., Solomon, L. M., and Harper, J. I. (1987). Percutaneous absorption in preterm infants. *Pediatr Dermatol* **4**, 234-7.

Wester, R. C., and Maibach, H. I. (1989). *In vivo methods for percutaneous absorption measurements*. Marcel Dekker, Inc., New York.

Wester, R. C., Melendres, J., Sedik, L., Maibach, H., and Riviere, J. E. (1998). Percutaneous absorption of salicylic acid, theophylline, 2, 4-dimethylamine, diethyl hexyl phthalic acid, and p-aminobenzoic acid in the isolated perfused porcine skin flap compared to man in vivo. *Toxicol Appl Pharmacol* **151**, 159-65.

Wheeler, J. P., and Stancliffe, J. D. (1998). Comparison of methods for monitoring solid particulate surface contamination in the workplace. *Ann Occup Hyg* **42**, 477-88.

Willems, B. A. T., Melnick, R. L., Kohn, M. C., and Portier, C. J. (2001). A physiologically based pharmacokinetic model for inhalation and intravenous administration of naphthalene in rats and mice. *Toxicol Appl Pharmacol* **176**, 81-91.

Williams, P. L., and Riviere, J. E. (1995). A biophysically based dermatopharmacokinetic compartment model for quantifying percutaneous penetration and absorption of topically applied agents. I. Theory. *J Pharm Sci* **84**, 599-608.

Xcellon (2004). acslXtreme Optimum user's guide version 1.4, Huntsville, AL.

Zeiger, E., and Smith, L. (1998). The first international conference on the environmental health and safety of jet fuel. *Environ Health Perspect* **106**, 763-764.